THE STRUCTURE OF THE SOUTHERN MILKY WAY

A thesis submitted for the degree of Doctor of Philosophy in the Australian National University

J. B. Whiteoak
Mount Stromlo Observatory
A. N. U.
November, 1961.

THE STRUCTURE OF THE SOUTHERN MILKY WAY

A thesis submitted for the degree of Doctor of Philosophy in the Australian National University

J. B. Whiteoak
Mount Stromlo Observatory
A. N. U.
November, 1961.

Prefatory Note.

The investigations described in the thesis were accomplished during the tenure of an Australian National University Research Scholarship (1959, 1960), and a General Motors-Holden's Post-Graduate Fellowship (1961), in the Department of Astronomy of the Research School of Physical Sciences. Except for Chapter 2, which describes work carried out jointly with other investigators, the studies reported herein were performed wholly by the candidate. Where authorship was shared, a major contribution was made by the candidate.

John. B. Whiteoak

TABLE OF CONTENTS

Acknowledgements

I am indebted greatly to the many persons of the Mt. Stromlo Observatory who have assisted me during the period when the work discussed in the thesis was carried out. First and foremost, Professor B. J. Bok has aided me in many ways, not only in the capacity of supervisor, where he has been a constant source of encouragement, but also as a result of his deep interest in the personal problems that occur from time to time. I am grateful also to Dr. A. W. Rodgers, who also acted as a supervisor while he was at the Observatory, for his wise counsel in various aspects of the study. In addition, I have benefitted from stimulating discussions with many members of the Mt. Stromlo Staff; in particular, Dr. B. E. Westerlund made many helpful comments regarding the context of the thesis. Dr. F. J. Kerr and Mr M. M. Komesaroff of the Radiophysics Laboratory, C.S.I.R.O., Sydney, have assisted by providing me with some of their results in advance of publication.

In the preparation of the subject matter, I am indebted to my wife, Mary, and Miss Flora Ogston, who typed the draft copies. To my mother goes my deepest thanks for the execution of the final typing of the thesis.

THE STRUCTURE OF THE SOUTHERN MILKY WAY

INTRODUCTION

The skies of the Southern hemisphere contain many of the objects important in the studies of galactic structure and stellar evolution. Apart from the Magellanic Clouds, the two nearest galaxies, there is a most interesting area of the Milky Way - that near the direction of the galactic centre. The greater part of it can be observed at observatories situated in the Northern hemisphere, but the region between $l^{II} = 290^{o}$ and $l^{II} = 350^{o}$ is inaccessible. There is a marked disparity between our knowledge of the Northern and Southern Milky Ways, and this is reflected particularly in our understanding of spiral structure, the optical interpretation of which depends almost entirely on Northern hemisphere observations.

The main object of this thesis is to add to the knowledge of the structure of the Southern Milky Way by:

(a) A study of the size and distribution of H II regions.

(b) The studies of two star concentrations - a visual grouping of early-type stars, and a young cluster.

In (a), a photographic survey for the detection of H II regions in the Southern Milky Way is carried out. Their distribution and apparent sizes as a function of galactic longitude are used to construct a qualitative representation of spiral structure which is compared with the current models. The aims of the investigations carried out in (b) are to study the characteristics of visual groupings of early-type stars and to aid the determination of distances of spiral arms in the Southern Milky Way.

Summary of Thesis

Chapter 1

Chapter 1 is a review of the present state of researches concerning spiral structure and O-B associations. The historical development of the attempts to detect spiral arms is discussed from the point of view of optical and radioastronomical investigations. The review shows the lack of accurate optical observations of Population I objects in the inner regions of the galaxy, and the consequent effect on the various representations of spiral structure. The general characteristics of OB associations are discussed; it is shown from the existing data that little is known of those situated in the Milky Way between galactic longitudes $l^{II} = 290^{o}$ and $l^{II} = 340^{o}$. In the study of their individual properties, it is concluded that the relation of associations to gas and dust, the existence of internal expansion, their membership and origin, are still uncertain.

Chapter 2

Chapter 2 deals with the detection and mapping of H II regions that are in the Southern Milky Way between longitudes $l^{II} = 220^{o}$ and $l^{II} = 40^{o}$. The experimental details of the production of an Atlas of H-alpha emission are given. Several of the more prominent southern H II regions are described. The distances of some of them, determined from studies of their exciting stars, are listed; on the assumption that the larger regions are in the nearer spiral arms, the distributions of sizes and distances with galactic longitude are examined in an effort to detect spiral structure. In the analysis, allowance is made for the effects of large areas of highly-absorbing interstellar material present in many directions.

Chapter 3

The results are presented of a photoelectric and spectrographic study of stars in the galactic cluster IC 2602 (θ Carina cluster). A description is given of the equipment used in the investigations discussed in this and the following chapter. The analysis of the results obtained for the probable members shows that the cluster consists of a young group of stars located at a relatively small distance from the sun. On the basis of objective prism spectra, and two-colour photographic magnitudes, a search for fainter possible members is carried out. The population of the cluster is compared with that predicted by the Initial Luminosity Function adopted by Limber[1]. The possible relationship of the cluster with the Scorpio-Centaurus association is discussed in a comparison of the characteristics of the two groups of stars. A brief study is made of the more distant galactic cluster, Melotte 101, which is situated in the same direction as IC 2602.

Chapter 4

In chapter 4, the details are given of a survey for the detection of stars of early spectral types between longitudes $l^{II} = 295^{o}$ and $l^{II} = 345^{o}$, and near the galactic-equator. The stars were identified by visual inspection of objective prism spectral plates taken of the region under study. Their distribution on the celestial sphere is examined for the presence of visual groupings. When the effect on the distribution of the dense obscuration near the galactic equator at most longitudes is considered, it appears that some of the groupings are situated in regions of the Milky Way less obscured than those adjacent to them, and may not be true associations.

(1) Limber, D.N., Ap.J., 131, 168, 1960.

A photoelectric and spectroscopic investigation of one of the detected O-B concentrations, centred at $l^{II} = 337^{o}$, is discussed. From an analysis of the diatances of individual stars, it is shown that several spatially-separated groupings are present in this direction. The population of the nearest is examined and compared with that predicted by the Initial Luminosity Function. The grouping could represent an association or a group of stars in a spiral arm that is traversed by the line of sight. In the part of the Milky Way occupied by the visual grouping are situated three galactic clusters, NGC 6167, NGC 6193 and NGC 6204. From the results of photoelectric studies of several members of each, distances of the clusters are derived and compared with that of the OB grouping.

Chapter 5

Chapter 5 contains a summary of the results obtained in chapters 2, 3, and 4. From the studies carried out, the distances of the stellar groupings are incorporated with those of other population I objects to define more accurately the spiral structure of the inner regions of the galaxy. The derived distribution of associations, clusters, high luminosity stars and H II regions are compared with that determined by Kerr for neutral atomic hydrogen. The difficulties encountered in the comparison of the optical results obtained by different observers are discussed.

The characteristics of the star groups discussed in chapters 3 and 4 are summarized and suggestions made for future studies.

CHAPTER 1

SPIRAL STRUCTURE AND OB ASSOCIATIONS.

1.1 The Development of the Model of Spiral Structure.

For many years prior to 1951, most astronomers believed that the galaxy possessed spiral structure, but could discover no means of tracing the spiral arms. However, in that year Baade[1], and Baade and Mayall[2] presented the results obtained from a photographic investigation with the Mount Wilson 100-inch and Mount Palomar 200-inch telescopes, of M31, the Andromeda Nebula. From a comparison of blue and red-sensitive plates of the galaxy, it was found that H-alpha emission could be detected. The discovery paved the way for spiral structure studies of our galaxy, for it provided a means of detecting one type of spiral arm tracer.

Since then, representations of spiral structure have been obtained by several methods using different criteria. They could be divided into two broad categories:

(1) Optical methods.

(2) Radioastronomical methods.

Category (1) consists of:

(a) the spatial distribution of Population I objects,

(b) the multiple structure shown by interstellar absorption lines of CaII and NaI in the spectra of distant stars,

(c) the distribution of brightness along the Milky Way.

In (2) is included:

(d) the distribution of neutral hydrogen in the galaxy,

(e) the sudden changes of the intensity of radio continuum radiation that occur at certain longitudes.

(1) Baade,W., Pub.Obs.Uni.Mich., 10, 7, 1951.
(2) Baade,W. and Mayall,N., 'Problems of Cosmical Aerodynamics,' 165. (Paris, 1951).

1. Optical Models of Spiral Structure.

(a). The distribution of extreme Population I objects.

In 1952, Morgan, Sharpless and Osterbrock[1] presented the results of an investigation of spiral structure, using H II regions as spiral tracers. The distances of the regions were determined from a study of their exciting stars. Between longitudes $l^{II} = 70^{o}$ and $l^{II} = 220^{o}$, there was evidence of a spiral arm (the Orion Arm) at a distance of 300 parsecs from the sun in the direction of the anti-centre. It contained several emission nebulae - that surrounding P Cyg, the North America Nebula, the Zeta-Per Nebula, the Orion Nebula and that near S Mon. From $l^{II} = 100^{o}$ to $l^{II} = 140^{o}$, a second arm (the Perseus Arm) was detected parallel to the first and about 2 kiloparsecs farther from the galactic centre. In the direction of the galactic centre, a third arm (the Sagittarius Arm), at a distance of 1500 parsecs from the sun, was defined by a series of O and B star groups extending from $l^{II} = 185^{o}$ in Carina to $l^{II} = 17^{o}$, the direction of the Small Sagittarius Cloud. The two arms farther from the galactic centre than the sun were inclined at an angle of 25 degrees with respect to the normal to a radius vector.

In 1953, Morgan, Whitford and Code[2] extended the original investigation by a study of the distribution of 27 O-B associations (fig.1). The distances of associations, determined from a consideration of several stars in each, should be more accurate than those of individual exciting stars of H II regions. The inferred spiral structure is similar to that of the previous interpretation, except for the

(1) Morgan,W.W., Sharpless,D. and Osterbrock,D., A.J.,57,3,1952.
(2) Morgan,W.W., Whitford,A.E. and Code,A.D., Ap.J.,118, 318, 1953.

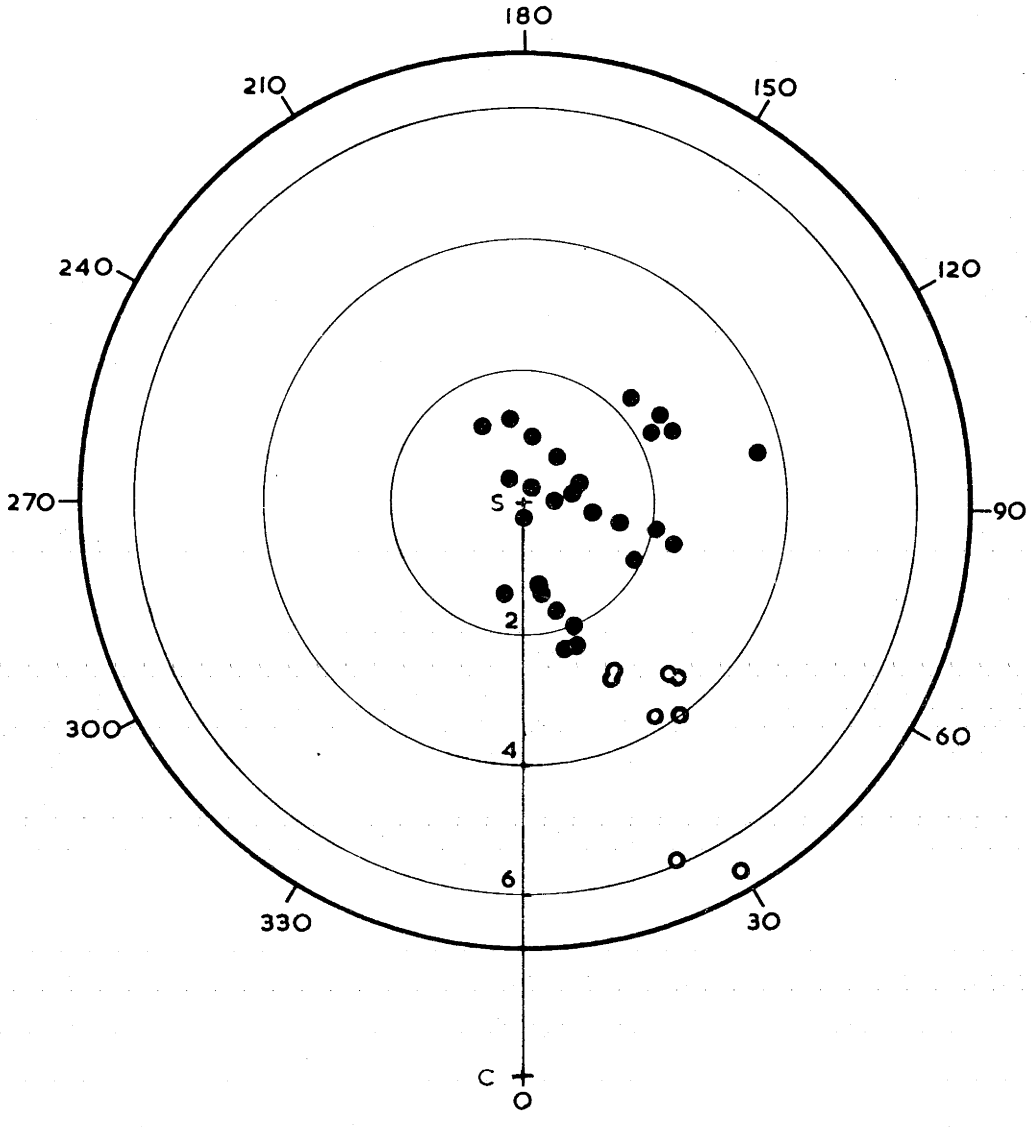

Fig. 1. Distribution of northern OB associations.

(The positions of eight distant OB Stars are shown as open circles.)

location of the sun within the Orion Arm. There is an apparent branching of this arm near the position of the sun. The distances of several individual stars (open circles) are used in an attempt to define more accurately the shape of the Sagittarius Arm. Apart from the stars and associations in the arm, two stars between the longitudes $l^{II} = 20^{o}$ and $l^{II} = 40^{o}$ appear to be situated at greater distances from the sun.

As Bok[1] has pointed out, the suggested spiral structures of Morgan, Whitford and Code, and more recent investigators may be criticized on three counts. The first is that the arms appear to be too highly inclined to a perpendicular to the radius vector from the galactic centre to the sun. Photographs of other galaxies indicate that spiral arms are generally more circular. The second criticism is that little more than half the Milky Way has been covered in the study of the associations. The third is that parts of the Orion Arm, including the Orion Nebula and its associated O and B Stars, are 15^{o} to 20^{o} south of the galactic plane. This would not be expected of a major feature of a spiral arm that may exist for at least one revolution, as it would imply that the arm is inclined at the quoted angle to the galactic plane.

In 1953, Weaver[2] attempted to construct a model of spiral structure from the distribution of B stars in galactic longitude. He assumed that the stars of spectral types earlier than B3 were uniformly distributed throughout spiral arms and that the interstellar absorption was either negligible or increased at the uniform rate of 1.0 magnitude per kiloparsec. The first assumption has been known to

(1) Bok,B.J., Obs.,79, 58, 1959.
(2) Weaver, H.F., A.J., 58, 177, 1953.

be incorrect since Shapley and Cannon[1], and Pannekoek[2] studied the space distribution of such stars in 1922 and 1929 respectively. As the second is also untrue, the model is of little value.

Hase (1954)[3] extended the type of investigation carried out earlier by Morgan, Sharpless and Osterbrock. The latter observers used the distribution of 25 H II regions; Hase determined the distances of the early-type stars associated with 150 of them. The distribution is shown in fig. 2. The suggested spiral arms are similar to those detected previously. The location of the Orion Arm at a distance of 300 parsecs from the sun in the direction of the anti-centre could be due to the fact that no H II regions between $l^{II} = 240^{o}$ and $l^{II} = 350^{o}$ were studied. An interesting feature is that the Sagittarius Arm appears to join the Orion Arm near the sun. If it is assumed that the furthermost H II regions shown at $l^{II} = 15^{o}$ in fig. 2 are in reality in an arm more distant than that containing the others present at this longitude, the modified representation of the Sagittarius Arm would be more parallel to the Orion Arm. Confirmation of this could be obtained from studies of regions at longitudes less than $l^{II} = 350^{o}$.

Such an investigation was carried out in 1955 by Gum[4], one of the first astronomers to derive a representation of spiral structure incorporating observations of the H II regions that are present in the Southern Milky Way (fig.3). His suggested position of the Sagittarius Arm depends greatly on the distances of some of these Southern H II regions. For the other two arms, the

(1) Shapley,H. and Cannon,A.J., H.C., 239, 1922.
(2) Pannekoek, A., Pub.Ast.Inst.Uni.Amst., No.2, 1929.
(3) Hase,V.F., Bull.Crim.Ast.Obs., 12, 88, 1954.
(4) Gum,C.S., Mem.R.A.S., 67, 155, 1955.

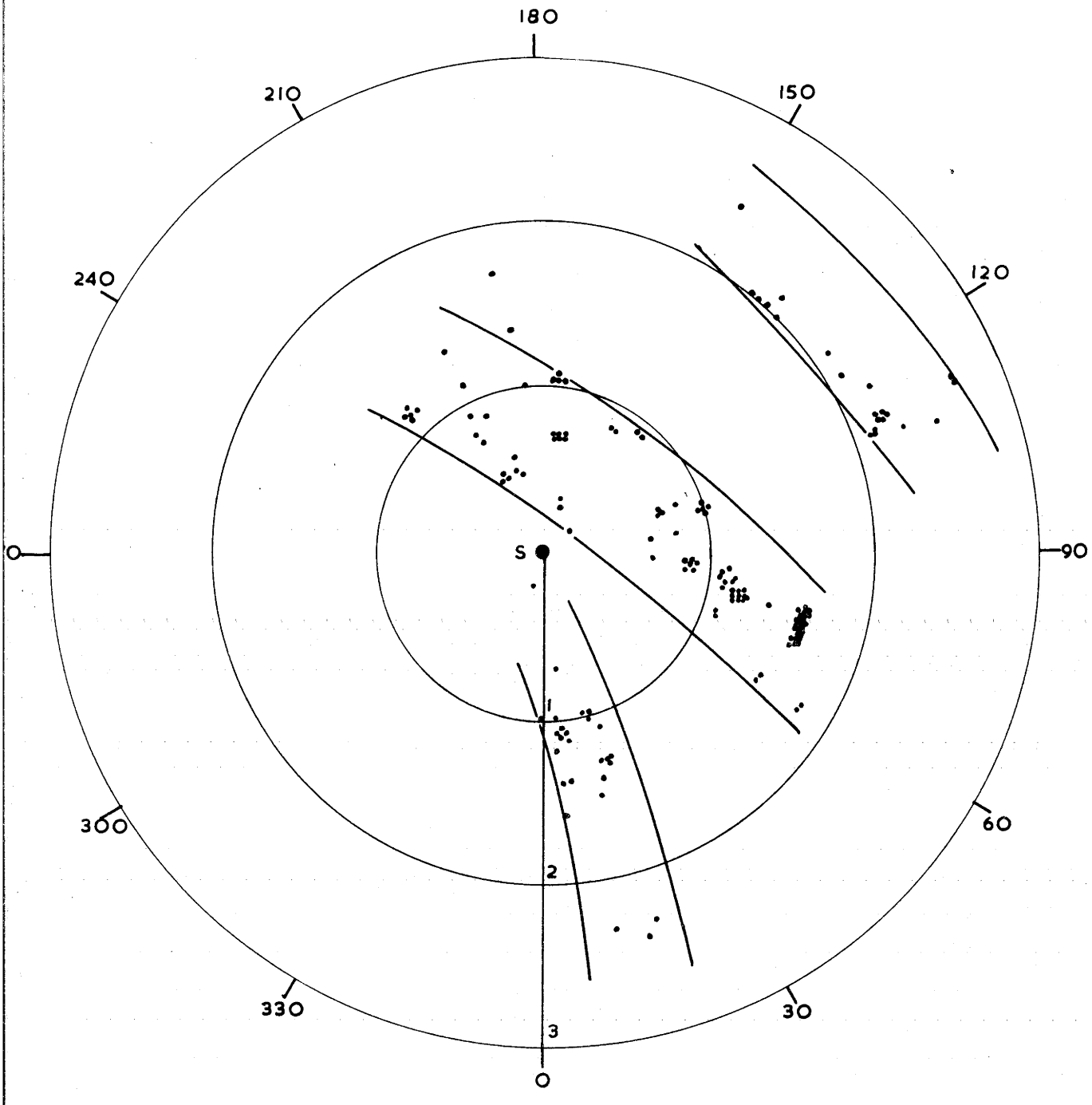

Fig.2. Spiral structure from distances of emission nebulae (Hase).

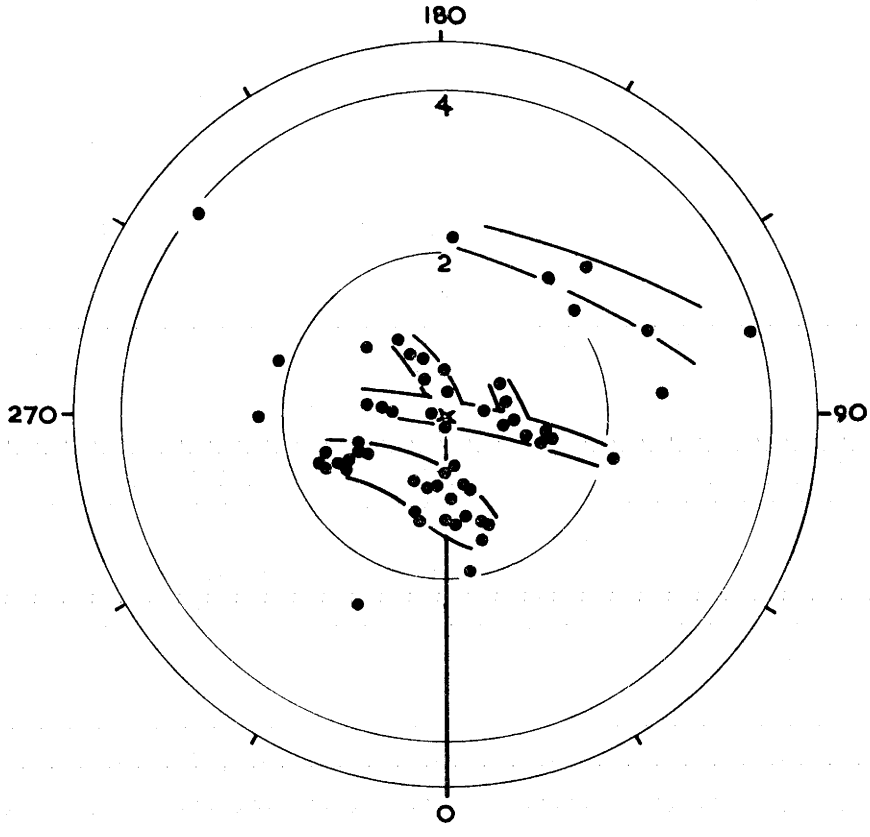

Fig.3. Spiral structure from the distribution of HII regions (Gum).

results of Morgan, Sharpless and Osterbrock were employed. The Perseus and Orion Arms are similar to those suggested by previous investigators. In addition to the forking of the latter, suggested by Morgan, Whitford and Code, Gum proposed the existence of a second branch that leaves the arm at $l^{II} = 78^{o}$. He suggested that the H II regions in Carina are located in the Sagittarius Arm, which could connect with the Orion Arm at $l^{II} = 270^{o}$. However, he has ignored the fact that between longitudes $l^{II} = 300^{o}$ and $l^{II} = 330^{o}$, there are no emission nebulae, a feature that could be interpreted as an inter-arm region in the line of sight.

An investigation similar to that of Morgan, Whitford and Code, but using the distances of 118 visual O-B star groups, was carried out by Kopylov[1] in 1957 (fig.4). The arms that he suggests are present are shown by the curved lines. There are several comments that can be made. In the figure there is very little evidence for the existence of the Perseus Arm. One can accept the presence of the Orion Arm from $l^{II} = 60^{o}$ to $l^{II} = 210^{o}$, but beyond these limits its position is doubtful. However, from the distribution in the figure, it is just as likely that the O-B groupings of Carina are situated in this and not the Sagittarius Arms as shown. A feature of the representation is that the Sagittarius Arm is replaced by two parallel arms 800 parsecs apart. On the basis of the available evidence, this part of the spiral pattern is not convincing. There are traces of another arm at a distance of about 3500 parsecs in the direction of the galactic centre. The positions of the spiral arms are similar to those in Gum's representation.

(1) Kopylov,I.M., A.J.U.S.S.R., 35, 359, 1958.

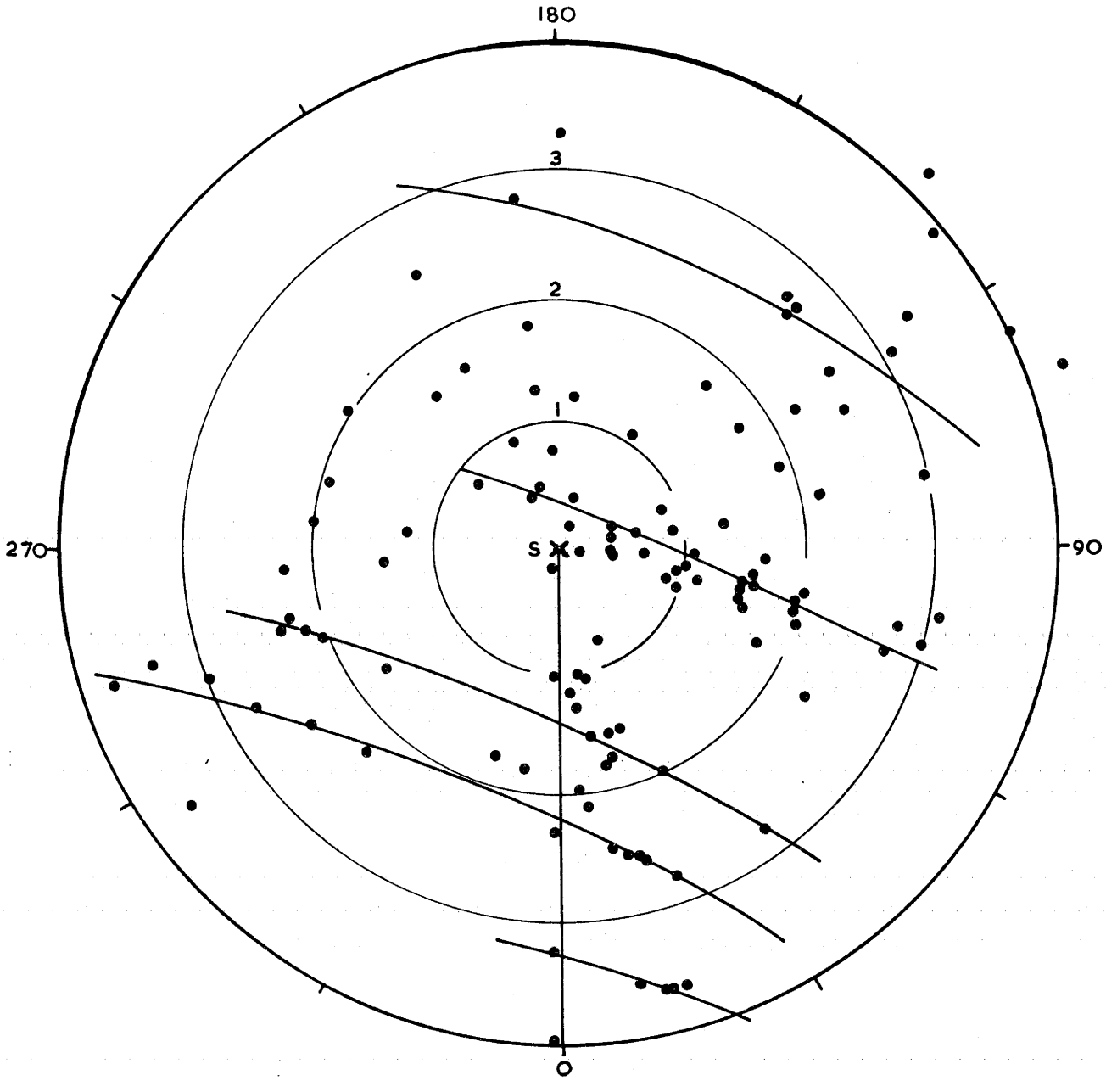

Fig.4. Distribution of OB groupings according to Kopylov.

(b). From observations of interstellar lines.

From an investigation of multiple interstellar absorption lines, Munch[1] in 1953 presented additional evidence independent of the previous method for the existence of spiral structure in the galaxy. At certain longitudes, the spectra of distant stars contain two separate components of these lines, which he interpreted as being due to the presence of two concentrations of interstellar material in the lines of sight, i.e. two spiral arms. Between longitudes $l^{II} = 70^{o}$ and $l^{II} = 180^{o}$, the velocities determined from single interstellar lines in the spectra of nearby stars and the red components of the multiple lines in those of distant stars were equivalent to the effects of galactic rotation at a distance of 400 parsecs from the sun. Between $l^{II} = 73^{o}$ and $l^{II} = 178^{o}$, the velocities determined by the violet line components correspond to rotation at a distance of 3 kiloparsecs. Thus Munch showed the existence of the Orion and Perseus Arms. The derived distances depend critically on the galactic rotation constants used (Munch employed the values listed by Oort[2] in 1952), and are only approximate, since stars in a large longitude range were considered. However, they are derived quite independently of those determined for exciting stars. The method can reveal unambiguously the existence of one or more spiral arms for which distances are equal to or less than those of the observed stars.

In 1956, Thackeray[3] discovered that several distant stars between longitudes $l^{II} = 330^{o}$ and $l^{II} = 30^{o}$ contain two components of the interstellar K line in their spectra.

(1) Munch,G., P.A.S.P., 65, 179, 1953.
(2) Oort,J.H., Ap.J., 116, 233, 1952.
(3) Thackeray,A.D., Nature, 178, 1458, 1956.

He concluded that the low-velocity component is produced by the concentration of interstellar matter associated with the Sagittarius Arm, and suggested that the high-velocity component corresponds to an inner arm which he termed the Scutum-Norma Arm. Except for the few distant stars shown in some of the previous distributions, this was the first positive optical evidence for the presence of the second inner arm.

(c). Spiral structure from the distribution of brightness along the Milky Way.

In 1960, Elsasser and Haug[1] carried out a photo-electric study in two colours of the brightness and colour distribution of the entire Milky Way. They determined the brightness in visual and photographic light of regions of the Milky Way $2\frac{1}{2}$ degrees square, and found the maximum value at each interval of $2\frac{1}{2}^{o}$ in galactic longitude. By considering the maxima at the chosen longitudes, and not necessarily the values occurring along the galactic equator, they attempted to overcome the effects of the irregular interstellar absorption that is present in the Milky Way. In the distribution of the maxima with longitude, several peaks are present. They suggested that, at the longitudes where the peaks are higher in photographic than in visual light, the effect is due to the radiation of early-type stars in spiral arms tangential to the lines of sight. The positions of the tangential points along the lines of sight were derived by assuming that the arms are circular. Pairs of tangential points were joined to give the representation shown in fig.5; the longitudes marked are the tangential directions. The way in which

(1) Elsasser,H. and Haug,U., Z.Fur.Ap., 50, 121, 1960.

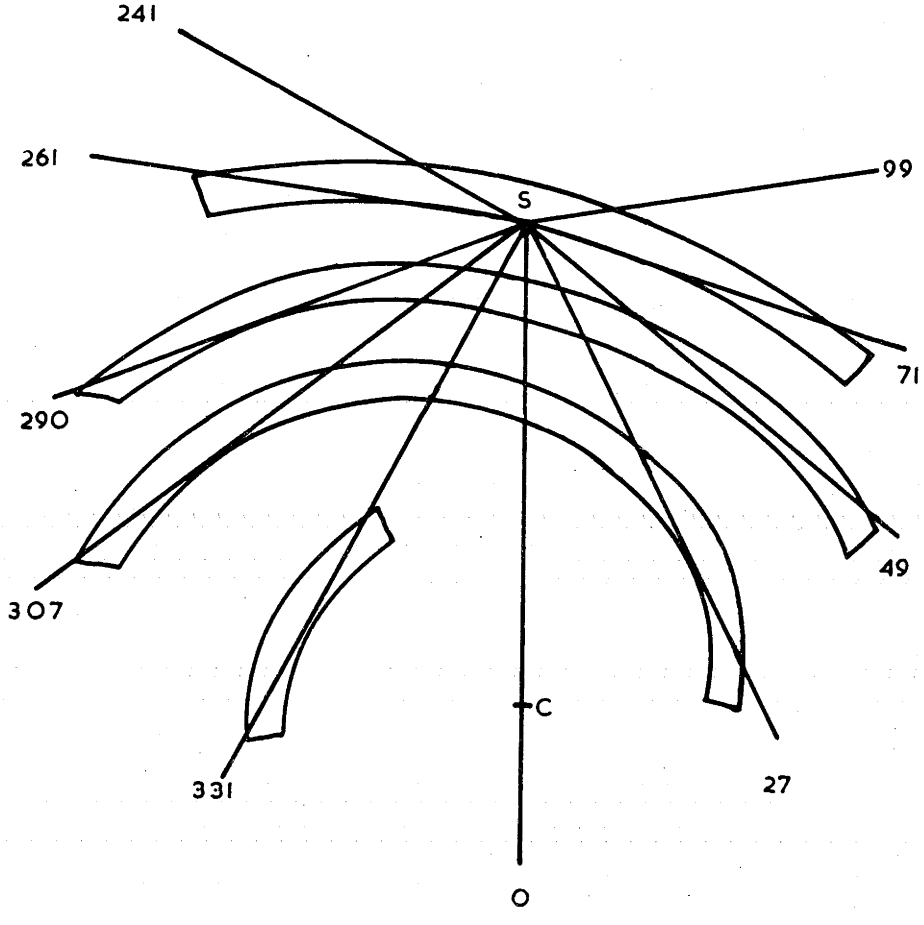

Fig.5. Structure from tangential directions of spiral arms (Elsasser and Haug).

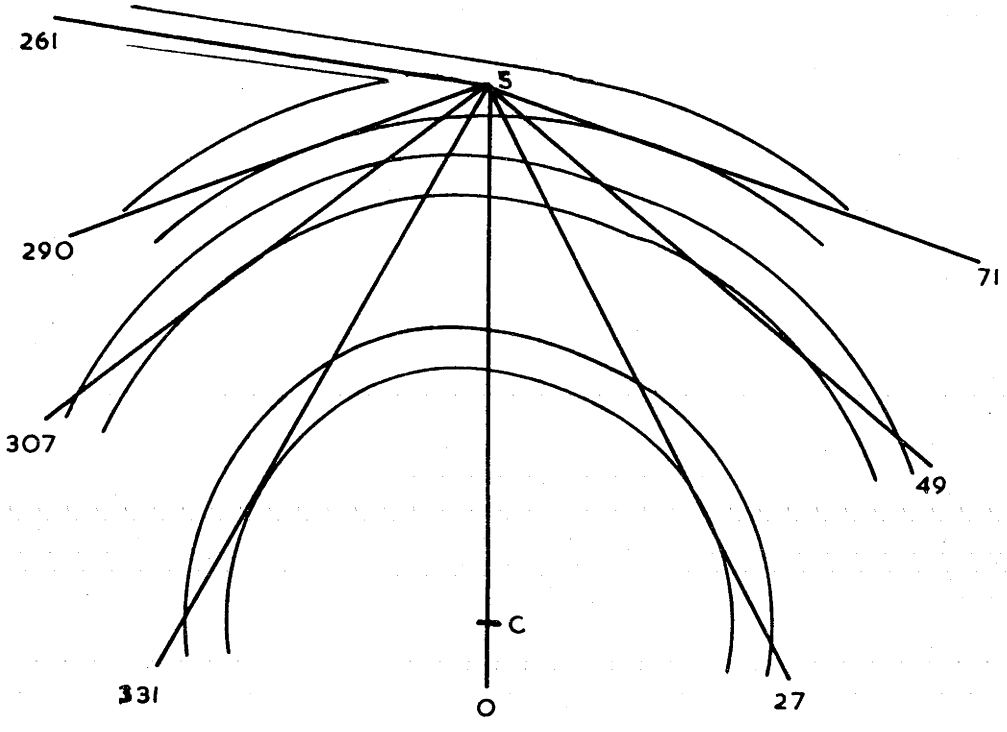

Fig.6. A modified version of fig.5 by adopting nearly circular arms.

the points were joined is open to criticism; Elsasser and Haug deliberately modified what could have been an interpretation of spiral arms more symmetrical about the direction towards the galactic centre to produce an asymmetrical picture conforming with the pattern of trailing arms. The spiral arms derived from 21 centimetre studies (to be discussed) are considerably more circular. If the tangential points were joined to preserve an almost circular representation of spiral arms, the results (fig.6) would be in better agreement with those derived from the distribution of neutral atomic hydrogen. A feature of the study is the existence of the Scutum-Norma Arm; some of the distant stars of early spectral type observed by Morgan, Whitford and Code may be located in this and not the Sagittarius Arm.

2. Spiral Structure from Radioastronomical Studies.

(d). Distribution of neutral atomic hydrogen.

The first evidence that the distribution of hydrogen gas showed spiral structure was detected by Christiansen and Hindman[1] in 1952. In a study of neutral hydrogen in several regions of the Milky Way, they observed the presence of multiple line profiles, caused by differences in the Doppler velocity shifts of the hydrogen line originating in separate concentrations of the gas in the line of sight.

A 21-cm study of spiral structure, assuming circular motion, was carried out by Van de Hulst, Muller and Oort[2] in 1954. They investigated the Milky Way between longitudes $l^{II} = 30^{o}$ and $l^{II} = 250^{o}$, but did not reduce the observations of regions nearer the galactic centre

(1) Christiansen,W.N. and Hindman,J.V., Aust.J.Sci.Rev., Ser.A, 5, 437, 1952.
(2) Van de Hulst,H.C., Muller,C.A. and Oort,J.H., B.A.N., 12, 117, 1954.

than the sun because of the ambiguity of the radial velocity-distance relationship. They detected a strong distant concentration at $l^{II} = 200^{o}$, presumed to be a possible continuation of the Perseus Arm.

Kerr, Hindman and Carpenter[1] in 1957 presented the first overall distribution of neutral atomic hydrogen (fig.7). For the outer regions of the northern part of the galaxy, they incorporated the distribution determined by Westerhout[2] on the basis of Schmidt's model of mass distribution for the conversion of radial velocities into distance. The distribution in the inner region is that derived by Schmidt[3] who used the extension of the gas in latitude to separate the contributions that have the same Doppler velocity but are located at different distances along the line of sight. On the southern side is represented a semi-qualitative pattern deduced from the velocities of the peak profile intensities.

The southern part shown in fig. 7 was later modified (Oort, Kerr and Westerhout[4]), the observations obtained at Sydney being reduced by a procedure similar to that used by the Leiden group, and on the basis of the same velocity - distance model (fig.8). A feature of the distribution is the apparent lack of hydrogen in the inner region of the southern side at distances of 6-8 kiloparsecs from the sun. It appears to be too heliocentric a feature to be a true representation, and it does not conform to the expected spiral pattern. Kerr[5] has concluded that it could be caused by the use of a velocity model that yields values which are too high

(1) Kerr,F.J.,Hindman,J.V. and Carpenter,M.S., Nature, 180 677, 1957.
(2) Westerhout,G., B.A.N., 13, 201, 1957.
(3) Schmidt,M., B.A.N., 13, 247, 1957.
(4) Oort,J.H., Kerr,F.J. and Westerhout,G., M.N.,118,379,1958.
(5) Kerr,F.J., private communication.

FIG.7 DISTRIBUTION OF HI IN THE GALACTIC PLANE.

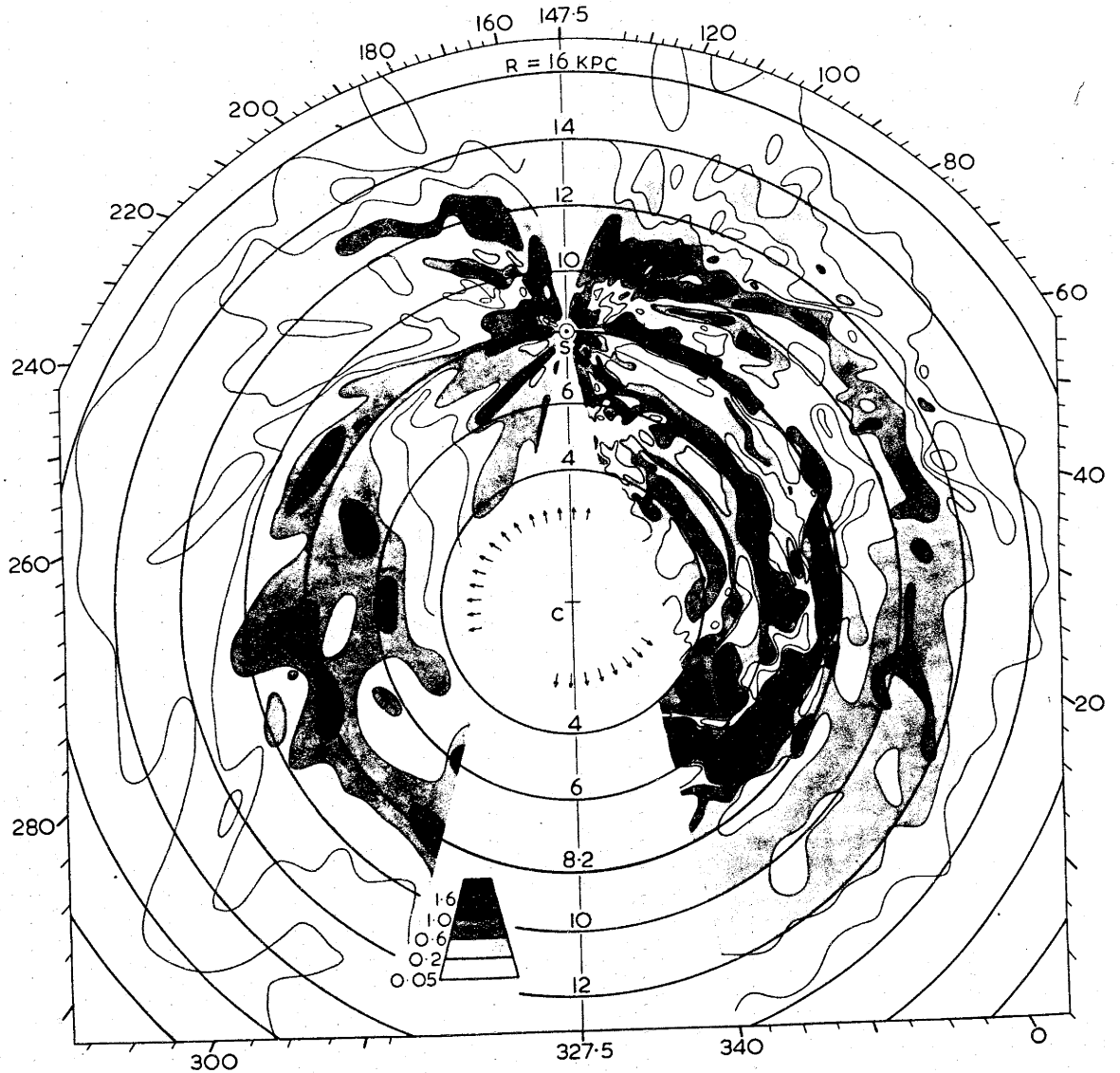

FIG. 8 Distribution of neutral hydrogen in the Galaxy, based on velocity model of BAN 475 (Unit = atom/cm^3.)

for the southern side of the galaxy; he suggested that the difficulty could be overcome by assuming that the local centre of rest and the gas at the sun's distance from the galactic centre are moving outwards with a velocity of 7 km/sec. The sun is too old to be taking part in the outward motion; as the X-component of the sun's velocity (the component with respect to the local standard of rest in the direction of the galactic centre) is 10.5 km/sec, the sun is in actual fact moving inwards. Postulating that the outward motion is a remnant of the large expansion velocities of the gas in the nuclear region of the galaxy (to be discussed), he adopted an inverse square law for the variation of velocity with distance from the galactic centre and constructed a further model (fig.9). It must be remembered that in reality, it is unlikely that the expansion is such a steady process. In the figure, several well-defined spiral arms can be traced over large ranges of longitude. The Perseus Arm extends from $l^{II} = 40^{o}$ to $l^{II} = 160^{o}$, at which point it is at a distance of 2500 parsecs from the sun; the maximum in the distribution at $l^{II} = 230^{o}$ may be a continuation of it. The Orion Arm is present at all the longitudes studied; in contrast to many optical models of spiral structure, it is almost circular. The presence of the Sagittarius Arm is shown by both the northern and southern observations. The apparent distribution of the gas near the sun, giving the impression that the three arms meet, may be due to the fact that near the direction of the galactic centre, the interpretation of the hydrogen-line profiles is difficult because the velocities of the random motions are comparable in size with those due to galactic rotation. The arms appear almost circular in contrast with those of

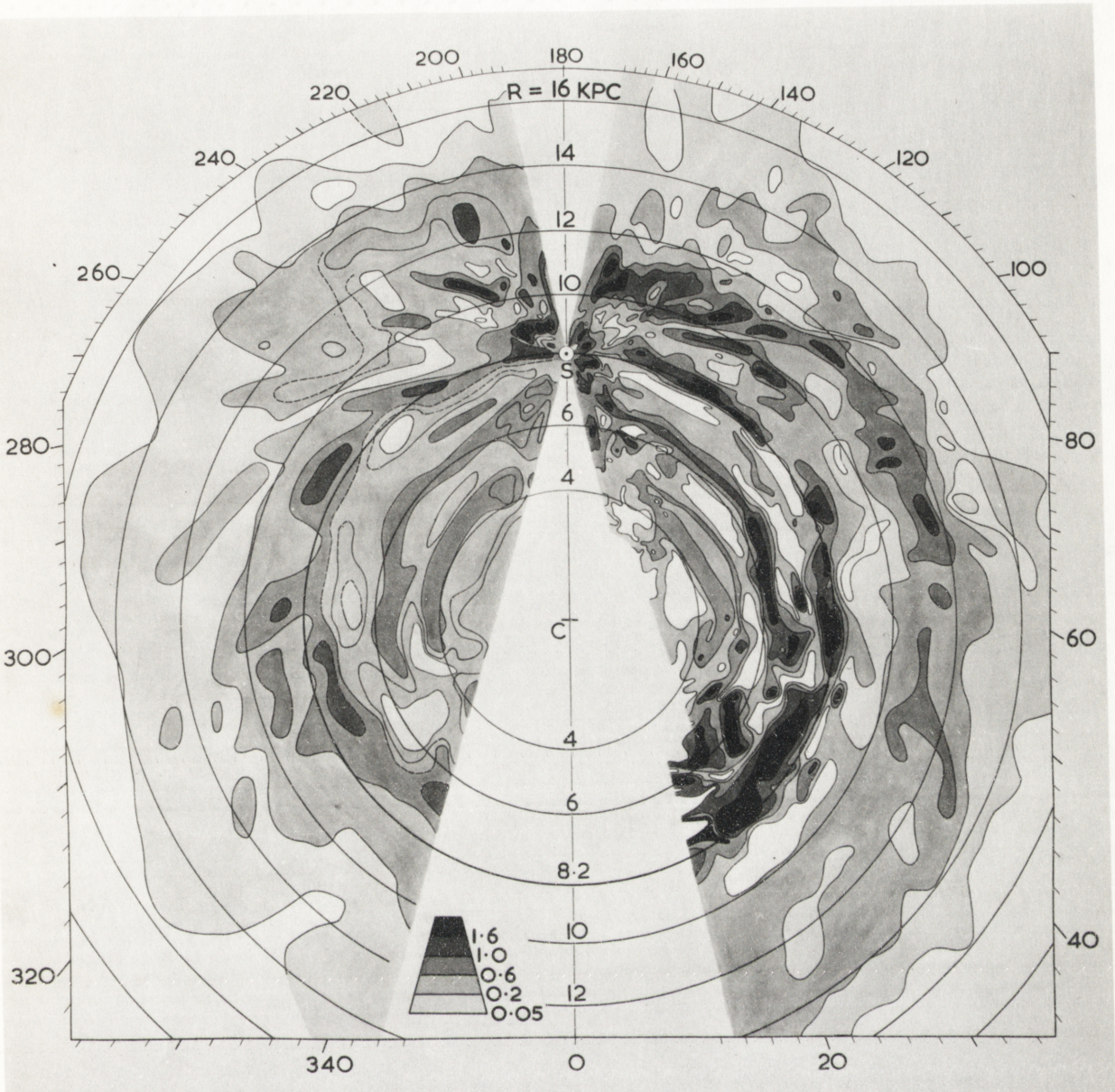

FIG.9 Distribution of neutral hydrogen in the Galaxy (unit-atom/cm^3)

based on a model involving both rotation and expansion

of most optical models. In fact, compared with those of other spiral galaxies, they seem a little too circular. According to de Vaucooleurs (unpublished), for spiral galaxies, the angle between an arm and a radius vector is approximately 72°; in Kerr's model, it is almost 90°.

In 1957, in a study of the hydrogen in the direction of the nuclear region of the galaxy, van Woerden, Rougoor and Oort[1] detected a prominent concentration (the 'expanding arm') expanding outwards at the rate of 53 km/sec. Previous evidence of it was shown by the presence of long faint wings in line profiles of the hydrogen situated within 25° of the direction of the galactic centre (Kwee, Muller and Westerhout[2]). The Australian radioastronomers observed it tangentially at $l^{II} = 338^{\circ}$, this corresponding to a distance of 3 kiloparsecs from the galactic centre.

(e) Spiral structure from radio continuum radiation.

In the distribution in longitude of the intensity of non-thermal radio emission at a wavelength of 3.5m (Mills, 1959[3]), there is a general diminution from a maximum in a direction near that of the galactic centre. At certain longitudes, there are distinct steps in the decrease; Mills inferred that in these directions, the line of sight is tangential to a spiral arm. He constructed a spiral structure pattern consisting of two equiangular spirals fitted as well as possible to the tangential directions (fig.10). The longitudes shown in the diagram are those at which the steps occur. The obtained fitting of the spirals to the specified lines of sight is surprisingly good; the diagram is a simplified version of the true structure, for in optical studies of galaxies, spiral arms can rarely be traced for more than one revolution.

(1) van Woerden,H.,Rougoor,W. and Oort,J.H., C.R. 244, 1691, 1957
(2) Kwee,K.K., Muller,C.A. and Westerhout,G.,B.A.N. 12, 211,1954.
(3) Mills,B.Y., P.A.S.P., 71, 267, 1959.

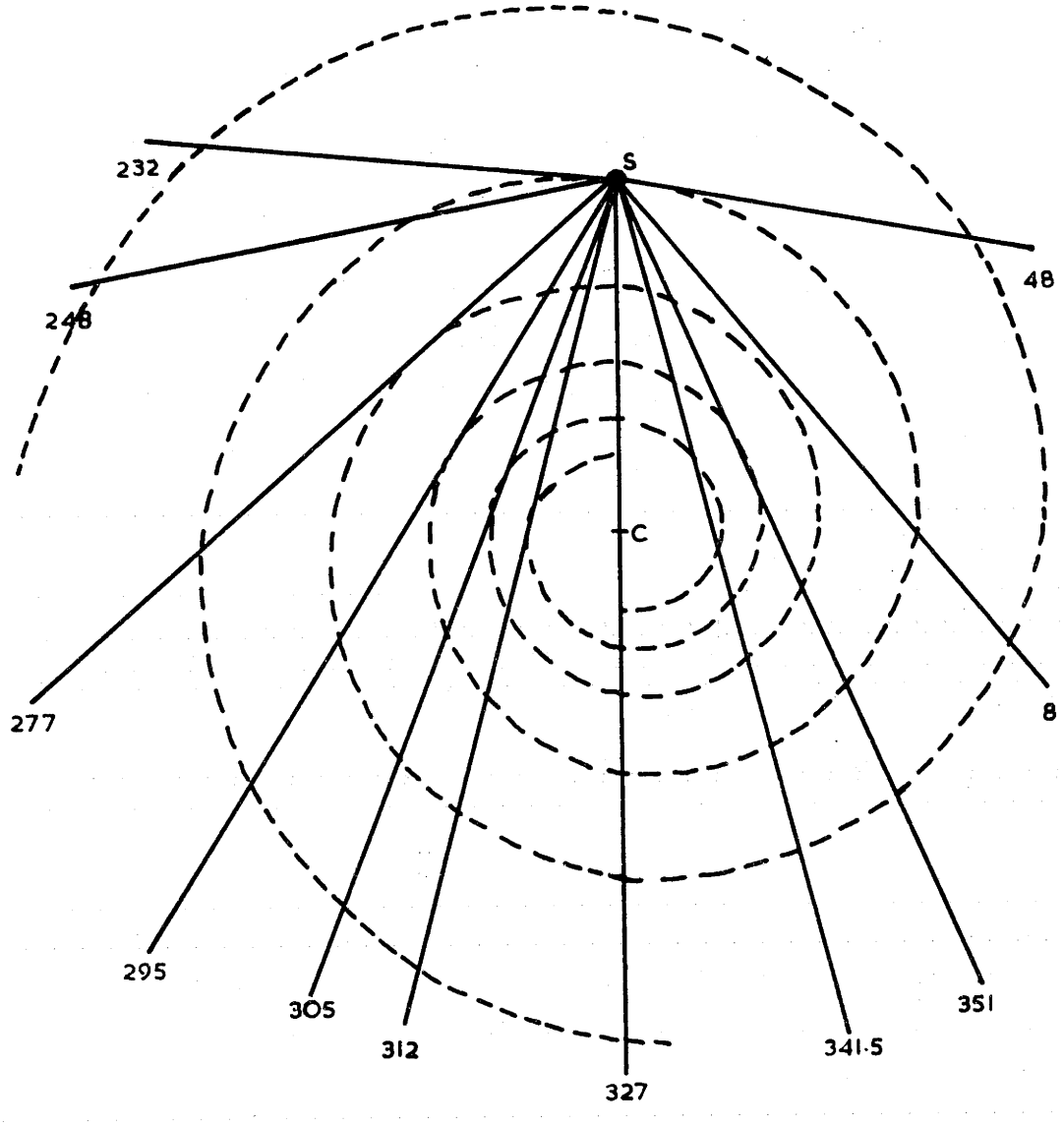

Fig.10. Galactic spiral pattern from radio continuum radiation.

In the figure, the Perseus Arm is situated at a minimum distance of 3500 parsecs from the sun, the sun is located in the Orion Arm, and the Sagittarius and Scutum-Norma Arms are 2000 parsecs and 4000 parsecs distant respectively in the direction of the galactic centre.

From a consideration of the models developed prior to 1959, Bok[1] proposed the existence of spiral arms that are more symmetrical about the direction of the galactic centre than suggested by the previous optical studies (fig.11). He accepted the presence of the Perseus Arm as formerly traced, but suggested that the optical representation of the Orion Arm should be replaced by another, the Carina-Cygnus Arm, with the sun located at its inner border. It contains several branches, the Orion Spur at $l^{II} = 203^{o}$, a spur parallel to this at $l^{II} = 217^{o}$, a distance of 500 parsecs from the arm, and a Vela Spur extending from it, near the sun, at a longitude $l^{II} = 288^{o}$. In it are included the spiral-tracing features in Carina. Thus Bok has interpreted more realistically the gap occurring between the longitudes $l^{II} = 300^{o}$ and $l^{II} = 330^{o}$ in the distribution of population I objects (present in the group of H II regions used by Gum), and demonstrated the importance of the Carina spiral tracers in the derivation of structure. The Orion and Vela Spurs are present also in the distribution of OB associations of Morgan, Whitford and Code. The Sagittarius Arm is at a distance of 2500 parsecs from the sun in the direction of the galactic centre, and parallel to the Carina-Cygnus Arm. The spiral arms suggested by Bok are similar to those in the distribution of neutral hydrogen, which might be expected since Bok's model was based in part on the latter.

(1) Bok, B.J., Obs., 79, 58, 1959.

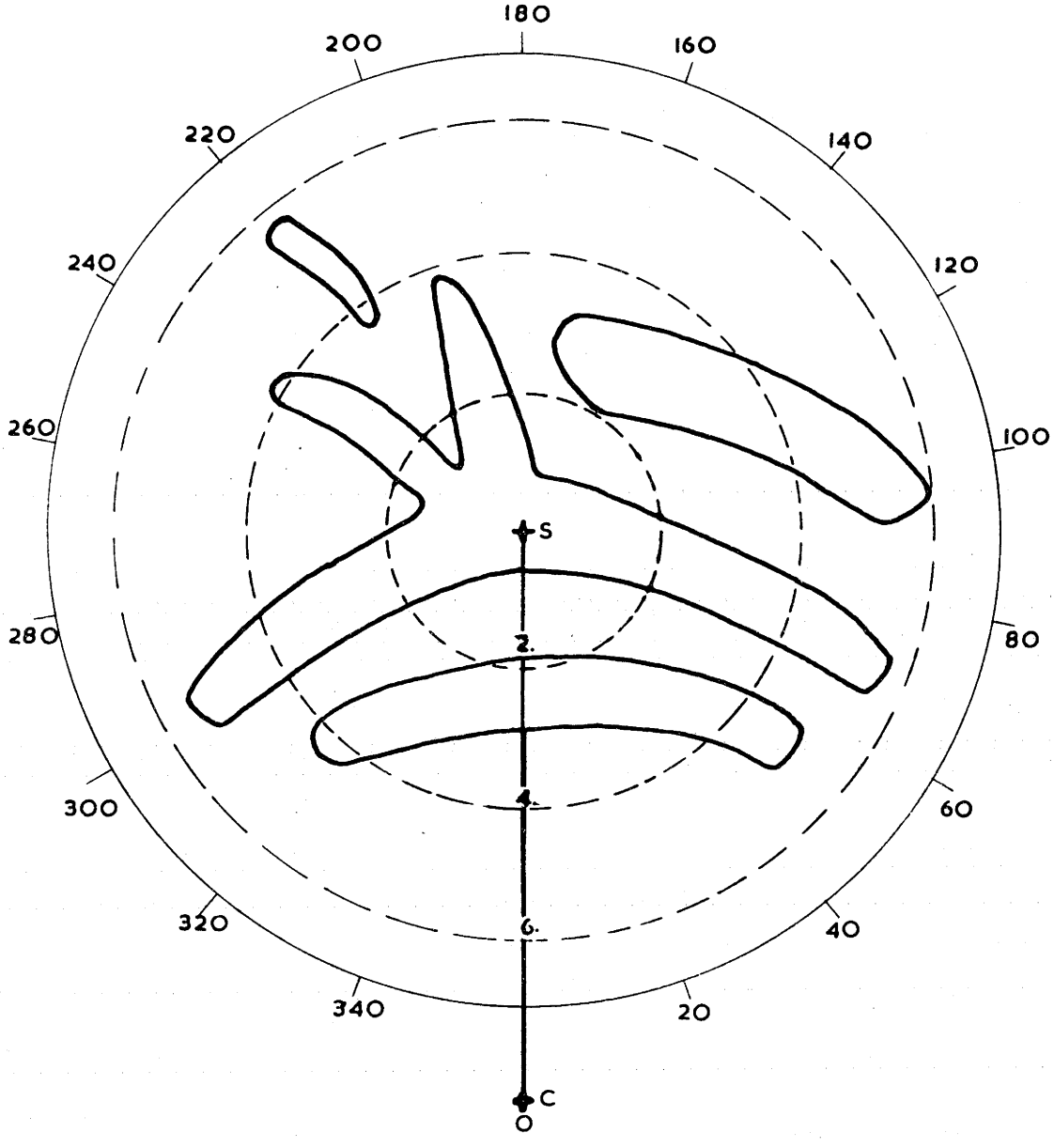

Fig.11. Bok's optical model of spiral structure.

1.2 Summary of the Models of Spiral Structure.

In a summary of the radio models, it is useful to compare the longitudes at which the tangential directions of the arms occur. Except for the model of Elsasser and Haug, such a comparison cannot be attempted in the case of optical diagrams, as the arms can be traced only for limited distances from the sun. In fig. 12, the tangential directions detected by Elsasser and Haug are compared with those of the arms of Kerr and Mills; there is reasonable agreement between the results obtained by the four observers.

In fig.13, the distribution of neutral atomic hydrogen with a density exceeding 0.6 atoms/cm^3 (Kerr) is compared with the positions of the associations of Morgan, Whitford and Code, and the arms of Elsasser and Haug. The spiral structure of Elsasser and Haug on the southern side of the galaxy has little in common with that of Kerr; on the northern side, there is quite good agreement. The majority of the associations are located within the HI arms; the location of those defining the Perseus Arm at the inner edge of the HI distribution, but not within it, could be due to the presence of dense obscuration at the distance of the gas. In the inner regions of the galaxy, there is little correlation between the distribution of associations and the arms of Elsasser's and Haug's model. A comparison between the model of Kerr, that of Bok, and the revised arms of Elsasser and Haug, is shown in fig.14. The agreement between the three is reasonably good. Bok's representation of the Sagittarius Arm is nearer the galactic centre than those of Kerr and Elsasser and Haug.

To summarize - in the vicinity of the sun, there appear to be four spiral arms with the following characteristics suggested by different astronomers:

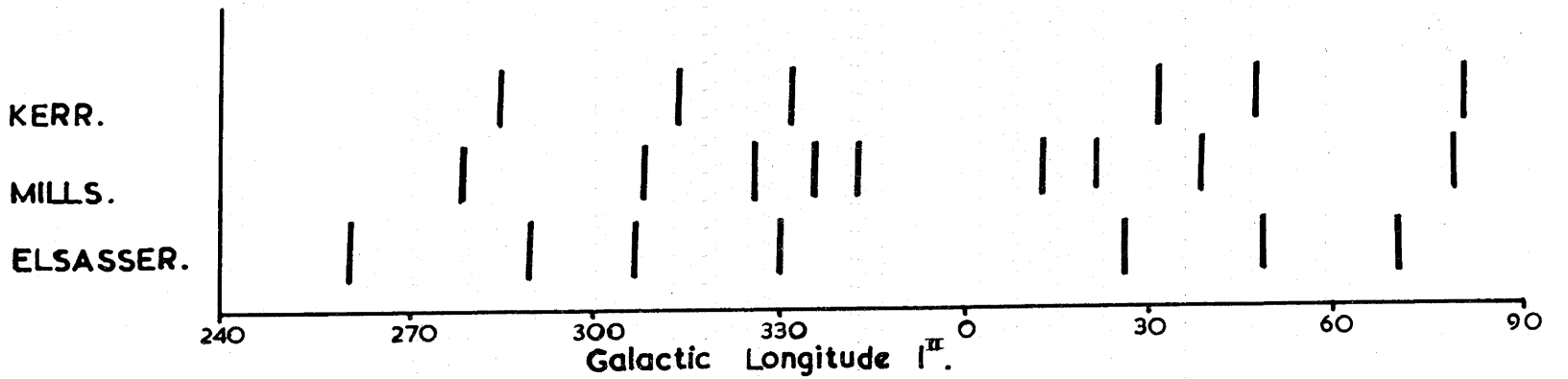

Fig.12. Tangential directions of spiral arms.

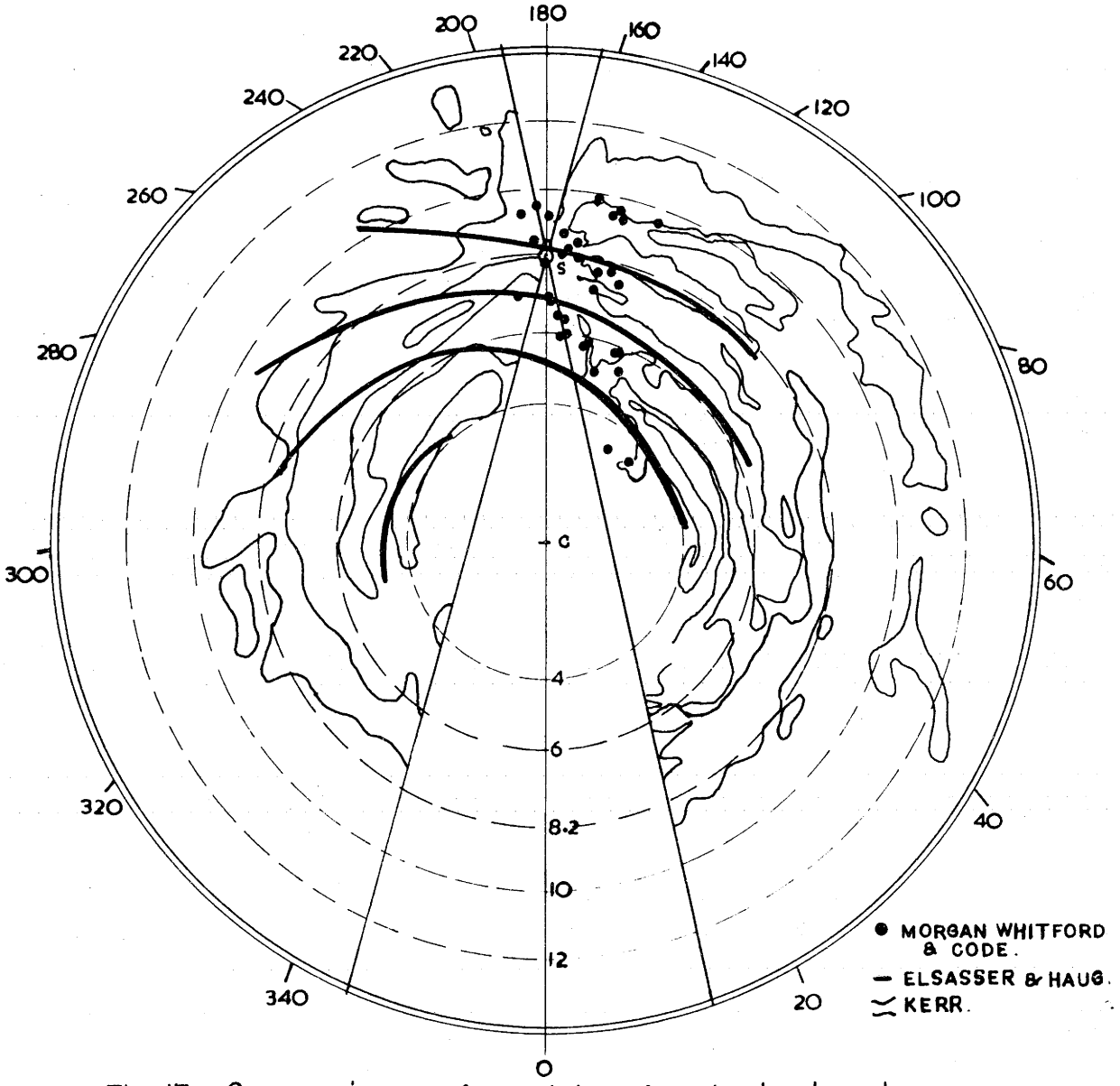

Fig.13. Comparison of models of spiral structure.

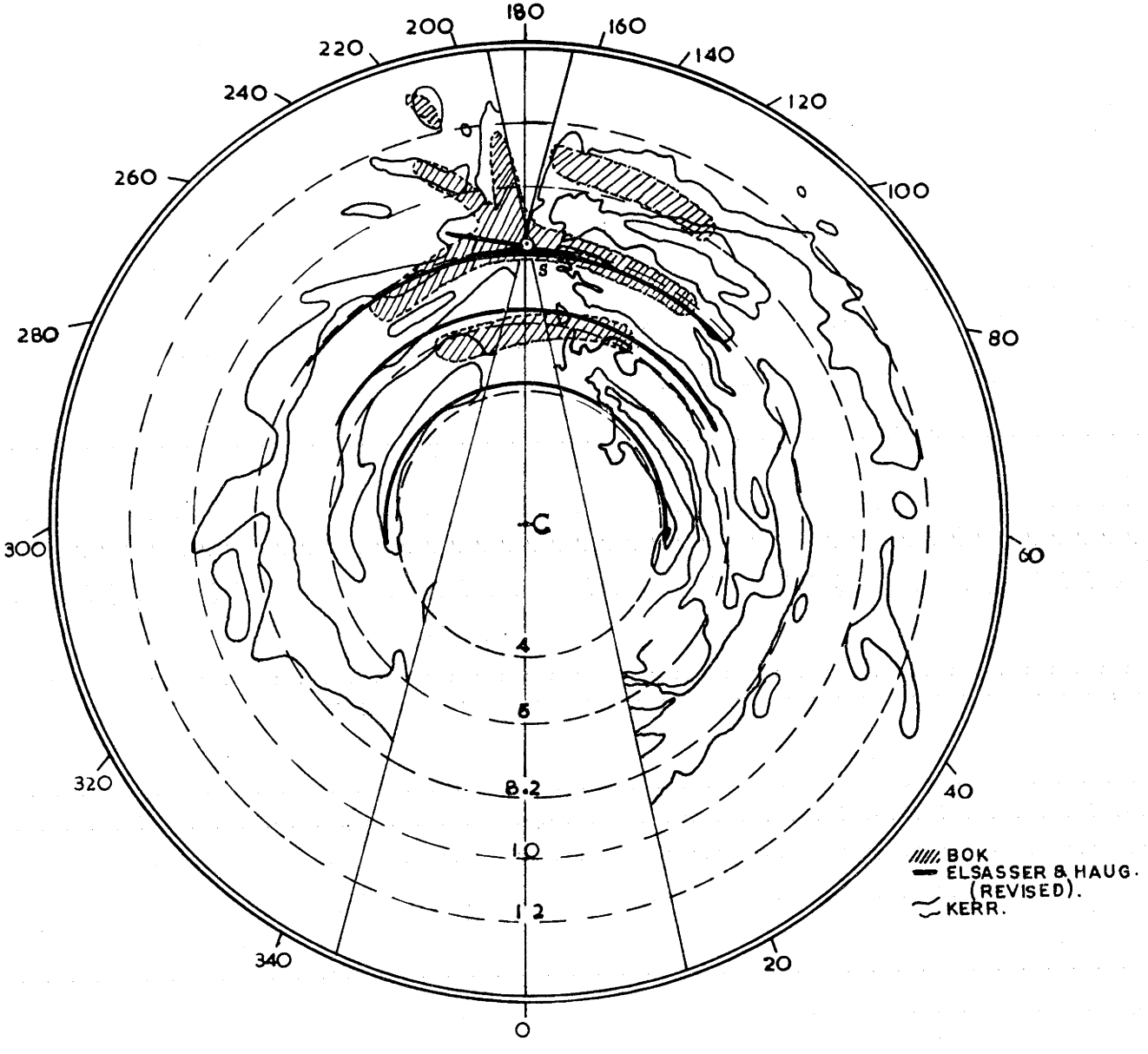

Fig.14. Comparison of models of spiral structure.

	Observer	Observed range of l^{II}	Min. dist from sun
Perseus Arm	M,S, and O	100°-140°	2300
	M,W and C	100°-170°	2500
	Munch	70°-180°	3000
	Hase	100°-150°	2200
	Kopylov	100°-200°	2500
	Bok	80°-130°	2200
	Kerr	40°-160°	2500
Orion Arm	M, S and O	70°-220°	300
	M,W and C	70°-210°	0
	Munch	70°-180°	400
	Hase	60°-210°	300
	Kopylov	60°-210°	0
	Bok	70°-300°	0
	Elsasser and Haug		0
	Kerr	15°-345°	0
Sagittarius Arm	M,S and O	285°-17°	1500
	M,W and C	335°-20°	1500
	Hase	0°-20°	0
	Gum	280°-10°	600
	Kopylov	280°-40°	1200;2000
	Bok	310°-50°	2500
	Elsasser and Haug		1800
	Kerr	30°-10°	1600
Scutum-Norma Arm	M.W and C	20°-40°	
	Thackeray	330°-30°	
	Kopylov	350°-20°	3200
	Elsasser		3800
	Kerr	330°-340°;20°-40°	3500

The data show that the best established arm is the

Perseus Arm, at a distance of approximately 2500 parsecs. The region of the Milky Way studied in this thesis is that in which are situated the last two arms mentioned. There is a great deal of uncertainty in their distances and directions in the optical models, and this is due to the fact that the Milky Way between longitudes $l^{II} = 290^{o}$ and $l^{II} = 350^{o}$ has been little studied. It appears more than likely that the Sagittarius Arm lies parallel to the Orion Arm rather than converging with it as in the models of Gum and Hase, and that the two arms are not as highly inclined as in the models of Morgan, Whitford and Code, and Kopylov.

The discussion would not be complete without an assessment of the limitations of the methods used to derive spiral structure. In the case of optical models constructed from the spatial distribution of early-type stars, the accuracy of the calculated distances depends on (a) the apparent magnitudes of the stars (b) their absolute magnitudes (c) the calculation of absorption affecting the stars' brightnesses. The greatest source of uncertainty is in (b) since the calibration, as a function of spectral type and luminosity class, is coarse for early type stars, has been altered considerably during the last decade, and is still not well-established, particularly for stars of high luminosity class. Therefore, a distribution of associations, where the distance of each is derived from the study of several members, is more accurate than that of H II regions, which may depend on the distances of single exciting stars. Such an approach minimises the adverse effects of the coarseness of the calibration. The distances to which spiral arms can be traced depend markedly on the presence of interstellar absorption and the ability to determine (b) observationally;

in general, the smaller the amount of absorption, the greater the distance at which stars can be observed. Studies of the multiplicity of interstellar absorption lines are also limited by galactic absorption. The method can predict, unambiguously, the presence of spiral arms, but the derived distances depend on the accuracy of the galactic rotation law. Investigations using the distribution of neutral hydrogen, unaffected by absorption, provide the only method of deriving the spiral structure of the whole galaxy. Based on the measurement of Doppler velocity shifts due to differential galactic rotation, the reduction procedure has many complications - the adoption of a relation between hydrogen density and temperature brightness, the relationship between distance and radial velocity, the ambiguity of the velocity-distance relationship in the inner part of the galaxy, and the corrections for the smoothing of profiles produced by instrumental effects and random velocities of gas clouds. Several of these apply to the derivation of distances from the observation of interstellar lines. In addition, the velocity-distance relationship is dependent on optical measurements; the hypothesis of Kerr, discussed previously, has yet to be proved. In view of the uncertainties, a more accurate representation of spiral structure would be obtained from a consideration of both optical and radio models, the former for the region of the galaxy near the sun, the latter for the more distant parts.

1.3 OB Associations.

Apart from the importance of associations in spiral structure, the study of their characteristics is of interest. The fact that O and B stars are located in groups near the galactic plane was observed by

Pannekoek[1] in 1929. The significance of the groupings was not fully realized until 1949, when Ambartsumian[2] proposed the existence of the Stellar Association. He defined it as a system of coeval stars with a space density much lower than that of the general galactic field in which it is situated. The term is usually applied to groups of O and B stars (OB associations), and irregular variable stars of the RW Aurigae type, one variety of which being T-Tauri stars (T associations). According to Ambartsumian, a unique feature of associations is that they have positive total energy and therefore are expanding, their members finally mixing with adjacent field stars. From estimated rates of expansion, he concluded that they are young stellar groups, a fact confirmed later by the calculated evolutionary ages of O and B stars. The existence of many associations in regions of interstellar matter and intense hydrogen emission where present star formation could be occurring also suggests their extreme youth.

The number of recognized associations has grown gradually during the last few years. The list of Morgan, Whitford and Code, published in 1953, contains 27. In 1958, Kopylov[3] carried out an investigation of 54 visual groups of stars of early spectral types, but pointed out that each was not necessarily an association, and could be composed of several spatial concentrations. One of the most comprehensive catalogues is that of Schmidt[4], containing 62 associations. In it are included the results of Morgan, Whitford and Code, Markarian[5],

(1) Pannekoek,A., Pub.Ast.Inst.Uni.Amst., No.2, 1929.
(2) Ambartsumian,V.A., A.J.U.S.S.R., 26, 3, 1949.
(3) Kopylov,I.M., A.J.U.S.S.R., 35, 390, 1958.
(4) Schmidt,Von K.H., A.N., 284, 76, 1957.
(5) Markarian,B.E., Dokl.Akad.Nauk.Armen.Sow.Repub., 15, 11, 1952.

and the groupings exhibited by the early-type stars observed by Hiltner[1]. His notation will be employed for the associations mentioned in the following pages. Between longitudes $l^{II} = 295^{o}$ and $l^{II} = 345^{o}$, the region studied in this thesis, only three associations are listed, viz. I Cru ($l^{II} = 294^{o}$ to $l^{II} = 309^{o}$), 1 Ara ($l^{II} = 336^{o}$ to $l^{II} = 342^{o}$), and I Sco ($l^{II} = 344^{o}$).

1.4 General Characteristics of Associations.

It was originally believed that OB associations consisted of stars only of spectral types O and early B, and that T associations contained only RW Aur type variables. In the case of the former groupings, particularly those that contain galactic clusters, there is evidence now that membership also includes stars of spectral types B3-B9 and A. The low space density of most associations impedes the detection of all but the most luminous members. In the vicinity of the association I Lac., Howard[2] detected a concentration of A stars, and suggested that it was due to the presence of stars of this type in the association. In studies of the cluster NGC 2264 and the association surrounding it (II Mon), Walker[3] observed a main sequence extending to stars of spectral type AO. In the HR diagram of the group, fainter members, which included T-Tauri stars, were situated above the main sequence. The presence of a main sequence extending to A5, and T-Tauri stars, was detected by Johnson[4] in the Orion association. An explanation for the sudden termination of a main sequence at its fainter end as a consequence of the effects of star formation was advanced by Henyey, Le Levier and Levee[5] in 1955. Their results show that while the

(1) Hiltner,W.A., Ap.J. Supp., 2, 389, 1956.
(2) Howard,W.E., Doctoral Thesis, Harvard Uni., 1958.
(3) Walker, M.F., Ap.J. Supp., 2, 365, 1956.
(4) Johnson,H.L., Ap.J., 126, 134, 1957.
(5) Henyey,L.G.,Le Levier,R. and Levee,R.D.,P.A.S.P.,67,154, 1955.

protostar is contracting gravitationally, before the commencement of thermonuclear processes, it remains off the main sequence, moving onto it only after the beginning of the hydrogen-burning stage. The more massive the star, the more rapidly will it proceed through the contraction stage. Therefore, at its low luminosity end, a cluster main sequence will terminate with stars in which the thermonuclear processes have just begun. As mentioned, this phenomenon has been detected observationally, although the reality of its existence in the clusters NGC 2264 and NGC 6530 has been criticized by Underhill[1] and The[2] respectively. Calculations of the dependence of the rate of gravitational contraction on stellar mass thus will provide an estimate of the age of the group of stars. Since T-Tauri stars are located amongst the group above the position on the main sequence characteristic of stars of their mass, one may deduce that they are still contracting gravitationally. A similar conclusion is suggested by their association with dense clouds of dust and interstellar gas where star formation still might be occurring.

If the suppositions are correct, one would expect all associations to contain T-Tauri stars if star formation is still taking place, and that there should be no real distinction between T-associations and OB associations other than that of age, i.e. the former are so young that no main sequence stars are present in them. Kholopov[3] has stated that all the associations near the sun, I Ori, S Mon, II Per, Cas-Tau, I Sag, and II Sco (if it is related to the dark nebula around the star Rho Oph) contain T-Tauri stars. According to him, the absolute magnitudes

(1) Underhill,A.B., Ap.J., 131, 526, 1960.
(2) The,P.S., Ap.J., 132, 40, 1960.
(3) Kholopov,P.N., A.J.U.S.S.R., 35, 434, 1958.

of RW type variables range from Mv = -5 to Mv = +10.5 for B-V = -0.3 to B-V = 1.8. The variable stars present in OB associations generally have absolute magnitudes fainter than Mv = +3, and the detection of them is difficult because of their low luminosities, although T- Tauri stars can be identified in objective prism spectral surveys on the basis of their hydrogen emission lines. As some associations are not surrounded by dense regions of gas and interstellar material, T-Tauri stars may not be present.

Supergiant stars and occasionally Wolf-Rayet stars are present in large associations. The supergiants of the association I Per are of spectral type M (Blanco[1], 1955); those of I Ori, an older group, are of types BO-B1. Several Wolf-Rayet stars have been observed in the association I Sco (Houck[2], 1956); Whether they are the most luminous main sequence stars of very young associations or evolved stars is uncertain.

The luminosity functions of associations derived from the brightest members are in general agreement with those of Sandage[3], Salpeter[4], Van Den Bergh[5] and Limber[6].

Many associations, e.g. I Sco (Houck, 1956), II Ori (Wade[7], 1957), I Ori (Menon[8], 1958), are situated in regions of dense clouds of dust, neutral and ionized hydrogen gas. In a study of 21cm radiation in the vicinity of several galactic clusters, Drake[9] found a relationship between the ratio of hydrogen mass to stellar

(1) Blanco,V.M., Ap.J., 122, 434, 1955.
(2) Houck,T.E., Doctoral Thesis, Uni.Wisc., 1956.
(3) Sandage,A., Ap.J., 126, 326, 1957.
(4) Salpeter,E.E., Ap.J., 125, 445, 1957.
(5) Van Den Bergh,S., Ap.J., 125, 445, 1957.
(6) Limber,D.N., Ap.J., 131, 168, 1960.
(7) Wade,C.M., Doctoral Thesis, Harvard Univ., 1957.
(8) Menon,T.K., Ap.J., 127, 28, 1958.
(9) Drake,F.D., Doctoral Thesis, Harvard Univ., 1958.

mass and the age of stellar grouping. The youngest clusters contained the greatest percentage of the gas. Dieter[1] has detected good correlations between the positions on the celestial sphere of associations and hydrogen gas with similar velocities. The value of the results depends on the validity of the assumptions that hydrogen is associated with a star group if it has a similar radial velocity, and that at a particular longitude, all gas with the same velocity is spatially concentrated. In a study of the association I Ori, Menon detected the presence of a slowly expanding sphere of neutral hydrogen surrounding the stars.

In most of the extensive studies of association-gas correlations, the position of the hydrogen relative to the stars is not that expected from the prevailing theories of formation of associations (Opik[2], Oort and Spitzer[3], and Bierman and Schluter[4]). In these, star formation occurs as a consequence of the compression of interstellar gas (by supernovae explosions according to Opik, by radiation pressure from O stars according to the other authors), which is expanding at the time that protostars are formed. As the velocities of stars and gas, initially the same, are diminished by encounters with field stars and interstellar matter, that of the gas decreasing more rapidly, an association should consist of a group of expanding stars at the centre of which is situated the parent interstellar matter. However, if radiation pressure is still present, the motion of the gas will be less affected by field encounters and as for I Sco and I Ori, the parent gas will be outside the

(1) Dieter,N.H., Ap.J., 132, 49, 1960.
(2) Opik,E.J., Irish A.J., 2, 219, 1952.
(3) Oort,J.H. and Spitzer,L., Ap.J., 121, 6, 1955.
(4) Bierman,L. and Schluter,A., Z.F. Naturf., 9a, 463, 1954.

association.

The presence of internal expansion in associations has not been proved conclusively. That it exists was suggested first by Blaauw[1] in a study of the proper motions of the stars of the association II Per; he detected the presence of systematic variations of the components of the proper motions in right ascension and declination with changes in these coordinates. Assuming uniform expansion from a region of relatively small size, he derived an expansion age of 1.3×10^6 years, and a velocity of expansion of 12 km.sec. From similar studies, the ages of the associations II Sco, II Sco, II Cep, and I Lac were determined to be 76×10^6 years (Blaauw), 2.8×10^6 years (Shteins and Abele[2], 1958), and 4.2×10^6 years (Blaauw and Morgan[3], 1953) respectively.

In a criticism of these results, Woolley and Eggen[4] have suggested that the expansion effect is due to systematic errors in the determinations of proper motions; they studied a group of field stars near I Lac and detected an apparent expansion similar to that present in the association. They could detect no expansion from a study of the radial velocity-distance relationship of members of the association. Kopylov[5] reached a similar conclusion from the investigation of proper motions of early-type stars occurring in several visual OB groupings, and concluded that there is no certain evidence of expansion.

The dimensions of associations vary considerably -

(1) Blaauw,A., B.A.N., 11, 405, 414, 1952.
(2) Shteins,K.A. and Abele,M.K.,A.J.U.S.S.R., 35, 70, 1958.
(3) Blaauw,A. and Morgan,W.W., Ap.J., 117, 73, 1953.
(4) Woolley,R.V.D.R. and Eggen,O., Obs., 78, 149, 1958.
(5) Kopylov,I.M., A.J.U.S.S.R., 35, 390, 1958.

according to Howard, they range from several to 170 parsecs. Most are ellipsoidal in shape, with their major axes orientated along the spiral arm in which they are situated. Typical dimensions of associations are - II Per - 40 x 25 parsecs (Blaauw and Morgan, 1953), II Sco - 290 x 100 parsecs (Blaauw, 1952), I Ori - 190 x 190 parsecs (Sharpless[1], 1952). I Lac - 120 x 70 parsecs (Blaauw and Morgan, 1953), I Gem - 120 x 120 parsecs (Crawford et al.,[2] 1955), and III Cep - 50 x 30 parsecs (Blaauw, Hiltner and Johnson[3], 1959).

The ages of associations are usually between 10^6 and 10^7 years. The most common method used in their determination is that based on the period that a star of a certain mass remains near the main sequence. Initial calculations of this time, based on homologous star models, were carried out by Schoenberg and Chandrasekhar[4]; more recent determinations are based on the theory arising from the studies of separate models of differing mass (Limber[5], 1960). The maximum age of a group of coeval stars is equivalent to the time that the brightest of them remains near the main sequence; the brighter the star, the sooner it becomes a giant or supergiant. Ages of associations determined by this method are: I Lac - 4.2×10^6 years (Harris[6], 1955), I Ori - 3×10^6 years (Johnson, 1957), and II Per - 4.7×10^6 years (Seyfert, Hardie and Grenchik[7], 1960). They are of the same order of magnitude as expansion ages,

(1) Sharpless,F., Ap.J., 116, 251, 1952.
(2) Crawford,D., Limber,D.N., Mendoza,E., Schulte,V.D., Steinman,H. and Swihart,T., Ap.J., 121, 24, 1955.
(3) Blaauw,A., Hiltner,W.A. and Johnson,H.L., Ap.J., 130, 69, 1959.
(4) Schoenberg,M. and Chandrasekhar,S., Ap.J., 96, 161, 1942.
(5) Limber,D.N., Ap.J., 131, 168, 1960.
(6) Harris,D.L., Ap.J., 121, 554, 1955.
(7) Seyfert,C.K., Hardie,R.H. and Grenchik,R.T., Ap.J., 132, 58, 1960.

in spite of the fact that expansion may not be real.

In a study of the mean radial velocities of 27 associations, Pismis[1] showed that after correcting for the effects of circular motion, residual values were present; they could be interpreted only as being due to expansion of the arms in which the star groups are located. The mean value of the expansion velocities is 3-4 km/sec. A more detailed investigation is needed to confirm this result, for in the study effected by Pismis, very few associations were used - only four between longitudes $l^{II} = 180^{o}$ and $l^{II} = 0^{o}$. The importance of this analysis lies in the fact that it shows an effect similar to that postulated by Kerr.

(1) Pismis,P., Ton.Bol., 19, 3, 1960.

CHAPTER 2

H-ALPHA EMISSION IN THE SOUTHERN MILKY WAY.

2.1 Introduction

It has been known for many years that hydrogen is an important constituent of our galaxy. Much of it is in the form of neutral atomic hydrogen, the distribution of which has been studied extensively by the observation of the radiation it emits with a wavelength of 21cm. The hydrogen in the neighbourhood of stars of early spectral types is ionized, and the energy radiated with the wavelengths of the Balmer series as a result of recombination can be detected optically. A means of detecting the presence of molecular hydrogen has yet to be found.

The pioneer work in the investigation of the regions of the sky in which ionized hydrogen is present (emission regions) was carried out between the years 1937 and 1939 by Struve and Elvey[1], and Greenstein and Henyey[2], at the Yerkes and McDonald Observatories. They used specially-designed spectrographs for the purpose. The work was later continued by Page[3] and Johnson[4].

Stromgren[5] in 1939 investigated theoretically the physical state of ionized interstellar hydrogen. He concluded that Balmer-line radiation is emitted by sharply bounded areas, which he termed HII regions, that surround stars of early spectral types. He expressed the radius of a region as a function of its electron temperature and

(1) Struve, O. and Elvey, C.T., Ap.J.,86,94,613,1937.
Ap.J.,88,364,1938.
Ap.J.,89,517,1939.

(2) Greenstein,J.L. and Henyey,L.G., Ap.J.,86,620,1937.
Ap.J.,87,79,1938.

(3) Page,T., Ap.J.,108.157,1948.

(4) Johnson,H.M., Ap.J.,118,162,970,1953.

(5) Stromgren,B., Ap.J.,89,526,1939.
Ap.J.,108,242,1948.

electron density, and the radius and surface temperature of the exciting star. However, in his calculations, he assumed that the effect of the Lyman continuum radiation scattered by the gas cloud was negligible, and that the optical depth of the Lyman continuum was independent of frequency. More elaborate calculations carried out by Jeffries and Pottasch[1] showed that the assumptions were invalid and that Stromgren's calculated radii were too small by factors of up to 10 in the case of ionized shells of gas, depending on the values of electron density, surface temperature etc. used (Pottasch[2]). Munch[3] recently criticized the calculations on the grounds that for the inner boundary condition of an ionized shell, Pottasch and Jeffries used the vanishing of the diffuse radiation field, whilst the correct condition should be the vanishing of the flux of the diffuse radiation in the inner volume enclosed by the shell. A smaller radius is derived when this modification is considered.

Struve[4] was one of the first observers to photograph H II regions in the light of one of the wavelengths of the radiation they emit; he employed a filter-photographic emulsion combination with an effective wavelength near H-alpha. This method is now used commonly for the detection and study of emission nebulae. Catalogues of H II regions for various sections of the Milky Way have been published by Cederblad[5], Minkowski[6], Strohmeier[7],

(1) Jeffries,J.T. and Pottasch,S.R., Ann.D'Ap.,22,318,1959.
(2) Pottasch,S.R., Ap.J.,132,269,1960.
(3) Munch,G., A.J.,65,495,1960.
(4) Struve,O., Ap.J.,86, 94,1937.
(5) Cederblad,S., Lund.Medd.Ser.II,No.119, 1946.
(6) Minkowski,R., P.A.S.P.,58,305,1946.
P.A.S.P.,59,257,1947.
(7) Strohmeier,W., Zs.F.Ap.,27,49,1950.

Courtes[1], Sharpless and Osterbrock[2], Hase and Shajn[3], Gum[4], Bok, Bester and Wade[5], Johnson[6] and Sharpless[7]. The details of each survey, compiled mostly by Sharpless, are shown in the following table. The columns are:

(1) Author or authors of the catalogue.
(2) Effective aperture of the camera.
(3) F-ratio of the camera.
(4) The type of H-alpha filter used - glass absorption, or interference type.
(5) The spectral region in which is situated the effective wavelength of the comparison filter-emulsion combination.
(6) The range of the survey in new galactic longitude, l^{II}.
(7) The number of H II regions detected in the survey.

Observer.	Eff.Ap.	F-ratio.	H-alpha	Comp.	l^{II} range.	No.
Cederblad (1946)					0-360	215
Strohmeier (1950)	3".9	1.5 1.2	Absn.	Blue	183-233	42
Courtes (1951)	2".2	1.4	Int.	Red		
Sharpless & Osterbrock (1952)	0".1	2.0	Absn.	Blue	356-225	16
Sharpless (1953)	48".0	2.44	Absn.	Blue	348-138	142
Bok,Bester, Wade. (1955)	3".0	1.5	Int.	Red	283-28	41
Johnson (1955)	6".3 5".7	1.2 1.35	Absn. Int.	Red I.Red	336-238	152
Hase & Shajn (1955)	17".7	1.4	Absn.	Blue	353-228	286
Gum (1955)	4".0 2".4	1.0 1.7	Absn.	Green	223-23	85
Sharpless (1959)	48".0	2.44	Absn.	Blue	North of dec.-27°.	313

(1) Courtes,G., C.R.,232,795,1283,1951.
(2) Sharpless,S. and Osterbrock,D.E., Ap.J.,115,89,1952.
(3) Hase,V.F. and Shajn,G.A., Bull.Crim.Ast.Obs.,15,11,1955.
(4) Gum,C.S., Mem.R.A.S.,67,155,1955.
(5) Bok,B.J.,Bester,M.J. and Wade,C.M.,Proc.Am.Acad.Arts & Sci., 86,9,1955.
(6) Johnson,H.M., Ap.J.,121,604,1955.
(7) Sharpless,S., Ap.J.,118,362,1953. Ap.J.,Supp.,4,257,1959.

The surveys in which a considerable region of the Southern Milky Way is studied will be discussed later in more detail. The table above shows that most of the surveys are of the Northern Milky Way.

2.2 A Survey of H II Regions in the Southern Milky Way.

The survey carried out to study the H II regions present in the Southern Milky Way consists of two parts:

(a) The detection and cataloguing of Southern H II regions (Rodgers, Campbell and Whiteoak, 1960[1]).

(b) The construction of an atlas consisting of photographs taken in H-alpha light of the Southern Milky Way, to show the regions pictorially (Rodgers, Campbell, Whiteoak, Bailey, and Hunt, 1960[2]).

It covers a region of sky 182° in longitude, extending from $l^{I} = 190^{\circ}$ ($l^{II} = 223^{\circ}$) to $l^{I} = 12^{\circ}$ ($l^{II} = 44^{\circ}$). Centred on the old galactic equator, it has a maximum width of 30°.

1. Equipment.

(a). Camera.

The regions of sky in the survey were photographed with an 8-inch f/1 flat-field Meinel-Pearson Schmidt camera, similar to that described by Meinel[3]. It was attached as a counterweight to the 6-inch Farnham refractor, the refractor being used for guiding during exposures. The diameter of the coma-free field of the camera is approximately 12°. The scale, determined by Johnson[4], is (1.08-0,01r)"/micron, where r is the distance from the

(1) Rodgers,A.W.,Campbell,C.T. & Whiteoak,J.B.,M.N.,121,103, 1960.
(2) Rodgers,A.W.,Campbell,C.T.,Whiteoak,J.B.,Bailey,H.H. and Hunt,V.O., 'An Atlas of H-alpha emission in the Southern Milky Way.' 1960.
(3) Meinel,A.B., Mitt.Sternw.Hamburg-Bergedorf,23,No.255,1956.
(4) Johnson,H.M., Mem.Mt.Stromlo Obs., No.15, 1960.

optical axis in degrees; for r greater than $5^{\circ}.7$, the formula breaks down, as does the quality of the stellar images. The resolving power of the camera in the red spectral region is about 17 microns.

A total of 78 different centres was required to cover completely the area of sky surveyed. It is composed of sets situated at $b^{I} = -9^{\circ}$, $b^{I} = 0^{\circ}$ and $b^{I} = +9^{\circ}$, of 26 field centres spaced 7° apart in galactic longitude. The observing program was arranged in two parts. In 1958, fields centred on the galactic equator were photographed. Later, plates were obtained of fields centred at $b^{I} = +9^{\circ}$ and $b^{I} = -9^{\circ}$ and at longitudes corresponding to those of the first set of observations. The planning proved to be unfortunate, for during the construction of mosaics, it was often difficult to match satisfactorily the prints of the fields photographed in the first part of the program with those acquired in the second group of observations. Whenever re-observation became necessary, plates of all the 18 fields of one mosaic were obtained on the same night.

2. Filters and Photographic Emulsions.

As in other surveys, to detect H-alpha emission, plates obtained by the use of a combination of filter and photographic emulsion that has a passband centred on H-alpha were compared with those derived from a combination the passband of which is centred on the nearby continuum and which transmits little H-alpha. The combinations, their effective wavelengths, and equivalent widths determined by Johnson, are shown in the following table:

Combination		Effective Wavelength	Equiv. Width
H-alpha	8mm OR1 + 103a-E	6560 A	326 A
Comparison	5mm OY1 + 103a-D	6070 A	495 A

As both of the filters are 8.25 inches in diameter, the camera was used at full aperture. At the wavelengths of 6300 A and 6364 A, those of the prominent night-sky lines of (OI), the transmission of the OR1 filter is less than 2%. Besides H-alpha, the filter also transmits the less prominent nebular spectral lines of NII (6548A, 6583A) and SII (6716A,6731A). The comparison combination transmits the nebular emission of HeI (5876A), but its intensity is only approximately 5% of the total intensity of the radiations near and including H-alpha (Aller and Liller[1]). The smallest images on the plates were greater than the 17 microns mentioned previously as the resolving power of the camera, due to the effect of the coarse grain of the 103a emulsions. To avoid noticeable sky fog on the plates, exposures were limited to a duration of 20 minutes and 7 minutes for the H-alpha and comparison combinations respectively. With these exposure times, a limiting stellar magnitude of $14\frac{1}{2}$ was attained.

3. Detection of H-alpha Emission.

Emission regions were detected by the comparison on a Grubb-Parsons Blink Comparator of H-alpha and comparison plates of each field photographed. The boundaries of extended emission of low surface brightness were estimated by visual comparison. Detection by the 'blinking' technique was found to be preferable to the 'negative-positive superposition' method of Gum[2], where the glass negative of the comparison plate is superposed on a positive transparency of the H-alpha plate, and the combination printed. The print shows regions of emission as dark areas against a grey background of cancelled-out star

(1) Aller, L.H. and Liller, W., Ap.J., 130, 45, 1959.
(2) Gum, C.S., Obs., 73, 123, 1953.

images. The advantage of the technique is that a permanent record of the detected H II regions is produced. However, the method of 'blinking' is much simpler, more rapid, and no resolution is lost by photographic copying processes. The exact nature of the emission is shown in the atlas, to be described later. Detection of H-alpha emission of low surface brightness was difficult in parts of the sky where both it and the star fields are bounded by absorption.

4. Catalogue of H II Regions.

As each field was blinked, the positions and dimensions of detected H II regions were noted. A catalogue of the 182 detected is shown in tables 1 and 2. The first table contains definite regions, the dimensions of which are greater than 4 minutes of arc. In table 2 are listed objects, of smaller dimensions, that are bright on H-alpha plates. It may include stellar or semi-stellar objects such as emission-line B stars, planetary nebulae, Wolf-Rayet and variable stars. Variable stars listed in the Russian Variable Star Catalogue[1], and those identified from an inspection of plates of a field that were obtained on different nights, have been omitted. The columns of the tables are:

(1) The current catalogue number.
(2) The new galactic longitude (l^{II}) of the estimated centre of each region.
(3) The new galactic latitude (b^{II}) of each centre.
(4) The right ascension for the epoch 1950.
(5) The declination of the epoch 1950.
(6) The approximate dimensions of the regions in minutes of arc.
(7) The assigned numbers of the regions according to other catalogues.

(1) Kukarkin,B.V.,Parenago,P.P.,Efremov,Y.I.and Kholopov,P.N., General Catalogue of Variable Stars,2nd Edition, 1958.

TABLE 1

Table of H II regions greater than 4' diam.

No.	l^{II}	b^{II}	R.A.1950	Dec.1950	Size (min of arc)	Comparison.
1	223.0	-1.5	07^h02	$-09^\circ30$	150X150	NGC2327,
	226.9	+0.3	07 14	-12 24		G2,3;HS111,113,114;E296.
2	223.8	-1.9	07 02	-10 27	14X14	IC2177;G1;HS109.
4	224.4	+3.2	07 21.5	-08 30	60X60	
5	227.8	-0.2	07 16.1	-13 09	8X8	NGC2359;G4;HS116;E298.
6	231.6	-4.3	07 08.0	-18 24	12X10	G5;E301.
7	232.6	+0.9	07 29.5	-16 51	17X15	(NGC2409);G6;E302.
9	234.4	-12.2	06 43	-24 20	90X30	E304.
10	234.4	-0.2	07 29.0	-18 54	18X14	E306.
11	234.6	-10.0	06 52	-23 35	60X20	E308.
12	234.7	+0.9	07 33.7	-18 42	6X3	G7; E307.
13	234.8	-0.1	07 30.1	-19 18	12X10	E309.
14	235.6	-4.1	07 17.0	-21 50	6X4	(NGC2367).
15	237.5	-7.3	07 08	-25 00	300X300	(NGC2362);E310.
16	243.3	+0.6	07 51.2	-26 15	33X33	(NGC2467);G9;E311.
19	253.8	-0.5	08 13.5	-35 42	48X40	G10.
20	254.5	0.0	08 17.5	-36 00	10X10	NGC2579;G11.
22	258.1	+12.2	09 13.5	-31 10	45X45	
27	260.1	+0.5	08 36.5	-40 12	100X100	G14.
32	261.6	+0.9	08 43.0	-41 09	27X27	G15.
33	263.0	+1.4	08 49.5	-41 54	95X80	G17.
35	264.6	+0.1	08 49.7	-43 55	30X30	G18.
36	265.2	+1.4	08 57.5	-43 33	12X6	G20.
37	267.0	+0.1	08 58.5	-45 45	13X3	NGC2736.
38	268.0	-1.0	08 57.5	-47 16	40X40	G22,23,24.

No.	l^{II}	b^{II}	R.A.1950	Dec.1950	Size	Comparison
40	269.3	-1.4	09 01.0	-48 27	8X8	G25.
41	270.3	+0.8	09 14.8	-47 45	8X4	
42	274.1	-1.3	09 22.4	-51 54	9X7	G26.
45	282.2	-0.1	10 10.0	-56 09	16X16	
46	282.4	-1.3	10 06.0	-57 15	15X15	
47	283.0	-2.7	10 03.5	-58 42	25X20	
48	283.5	-1.0	10 14.0	-57 36	15X10	NGC3199;G28.
49	284.3	-0.3	10 22	-57 27	90X35	(NGC3247);G29.
50	284.3	+0.4	10 24.5	-56 54	12X12	
51	286.0	+0.5	10 36.1	-57 42	12X12	
52	287.2	+0.4	10 43.5	-58 18	15X15	BBW25500;G32.
53	287.4	-0.9	10 40	-59 30	210X210	NGC3293,3324,3372; IC2599;BBW25500; G30,31,33.
54	288.8	+0.7	10 56	-58 42	210X60	(NGC3503,3572); G34,a,b,35,36,37.
	291.1	-0.3	11 09	-60 36		
55	290.4	-3.0	10 54.2	-62 45	8X8	
57	291.6	-0.5	11 12.5	-60 56	170X40	NGC3603;G38a,b.
58	292.4	-4.9	11 04.3	-65 18	7X7	
59	293.0	+4.5	11 35	-56 40	180X150	
60	293.7	-1.4	11 26.5	-62 30	50X50	IC2872;BBW26201;G39,40.
61	294.2	-2.3	11 28.3	-63 30	15X15	G41.
62	294.8	-1.5	11 35	-62 54	80X80	IC2944,8;BBW26201;G42.
63	296.7	+7.1	12 05	-55 00	250X40	
	299.5	+13.5	12 28	-49 00		
65	301.0	+1.2	12 31.5	-61 18	11X6	G43.
68	301.7	+1.0	12 37.3	-61 36	15X15	
69	302.2	+0.3	12 41.5	-62 18	5X3	G45
74	305.2	0.0	13 07.8	-62 33	15X12	

No.	l^{II}	b^{II}	R.A.1950	Dec.1950	Size	Comparison
75	306.3	+0.2	13 16.5	-62 15	18X13	BBW27300;G48a.
78	307.9	+0.2	13 30.5	-62 00	45X30	BBW27500;G48b.
79	308.7	+0.6	13 36.5	-61 30	9X5	BBW27600;G48c.
80	309.3	-0.5	13 43.5	-62 24	21X10	BBW27700;G48d.
82	311.0	+0.4	13 55.7	-61 12	5X4	
83	311.9	-0.5	14 05.0	-61 50	60X50	BBW27901.
85	313.5	-0.4	14 17.0	-61 10	25X20	BBW28100.
91	321.2	-0.5	15 12.5	-58 01	11X10	BBW28801.
92	322.2	+0.6	15 14.5	-56 30	8X5	BBW28900.
94	326.2	+0.9	15 37.0	-54 00	20X20	BBW29400a.
97	327.1	-0.5	15 47.7	-54 36	6X5	BBW29401.
98	327.6	-0.8	15 51.5	-54 30	6X5	BBW29501;G49.
102	331.9	-1.0	16 14.0	-51 48	12X8	BBW29902.
103	332.4	-0.4	16 13.3	-51 00	5X3	
104	332.9	-1.4	16 20.2	-51 24	20X20	
105	332.9	+1.8	16 06.3	-49 00	45X35	BBW30000;G51.
106	332.9	-0.6	16 17.0	-50 48	35X20	
107	336.4	-0.2	16 29.8	-48 03	8X4	NGC6164,5;G52.
108	336.5	-1.3	16 35.0	-48 40	210X120	(NGC6193);BBW30402;G53.
110	340.9	-0.8	16 50.0	-45 00	7X3	G54.
111	341.1	-1.0	16 51.5	-45 00	5X3	G54.
113	342.7	+1.8	16 45	-42 00	360X300	(NGC6231);BBW31100;G55.
114	343.9	-4.7	17 18	-45 00	330X330	
116	344.8	+1.8	16 52.3	-40 26	110X75	IC4628;BBW31100;G56.
119	347.7	+1.9	17 01.3	-38 00	180X145	(NGC6281);BBW31500; G57a,b;E2.
120	348.3	+0.5	17 09.0	-38 24	6X6	G58;E3.
123	349.5	-0.8	17 17.8	-38 09	75X75	NGC6337;G59;E5.
125	350.0	+0.2	17 15.0	-37 09	8X8	

No.	l^{II}	b^{II}	R.A.1950	Dec.1950	Size	Comparison.
126	350.6	+1.0	17 13.5	-36 18	16X4	BBW31800a.
127	351.4	+0.7	17 17.0	-35 48	50X25	NGC6334;HS119; BBW31800b;G61,62,63, 64a,b,c;E8.
128	351.4	-0.1	17 20.4	-36 15	10X10	
129	351.9	+12.7	16 34.0	-28 00	180X180	G65.
130	352.4	+2.1	17 14.2	-34 06	30X20	E10.
131	353.2	+0.7	17 22	-34 18	170X55	(NGC6357);HS120; BBW32100;G66;E11.
132	355.4	+0.2	17 30	-32 42	110X80	(NGC6383);HS121; BBW32301;G67;E12.
133	355.9	+1.5	17 26.0	-31 36	45X40	BBW32300;G68;E13.
134	358.5	-1.9	17 46.1	-31 14	60X50	BBW32603;G69;E15.
137	359.8	-0.2	17 42.6	-29 18	18X18	BBW32801;E16.
138	0.1	+0.2	17 41.7	-28 49	8X4	E17.
140	0.2	-0.4	17 44.2	-29 02	12X12	BBW32701;E19.
141	0.4	-0.2	17 44.0	-28 46	6X4	E20.
143	3.5	+2.1	17 42.5	-24 54	7X6	(NGC6432).
144	4.4	+0.5	17 50.7	-25 00	85X65	HS123;BBW33201;G71;E22.
145	6.6	+0.1	17 57	-23 15	90X35	HS124;G74a,b;E26.
146	6.6	-1.5	18 03	-24 00	120X90	NGC6523,(6530),6559; HS126;BBW33402;G72,75; E25,29.
147	7.2	-0.2	17 59.5	-22 54	16X16	NGC6514;HS125;G76;E30.
149	8.7	-0.6	18 04.0	-21 45	120X30	HS129;G77a;E34.
151	11.0	-1.8	18 13.5	-20 25	100X35	NGC6526;HS134;G77b,E35.
153	12.2	-1.8	18 16.0	-19 20	60X20	(IC1283,4);HS140; BBW33903;G78;E37.
154	12.7	+2.0	18 03.0	-17 00	40X30	
155	12.9	+0.3	18 09.3	-17 41	10X10	HS133;E40.
156	13.7	-0.8	18 15.0	-17 30	50X50	HS136;E43.
157	14.3	+0.1	18 13.2	-16 36	60X60	(IC4701);HS137; BBW34101;G79;E44.

No.	l^{II}	b^{II}	R.A.1950	Dec.1950	Size	Comparison.
158	15.2	+3.3	18 03.5	-14 12	23X23	HS128;BBW34201;G80;E46.
159	15.3	-1.8	18 22.0	-16 36	15X15	
160	15.4	-0.8	18 18.5	-16 00	70X60	(NGC6618);(IC4706,7); HS144,145;BBW34202; G81a,b;E45.
161	16.1	-0.3	18 18.0	-15 09	80X40	HS143.
162	16.7	-0.5	18 20.0	-14 40	22X10	HS146;BBW34401;G82;E48.
163	16.9	-2.3	18 27.1	-15 24	10X9	
164	16.9	-1.2	18 23.0	-14 51	8X6	HS148;E50.
165	17.0	+0.8	18 16	-13 54	90X66	(NGC6611);HS142; BBW34400;G83;E49.
166	18.4	-0.3	18 22.6	-13 09	15X15	HS147;E53.
167	19.0	+1.3	18 18	-11 54	180X90	(NGC6604);BBW34600; G84,85;E54.
169	22.0	+0.1	18 28.2	-09 48	7X7	HS150;E56.
170	22.6	+0.3	18 28.5	-09 09	7X5	
171	23.2	+0.6	18 28.6	-08 27	5X5	HS151;E58.
172	24.6	-0.1	18 33.8	-07 32	7X7	HS155;E59.
173	25.4	+0.2	18 34.0	-06 41	17X17	HS154;BBW35201;E60.
174	28.8	+3.4	18 29.2	-02 13	5X4	HS152;E64.
175	29.1	-0.7	18 44.2	-03 48	7X5	HS159;(NGC6823);E65.
176	30.5	+0.4	18 42.7	-02 04	8X8	HS158;E66.
177	31.9	+1.4	18 41.8	-00 24	12X12	HS156;E69.
179	36.4	-1.7	19 01.2	+02 09	20X15	E72.
181	38.8	+2.0	18 52.3	+06 00	5X5	

TABLE 2

List of possible regions less than 4° diam.

No.	l^{II}	b^{II}	R.A.1950	Dec.1950	Size (min of arc)	Comparison.
3	224.2	+1.2	$07^h14.0$	$-09^\circ18$	4X4	HS115;E294.
8	233.9	-0.1	07 28.3	-18 27	3X2	E305.
17	243.5	-1.0	07 45.4	-27 13	2X2	
18	250.3	-2.2	07 57.2	-33 42	1X1	
21	257.6	+0.6	08 28.8	-38 10	1X1	
23	258.5	+1.4	08 35.0	-38 21	2X1	
24	258.7	-1.4	08 23.6	-40 12	3X2	
25	259.2	+1.3	08 36.9	-39 02	2X1	
26	259.7	+2.9	08 44.6	-38 27	3X3	
28	260.1	-3.4	08 19.6	-42 33	2X1	
29	260.2	-3.3	08 20.0	-42 32	2X2	G13.
30	260.2	-3.1	08 21.1	-42 29	2X2	
31	260.7	-3.2	08 22.3	-42 55	3X2	
34	264.4	+1.4	08 54.4	-42 56	2X2	G19.
39	269.2	-1.1	09 01.9	-48 12	2X2	
43	277.2	-3.8	09 25.5	-55 54	2X2	NGC2899;G27.
44	277.8	-3.6	09 29.6	-56 05	2X2	
56	291.1	-2.1	11 03.3	-62 12	2X1	
64	299.4	-0.3	12 16.7	-62 41	3X2	
66	301.1	+0.9	12 32.6	-61 39	2X1	G44.
67	301.2	+0.8	12 33.0	-61 45	4X4	
70	302.7	-1.0	12 45.6	-63 34	1X1	
71	302.9	+1.3	12 47.3	-61 18	4X3	G46.
72	303.2	+1.6	12 50.3	-61 00	2X2	
73	303.4	+1.4	12 52.0	-61 12	2X2	
76	307.2	-3.5	13 29.8	-65 45	3X2	NGC5189;G47.
77	307.6	-5.0	13 35.4	-67 10	1X1	

No.	l^{II}	b^{II}	R.A.1950	Dec.1950	Size	Comparison.
81	310.6	+0.6	13 51.9	-61 06	1X1	
84	312.6	-2.7	14 16.4	-63 40	1X1	
86	315.0	-2.3	14 35.5	-62 27	3X3	
87	320.2	+0.8	15 01.0	-57 19	2X2	
88	320.2	+0.5	15 02.7	-57 36	3X2	
89	320.4	-1.0	15 09.5	-58 46	4X4	
90	321.0	+2.2	15 01.5	-55 46	0.5X0.5	
93	322.6	-2.5	15 29.7	-58 54	2X2	
95	326.7	+0.8	15 39.7	-53 47	3X2	BBW29400c.
96	326.9	-1.0	15 48.9	-55 06	2X2	
99	328.7	-0.5	15 55.8	-53 35	4X2	G50.
100	329.1	+2.0	15 47.7	-51 22	1X1	
101	331.7	-1.0	16 12.6	-51 54	2X2	
109	339.7	-0.3	16 43.0	-45 39	2X2	
112	341.7	+5.6	16 27.0	-40 12	2X2	
115	344.4	+7.3	16 29.6	-37 06	4X2	
117	345.5	-1.0	17 06.2	-41 33	2X2	
118	347.3	-0.5	17 10.0	-39 48	2X2	
121	348.4	-1.1	17 15.5	-39 15	3X2	E4.
122	348.9	-1.1	17 17.1	-38 54	2X2	
124	349.6	+1.1	17 10.4	-37 00	3X2	NGC6302;G60;E6.
135	359.0	-0.7	17 42.4	-30 12	2X2	
136	359.0	-3.6	17 54.4	-31 40	1X1	
139	0.1	-0.3	17 43.8	-29 02	2X2	
142	0.6	-0.7	17 46.5	-28 50	2X2	E21.
148	8.2	+0.6	17 58.5	-21 35	2X2	
150	9.3	+0.3	18 02.1	-20 48	2X2	
152	12.2	+4.3	17 53.3	-16 19	2X2	

No.	l^{II}	b^{II}	R.A.1950	Dec.1950	Size	Comparison.
168	21.3	+2.5	18 18.0	-09 16	1X1	
178	36.3	-1.2	18 59.2	+02 19	2X2	
180	38.4	+3.5	18 46.3	+06 19	1X1	
182	40.0	-1.3	19 06.3	+05 32	3X3	E74.

(a). Coordinates.

Equatorial coordinates were marked, with an estimated accuracy of ± 4 minutes of arc, on prints of the photographed fields. Transformations from equatorial to new galactic coordinates were effected with the computer SILLIAC of the University of Sydney. The new galactic coordinates are those recommended by Commission 33b of the I.A.U. (Pawsey, Gum, Westerhout and Blaauw[1]).

(b). Comparison with other surveys.

Comparisons are made with the surveys of Dreyer[2] (1953), Gum (1955), Hase and Shajn (1955), Bok, Bester and Wade (1955), and Sharpless (1959). In column 9 they are designated thus: NGC and IC - Dreyer (those shown in parenthesis represent associated clusters), G - Gum, HS - Hase and Shajn, BBW - Bok, Bester and Wade, and E - Sharpless.

The Vela-Puppis Nebula (centred at about $\alpha = 7^h50$, $\delta = -45^\circ$) was not catalogued as it could not be adequately described; it will be discussed more fully later. Some of the adjacent H II regions appearing in the list may be extensions of it.

5. An Atlas of H-alpha Emission.

The atlas is a pictorial representation of the H II regions the detection of which has been discussed previously.

(1) Blaauw,A.,Gum,C.S.,Pawsey,J.L. and Westerhout,G., Ap.J., 130, 702, 1959.
(2) Dreyer,J.L.E., New General Catalogue, 1953

It consists of five mosaics, each of 18 prints of H-alpha plates, and corresponding charts on which the positions of detected emission have been marked. Each mosaic covers six fields of longitude and three in latitude. To achieve continuity, the final three centres of one mosaic are repeated at the beginning of that following it. There was no need to reproduce the mosaics and charts in this chapter, with a loss of detail and quality, when reference can be made to the original Atlas.

(a). Identification charts.

The parts of the Milky Way in which emission was detected are marked in dark outline on the charts. Areas of higher intensity within the boundaries of large H II regions are bounded by fine outlines. Accurate intensities of H-alpha emission in the area of sky surveyed have been determined by Johnson[1] who employed the same equipment and field centres. Small H II regions that are present in the same directions as large distributions of emission, but may be spatially separated from them, are represented on the charts as areas bounded by fine as well as dark outlines. The imposed boundaries of the small regions do not indicate true dimensions, only positions, as the former would be too small to be represented on the charts. The numbers assigned to the regions are those of the catalogue of tables 1 and 2. Some correspond not to discrete H II regions, but to bright areas within larger distributions of extended emission of lower intensity.

Marked on each chart are equatorial coordinates, new and old galactic coordinates. As mentioned, the equatorial coordinates were originally marked on individual prints

(1) Johnson, H.M., Mem. Mt. Stromlo Obs., No. 15, 1960.

with an accuracy of ± 4 minutes of arc, but due to small deformations of the scale at the edges of the field of the camera, some smoothing was necessary during the construction of the mosaics. Ohlsson's galactic coordinates tables[1] and the precession tables of Allen[2] were employed to determine old galactic coordinates (fine, continuous lines). The transformation from equatorial to new galactic coordinates (heavy, broken lines) was effected with the Mount Stromlo IBM 610 computer. In a regenerating program, values of right ascension and declination were calculated for intervals of 3° in new galactic latitude and longitude for b^{II} between -15° and $+15^{\circ}$, and l^{II} between 217° and 44°.

Several prominent stars have been marked on the charts for reference purposes. Reference is aided further by the similarity of the scales of the mosaics and their corresponding charts.

To provide an overall picture of the distribution of H-alpha along the Southern Milky Way, a chart has been prepared on which is shown the total distribution of detected emission.

(b). Comparison with the surveys of Gum, and Bok, Bester and Wade.

Both the surveys of Gum, and Bok, Bester and Wade, mentioned at the beginning of the chapter, include areas of the sky observed in the present investigation. Gum photographed the region between longitudes $l^{II} = 220^{\circ}$ and $l^{II} = 20^{\circ}$ with a 2.4-inch f/1.7 Schmidt camera and glass filters. Because of the better resolution of the 8-inch Schmidt and the more sensitive method of detection used, the present survey has resulted in the discovery of greater

(1) Ohlsson,J., Lund Obs. Tables, 1956.
(2) Allen,C.W.,'Astrophysical Quantities',Uni.Lond.Press,1955.

A chart showing the H II regions detected in the H-alpha emission survey. New galactic coordinates are used.

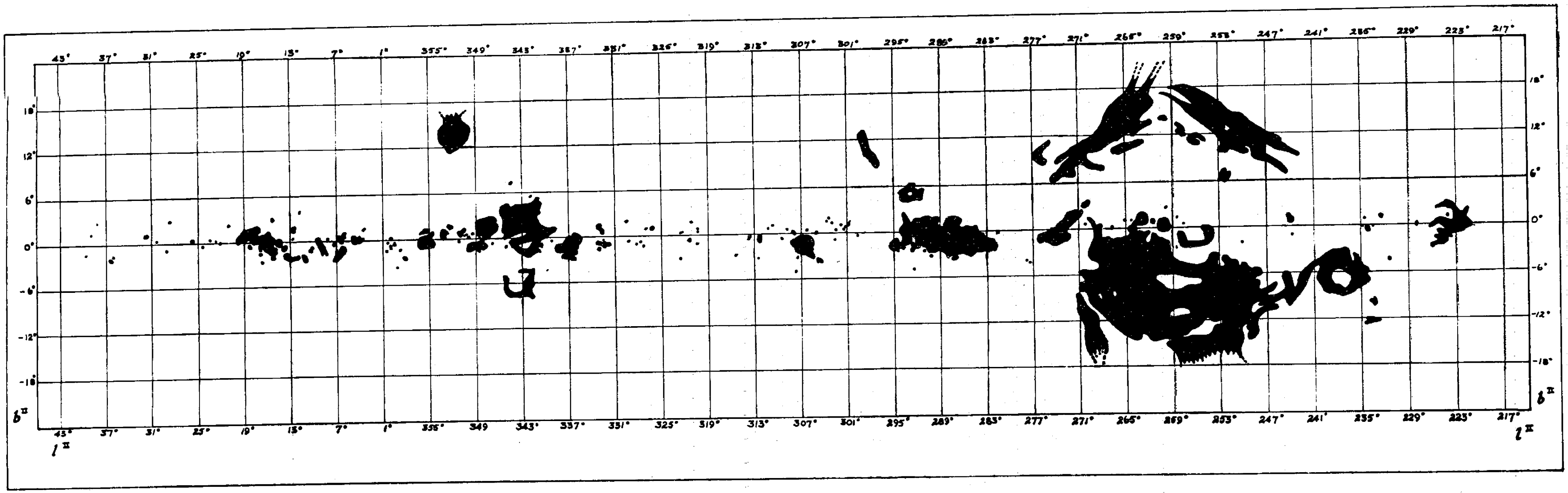

l^{II}
b^{II}
43°
37°
31°
25°
19°
13°
7°
1°
355°
349°
343°
337°
331°
325°
319°
313°
307°
301°
295°
289°
283°
277°
271°
265°
259°
253°
247°
241°
235°
229°
223°
217°
18°
12°
6°
0°
-6°
-12°
-18°

numbers of small regions and areas of faint emission. Gum estimated that the faintest regions he could detect had an emission measure of 600; the limiting value of the present study is approximately 400, though it would be higher in the parts of the sky near the galactic centre because of the greater brightness of the Milky Way. Bok, Bester and Wade employed a 3-inch f/1.5 Zeiss-Sonar camera and Baird 50A passband interference filters for a survey between $l^{II} = 283^{o}$ and $l^{II} = 28^{o}$. In contrast with the present survey, they detected large areas of faint emission between longitudes $l^{II} = 283^{o}$ and $l^{II} = 310^{o}$, and $l^{II} = 336^{o}$ and $l^{II} = 350^{o}$.

2.3 The Vela-Puppis Nebula.

Many of the emission nebulae show complex structure over large areas, and very few have the spherical structure deduced by Stromgren. This complexity is due in part to the effects of non-uniform overlying obscuration which hinders the detection of exciting stars, as it is often impossible to determine the true centre of a nebula. Existing spectral data i.e. that of the Henry Draper Catalogue, are insufficient to identify the possible exciting stars of the small distant H II regions.

The most prominent southern H II region is that located in the constellations of Vela and Puppis, commonly known as the Vela-Puppis or Gum Nebula. It was first detected by Gum[1] in 1952 as a huge H II region in the shape of a broken loop, about 20^{o} in diameter, with its centre at $l^{II} = 258^{o}$, $b^{II} = -9^{o}$. He attributed its presence to the excitation of hydrogen by the stars Zeta Pup (O5) and $Gamma_2$ Vel (WC7), both of second visual magnitude. A nearby emission region in the constellation

(1) Gum, C.S., Obs., 72, 151, 1952.

A composite of two mosaics of the Atlas, showing the Vela-Puppis Nebula. On the accompanying chart are marked the detected regions of emission.

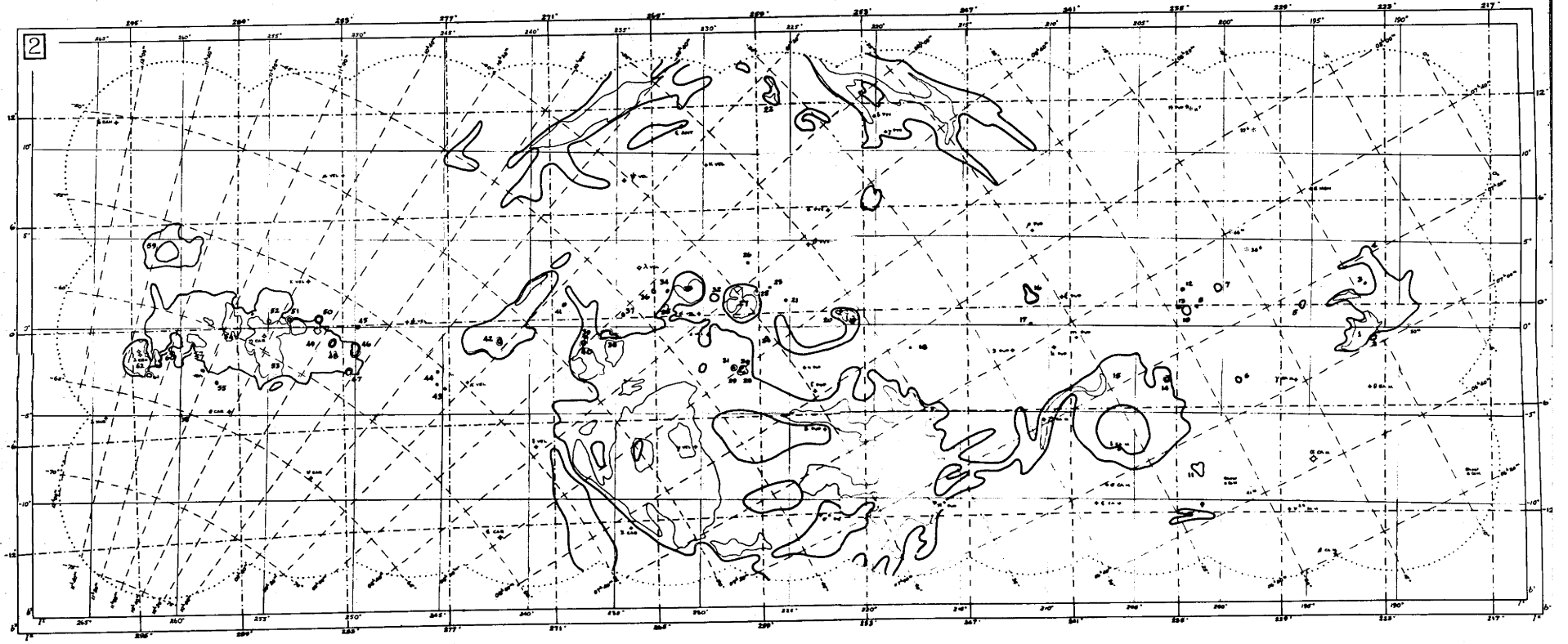
2

Antlia he assumed to be due to the same stars. He derived the distance of the nebula from that of the star $Gamma_1$ Vel, a suspected proper motion companion of $Gamma_2$ Vel. Its Henry Draper spectral type is B3, and Gum assigned it an absolute magnitude of -1.3. From its apparent magnitude $m_v = 4.8$, and an assumption of no absorption, he determined a distance of 170 parsecs. In a later publication[1], the value was altered to 250 parsecs.

Prior to Gum's investigation, several other observers had detected small areas of the nebula. Cederblad catalogued several nebulous condensations between $\alpha = 8^h25$ and 8^h42, and $\delta = -40^\circ$ and -47°. Shapley and Paraskevopoulos[2] detected a 'string' nebula (prominent in mosaics 1 and 2), 4.5° in length, and centred at $\alpha = 8^h30$, $\delta = -42^\circ35$.

Abt, Morgan and Stromgren[3] have photographed in H-alpha light the area of the sky in which the nebula is located. Their prints show the presence of a greater extent of faint emission than detected by Gum, but less than that in the mosaics.

The present survey shows that the size of nebula is considerably greater than originally suspected. In the region of the sky where it is situated, fields at greater galactic latitudes were photographed in an attempt to detect as much emission as possible associated with the nebula. In the diagram showing the total distribution of H II regions, the broken loop of emission originally detected by Gum appears as an almost spherical region. Apart from an increase in the amount of emission detected in Antlia (from $l^{II} = 260^\circ$, $b^{II} = 20^\circ$ to $l^{II} = 277^\circ$, $b^{II} = 6^\circ$), with a 'fanning-out' at the end of lower latitude,

(1) Gum,C.S., Mem.R.A.S.,67, 155, 1953.
(2) Shapley,H. & Paraskevopoulos,J.S., H.B.,No.914,8,1940.
(3) Abt,H.A.,Morgan,W.W. & Stromgren,B., Ap.J.,126,322,1957.

there is an area in Pyxis (from $l^{II} = 243^{o}$, $b^{II} = 8^{o}$ to $l^{II} = 259^{o}$, $b^{II} = 18^{o}$). The main region of emission extends to the H II region in Canis Majoris ($l^{II} = 238^{o}$, $b^{II} = -6^{o}$) the nebulosity of which has a similar filamentary nature, and which may be related to the Vela-Puppis Nebula or at least be situated at the same distance from the sun, although Abt, Morgan and Stromgren have suggested that it is at a greater distance. On the assumption that all the emission regions discussed are part of the nebula, it is almost circular in appearance, centred at $l^{II} = 259^{o}$, $b^{II} = 0^{o}$, and has a diameter of 36^{o} or greater.

The distance from the sun of the H II region is still uncertain. Of the three possible exciting stars Zeta Pup, $Gamma_1$ and $Gamma_2$ Vel, only the second can be used for a distance determination; according to Smith[1], the first is classified as O5f and the last as WC7+O, and well-determined absolute magnitudes for stars of these types are not available. For $Gamma_1$ Velorum, from three sets of observations, its magnitude and colours are: V = 4.24, B-V = -0.21, U-B = 0.88. With the aid of Johnson's "Q" method[2] and assuming that it is a main sequence star (no spectra of the star are available at present), the unreddened values are: V = 4.15, B-V = -0.24, U-B = -0.90, and the visual absorption, $A_V = 0^{m}.09$. The colours correspond to a star of spectral and luminosity type B1.5V. This is in reasonable agreement with the type B2IV quoted by Smith, but earlier than the Henry Draper type, B_3. If the three stars mentioned above are coeval, the brightest main sequence star would

(1) Smith, H.J., Doctoral Thesis, Harvard Uni. 1955.
(2) Johnson,H.L., Lowell Obs.Bull., No.90, 1958.

be of spectral type O5, and the appropriate value of the absolute magnitude of Gamma$_1$ Vel is that assigned to a zero-age main sequence star of type B1.5 - -2.0 according to Johnson and Iriarte[1]. The determined distance of the star therefore is 175 parsecs. This estimate should be regarded as a minimum value as the star may be more luminous than assumed. The linear diameter of the nebula is equal to or greater than 130 parsecs. If it is assumed that the two brightest exciting stars are embedded in a uniform region of hydrogen of density N_H atoms/cm^3, then Stromgren's equation[2] is:

$$N_H = (An^{1/3}r^{-1})^{3/2}$$

where r = the radius of the emission region.
n = the number of exciting stars.
A = a value listed by Stromgren as a function of spectral type of the exciting stars.

In this case, as both stars are of very early spectral type, A = 140. The equation is corrected in the manner suggested by Pottasch[3] and the determined density is approximately 2 atoms/cm^3.

The emission measure is defined as:

$$E = \int NiNedl$$

where Ni = ion density.
Ne = electron density.
dl = element of path length in parsecs in the line of sight.

As virtually all the free electrons in the nebula are contributed by the ionization of hydrogen, Ni = Ne. Assuming a uniform density throughout the emission region,

(1) Johnson,H.L. and Iriarte,B., Lowell Obs. Bull.,No.91,1958.
(2) Stromgren,B., Ap.J., 108, 242, 1948.
(3) Pottasch,S.R., Ap.J., 132, 260, 1950.

$$E = 2N_H^2 r = 500.$$

This value has little significance as the region is not of uniform density, suggested by the fact that some areas of the nebula have a considerably higher emission measure than the value calculated; if the apparent non-uniformity was due only to the effects of overlying obscuration, the maximum emission measure would be 500. However, some of the apparent non-uniformity in intensity of the ionized gas of the nebula may be due to the presence of interstellar material overlying parts of it, for edges of regions of obscuration appear to coincide with those of nebulosity. This suggestion is not inconsistent with the fact that the colours of Gamma$_1$ Vel are little reddened, as the star is located in a direction that appears to be relatively unobscured. One of the regions in question, the Vela Dark Nebula ($l^{II} = 265^o$, $b^{II} = 0^o$), has been assigned a distance of 600 parsecs, by Greenstein[1], from a comparison of star counts in its direction with those of a nearby unobscured area. As the estimate is only approximate, it is possible that it is too large. For the Nebula, the nature of its filamentary structure, the determined distance of Gamma$_1$ Vel, and the fact that the greater its distance, the lower is the estimate of its emission measure, suggest that it is a local feature.

The radio emission from the region of the Vela-Puppis Nebula has been studied by Risbeth[2]. Apart from the detection of several H II regions that are visible in emission at a wavelength of 3.5m, and in absorption at 12.5m, the outstanding feature is the presence of a group of strong non-thermal sources near the galactic equator. The brightest part of the nebula, near Gamma Velorum, is shown on the 3.5m

(1) Greenstein, J.L., H.A., 105, 359, 1936.
(2) Risbeth, H., Aust. J. Phys., 11, 550, 1958.

isophotes as a spur, several degrees wide, extending southwards from the band of radio-emission along the galactic equator; the determined emission measure, E = 1000, may include a contribution from the background radiation. Other parts of the H II region are not visible, possibly because of the effect of the pronounced brightness gradient of the non-thermal emission in the area. At the wavelength of 15.2m, a large area shown in absorption agrees in position with the optical region; the estimated emission measure is 800 but the determination may be effected by radiation originating between the nebula and the sun. There are several radio features present in directions where no H-alpha emission has been detected optically e.g. at $l^{II} = 266^{o}$, $b^{II} = 10^{o}$; such inconsistencies could be due to the effects of interstellar absorption, particularly in the region quoted. Other small H II regions not necessarily associated with the Vela-Puppis Nebula were detected in the radio survey, e.g. numbers 38, 24, 32, and 36 of the present catalogue coincide in positions with the sources R61, R55, R57 and R62 respectively, of Risbeth's catalogue.

As mentioned, the most conspicuous radio features of the Vela-Puppis region are the intense non-thermal regions, the presence of which are indicated by the high brightness temperatures recorded at a wavelength of 15.2m. The source Puppis A (IAU 08s4A) discovered by Stanley and Slee[1] in 1950, corresponds to the small bright H II regions numbers 28, 30 and 31. It was identified by Baade and Minkowski[2], on the basis of the position determined by Stanley and Slee and the angular size measured by Mills[3], with a network of gaseous filaments having a high velocity

(1) Stanley,G.J. and Slee,O.B., Aust.J.Sci.Res.,A3,234,1950.
(2) Baade,W. and Minkowski,R., Ap.J.,119,206,1954.
(3) Mills,B.Y., Aust.J.Sci.Res.,A5,266,1952.

dispersion of 150-200 km/sec. It is similar to that observed in Cassiopeia. A more recent study of the source at 3.5m has been carried out by Sheridan[1].

The strong non-thermal sources Vela-X, Vela-Y and Vela-Z may be associated with a group of filaments of H-alpha emission centred at $l^{II} = 263^{o}$, $b^{II} = -2^{o}$. However, photographs of it have been examined by Basinski, Bok and Gottlieb[2] who concluded that this nebulosity does not resemble the structure of the emission near Puppis A, with the result that the optical identification is still in doubt. Risbeth has suggested that the radio sources may represent regions of interaction between clouds of interstellar material.

2.4 Distances of H II Regions.

Some estimates of distances of H II regions are listed in table 3. The columns are:

(1) The current number of the region.
(2) Its approximate new galactic longitude, l^{II}.
(3) The determined distance in parsecs.
(4) Notes on (3). In the column are listed the exciting stars studied. Many of the distances are more recent estimates of those of exciting stars listed by Gum[3]. Others are of associated features such as clusters and associations.
(5) The number of the reference to the paper from which the value in (3) was taken.

The values listed in (3) are the best available to date, but some may not be very reliable. For example, the estimates of Gum[3], based on the B star catalogues of

(1) Sheridan,K.V., Aust.J.Phys.,11,400,1958.
(2) Basinski,J.,Bok,B.J. & Gottlieb,K., 'Paris Symposium on Radio Astronomy',Ed.Bracewell,R.N.,(Stanford Uni. Press,1959.)
(3) Gum,C.S., Mem.R.A.S.,67,155,1955.

TABLE 3

Distances of H II regions

No.	Approx. l^{II}	Dist. (p.s.)	Notes	Ref.
1	225°	1100		(1)
2	224	550	HD53367	(2)
14	236	2100	NGC2367	(3)
15	238	1500	NGC2362	(4)
16	243	3500	HD64315	(5)
19	254	2100	HD69464	(2)
Vela-Pupp.	259	175	Discussed in chapter 2	
27	260	910	HD73882	(2)
32	262	760	HD74804	(2)
33	263	600	HD75759	(2)
48	284	3800	HD89358	(2)
49	284	2800	NGC3247	(6)
53	287	1500	OB Concentration	(7)
54	290	3630	HD97471	(8)
57	292	760	HD97950	(2)
60	294	2880	HD99897	(8)
61	294	1750	HD100099	(2)
62	295	630	OB Concentration	(2)
Crucis	306	2200	1 Cru. Association	(9)
105	333	2200	HD144900 HD144918	(8)
107	336	1400	HD148937	(10)
108	337	1300	NGC6193 (chapter 4)	
113	343	1450	I Sco Association	(11)
116	345	1450	I Sco Association	(11)
119	348	820	NGC6231	(3)

No.	Approx. l^{II}	Dist. (P.s.)	Notes	Ref.
127	351	1400	OB Concentration	(12)
129	352	150	II Sco Association (Chapter 3)	
132	355	1450	HD159176	(5)
133	356	720	HD158186	(2)
134	359	1000	HD161853	(2)
135	359	3000	Star number 655	(5)
137	0	3500	HDE316232	(5)
140	0	3200	HDE316311	(5)
144	4	1100	HD162978	(5)
145	7	1400	HD164971	(2)
146	7	1400	NGC6530	(13)
147	7	2300	HD164492	(5)
149	9	760	HD165516	(14)
151	11	660	HD167263	(14)
153	12	1500	HD167722 HD167815	(15)
157	14	1450	HD167633	(2)
158	15	2800	HD165319	(5)
160	15	1500	NGC6618	(16)
165	17	2500	NGC6611	(13)
167	19	1400	NGC6604	(1)
175	29	1650	NGC6823	(13)

References

(1) Sharpless,S. and Osterbrock,D., Ap.J., 115, 89, 1952.
(2) Gum,C.S., Mem.R.A.S., 67, 155, 1955.
(3) Barkhatova,K.A., AZh., 27, 182, 1950.
(4) Johnson,H.L., Ap.J., 123, 267, 1956.
(5) Hiltner,W.A., Ap.J. Supp., 2, 389, 1956.

(6) Collinder,P., Ld.An.2, Cr., 1931.

(7) Bok,B.J., 'Vistas in Astronomy', 2, 1522, 1956.

(8) Feast,M.W., Stoy,R.H., Thackeray,A.D. and Wesselink,A.J., M.N., 122, 239, 1961.

(9) Houck,T.E., Doctoral Thesis, Univ. Wisc., 1956.

(10) Westerlund, B., Arkiv F.Ast., Bd.2, no.44, 467, 1960.

(11) Morgan,W.W., Whitford,A.E. and Code,A.D.,Ap.J.,118, 318, 1953.

(12) Hoffleit,D., Ap.J., 124, 61, 1956.

(13) Johnson,H.L., Hoag,A.A., Iriarte,B., Mitchell,R.I. and Hallam,K.L., Lowell Obs. Bull., 5, 133, 1961.

(14) Oosterhoff, P.Th., B.A.N., 11, 299, 1951.

(15) Stebbins,J., Huffer,C.M. and Whitford,A.E., Ap.J., 91, 20, 1940.

(16) Markarian,B.E., Buir. Soob., 9, 7, 1951.

Stebbins, Huffer and Whitford[1], and Oosterhoff[2], are in general considerably smaller than more recent determinations effected with UBV photometry and MK spectral types and luminosity classes. The disparity is due probably to the fact that for the calculation of the distance moduli listed in the two catalogues, mean absolute magnitudes / spectral type were used; the most recent estimates incorporate separate values / spectral type / luminosity class.

The data of table 3 will be used in chapter 5 when a re-assessment of spiral structure is carried out.

2.5 Comparison With a 19.7 Mc/s Survey.

The investigation of the distribution of intensity at a frequency of 19.7 Mc/s is the radio astronomical counterpart to an H-alpha emission survey. At this frequency, the brightness temperature of galactic non-thermal radiation (the distribution of which has been discussed in 1.1, section 2(e)) is of the order of 10^5 °K; since those of H II regions are generally 10^4 °K, an area of sky containing ionized hydrogen should appear in absorption (as a 'trough' in a drift scan, at constant declination, across the particular area) if there is a background of non-thermal emission in its general direction. At high frequencies, the intensity of non-thermal radiation is less, with the result that H II regions are visible in emission and can be confused with non-thermal radio sources.

A survey at 19.7 Mc/s has been carried out by Shain[3]. The results, prepared for publication by Komesaroff[4], are shown in fig.1. In a comparison with the distribution of

(1) Stebbins,J.,Huffer,C.M. and Whitford,A.E.,Ap.J.,91,20,1940.
(2) Oosterhoff,P.Th., B.A.N.,11, 299, 1951.
(3) Shain,C.A., Aust.J.Phys., 10, 195, 1957.
(4) The author is indebted to M.M.Komesaroff for making available the results in advance of publication.

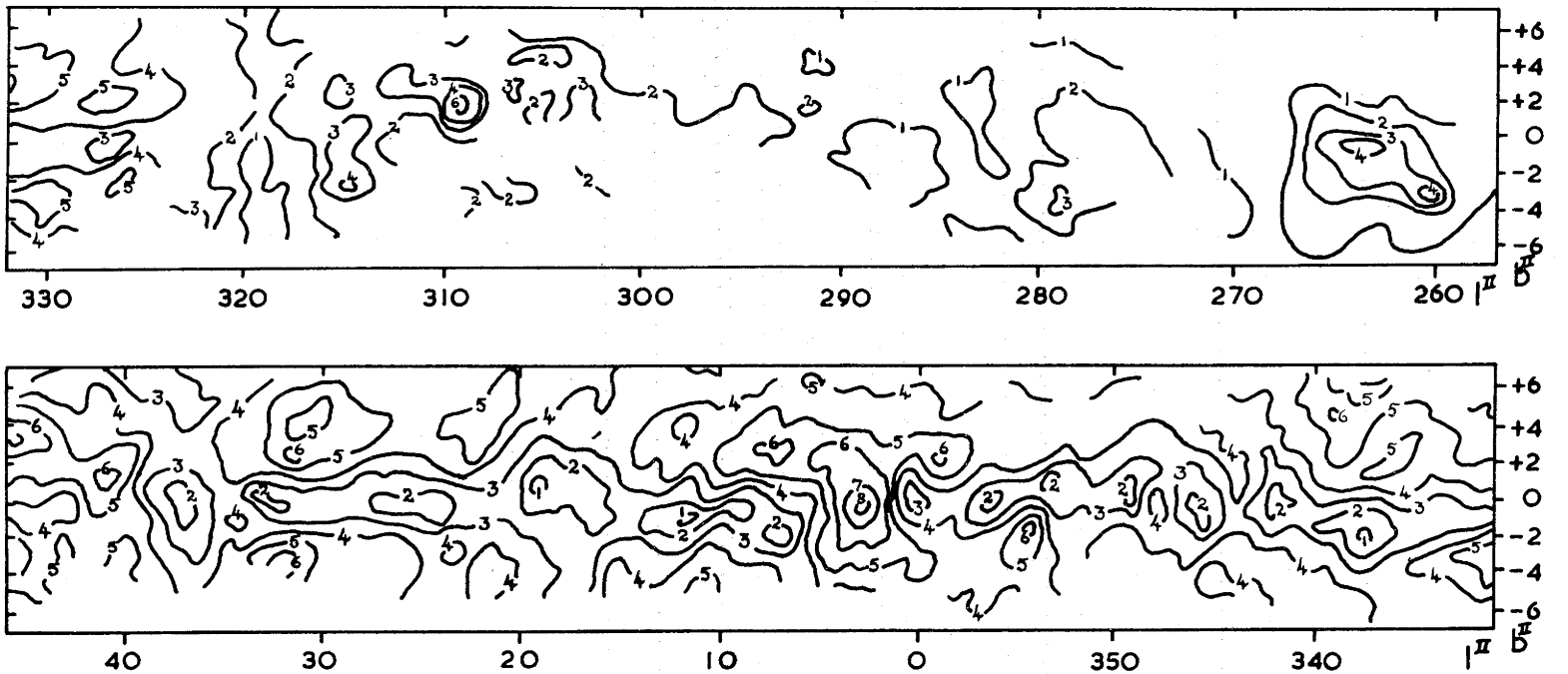

Scale:

1	1.0×10^5 °K	5	3.0×10^5
2	1.5×10^5	6	3.5×10^5
3	2.0×10^5	7	4.0×10^5
4	2.5×10^5	8	4.5×10^5

Fig.1. Distribution of brightness at 19·7 Mc/s, along the Southern Milky Way.

H II regions, certain points must be remembered:

(a). The resolution is lower than the optical study because of the $1^{o}.4$ aerial beamwidth.

(b). It has been found by Mills[1] that the brightness temperature of non-thermal radiation along the galactic equator is not constant (it has been discussed in chapter 1). This effect, together with the presence of discrete non-thermal radio sources, will affect the observed brightness.

(c). The radiation observed in the direction of an H II region may include a contribution from the non-thermal radiation originating between the H-alpha emission and the sun. Shain[2] has suggested that in the inner part of the galaxy, a value of $50^{o}{,}000\ ^{o}K$ is attained at a distance less than 600 parsecs.

1. Comparison of Optical and Radio results.

Little information can be derived from fig.1 between longitudes $l^{II} = 270^{o}$ and $l^{II} = 305^{o}$ because of the incompleteness of the radio investigation. The main characteristics of a comparison of the optical distribution of H II regions with the 19.7 Mc/s survey are:

1) In the direction of the Vela-Puppis Nebula ($l^{II} = 260^{o}$), the radio survey shows a region in emission. As mentioned, this is due to the presence of non-thermal radio sources. A more detailed discussion of this has been given already.

2) There is an ill-defined 'trough' in the direction of the Eta Carina Nebula ($l^{II} = 280^{o}$-295^{o}). In a 1400 Mc/s

(1) Mills,B.Y., P.A.S.P., 71, 267, 1959.
(2) Shain,C.A., 'Paris Symposium on Radio Astronomy' (Ed. Bracewell,R.N.),Stanford Uni.Press,1959.

radio study of the H II region, Wade[1] determined an emission measure of 54,000, so that it should be a prominent feature in the figure. However, the brightness temperature is low in the area near the nebula, due either to the presence of H-alpha emission which has not been detected optically, or to the lack of non-thermal radiation. The latter conclusion is correct, for in the 85.5 Mc/s survey of Hill, Slee and Mills[2], which shows H II regions in emission, the brightness temperature is also relatively low in this direction.

3) In the radio survey, there is a 'trough' at $l^{II} = 319^{o}$ that is unusual as it is perpendicular to the galactic equator. It may be associated with the group of H II regions present in this direction as there is a local maximum in the survey of Hill, Slee and Mills, and the ratio of brightness temperatures, T(19.7): T(85.5) is much less than 50, the value expected if H-alpha emission is not present.

4) From $l^{II} = 319^{o}$ onwards, there is excellent correlation of the positions and shapes of absorption features and H II regions. The results of the radio survey suggest that many of the latter are connected by faint emission or emission covered by obscuration. Several of the small groups of regions are visible as single large areas in the radio survey. They could be due either to the effects of obscuration on the optical results or the poor resolution due to the beamwidth of the aerial.

5) In the 19.7 Mc/s survey, there is a prominent area of emission at $l^{II} = 3^{o}$. It has been suggested

(1) Wade,C.M., Aust.J.Phys., 12, 418, 1959.
(2) Hill,E.R.,Slee,O.B. & Mills,B.Y.,Aust.J.Phys.,11,530,1958.

by Shain that it is a 'window' in the distribution of H-alpha emission, although there are several H II regions in this direction. An indication that there is overlying H-alpha emission is given by the results of other surveys at higher frequencies, which predict a temperature of 700,000°K at 19.7 Mc/s, in contrast with the value 400,000°K observed. From this, it appears that the feature is due to a maximum in the background non-thermal radiation.

2. Conclusion

The results of the comparison suggest that there is a large band of H-alpha emission along the galactic equator near the direction of the galactic centre. The 19.7 Mc/s survey has shown its usefulness as a H II region detector, but in an extensive interpretation of the distribution, points (a), (b), and (c) must be considered. Although it cannot be used to detect the small regions observed optically, the results are not affected by interstellar absorption, and can indicate the true dimensions of large areas of H-alpha emission.

Plate (1) A 20/26-inch Schmidt photograph in visual light, showing the cluster IC 2602. The cluster Mel. 101 is the compact grouping of stars in the lower part of the plate. North is at the top, East is to the left. The scale of the field is 16'/inch.

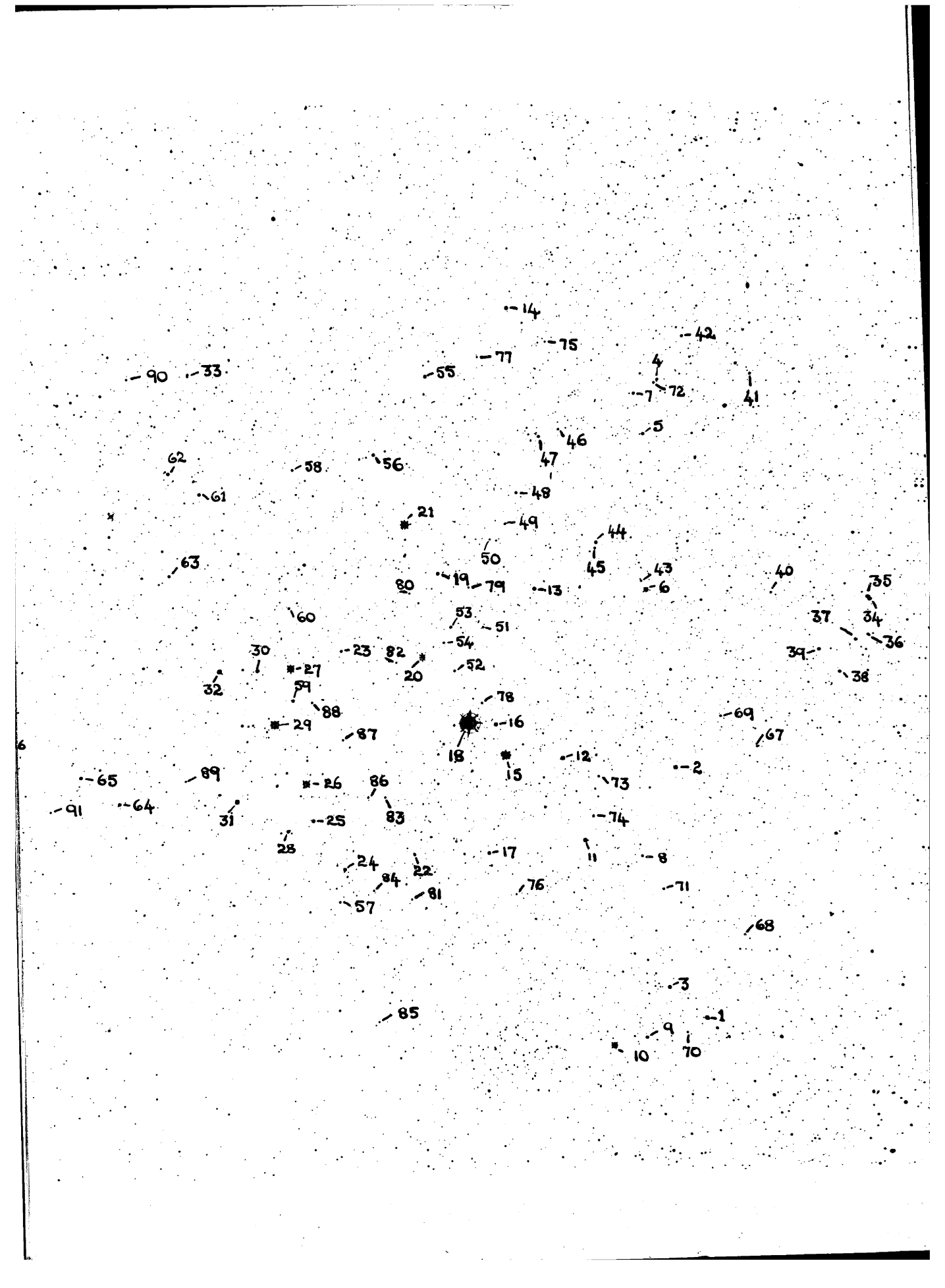
14
75
42
77
4
90
33
55
72
41
7
5
46
62
58
56
47
61
48
21
49
44
50
63
45
43
40
35
80
19
79
13
6
60
53
51
37
34
54
30
23
82
36
27
20
52
39
32
59
78
88
69
29
16
67
87
18
12
2
65
89
26
86
15
73
91
64
31
25
83
74
28
17
11
8
24
22
84
76
71
57
81
68
3
85
1
9
10
70

Star Clusters[1] as consisting of 33 stars - 8 brighter than 7th magnitude, 6 brighter than 8th, and 9 brighter than 9th. It was first studied about 40 years ago; Raab[2] in 1922 assumed a mean apparent magnitude for its members and derived a distance of 160 parsecs. Edwards[3] and Doig[4], from spectroscopic studies of several members, determined a value of 250 parsecs. Later estimates by Russian astronomers were 220, 200 and 210 parsecs, obtained by Barkhatova[5], Markarian[6] and Kopylov[7] respectively. As these three astronomers used the magnitudes and spectral types of the Henry Draper Catalogue[8], it is not surprising that their results are similar. Markarian[9] has pointed out that the cluster is too near the sun to be a local condensation of the I Car Association. From a study of the proper motions of some of its members, he concluded[10] that the group is expanding. In a recent photo-electric investigation of the brighter members of the cluster, Braes[11] derived a distance of 150 parsecs; later, he changed the value to 158 parsecs[12]. From the absolute magnitude of the brightest main sequence star, Theta Car, and the position on the main sequence that the effects of gravitational contraction occur, he obtained an age of 15×10^6 years.

The investigations described in this chapter are

(1) Gould,B.A., C.R., 19, 292, 1897.
(2) Raab,S., Lund.Ast.Obs.Medd., 11, 28, 1922.
(3) Edwards,D.L., M.N., 84, 366, 1923.
(4) Doig,P., J.B.A.A.,35,201,1925; J.B.A.A.,36,107,289,1926.
(5) Barkhatova,K.A., AZh., 27, 183, 1950.
(6) Markarian,B.E., Buir.Soob., 9, 6, 1951.
(7) Kopylov,I.M., Crim.Pubs., 8, 122, 1952.
(8) Cannon,A.J., H.A., 96, 1930.
(9) Markarian,B.E., Buir.Soob., 9, 8, 1951.
(10) Markarian,B.E., Buir.Soob., 11, 19, 1953.
(11) Braes,L.L.E., M.N.A.S.S.A., 20, 7, 1961.
(12) Data kindly made available to the author in advance of publication.

part of a joint program that was initiated at Mt. Stromlo by Drs H. Gollnow and G. Hagemann in 1956. Plates for the determination of proper motions have been taken by Mr H. Wood and associates at Sydney Observatory and Mr C. Jackson at the Yale-Columbia Southern Station. Drs H. Gollnow and A. Przybylski are determining radial velocities using spectra obtained on the 74-inch reflector.

3.3 Observations.

1. Photoelectric Observations.

Three telescopes were used to obtain three-colour photoelectric observations of 67 suspected cluster members. The investigation was commenced with the Mount Stromlo 20-inch f/18 reflector, but most of the observing was carried out with the Mount Stromlo 50-inch f/18 reflector and the Mount Bingar 26-inch f/12 reflector. The photoelectric equipment consisted of an EMI photomultiplier, replaced by a refrigerated RCA 1P21 for the more recent observations, a GR amplifier, or an amplifier constructed at Mount Stromlo, and a Brown Potentiometer. The filters used were those recommended by Johnson and Morgan[1] for the linear transformation from instrumental magnitudes to the UBV system. The combinations of filters and photomultipliers are shown in the following table:

Telescope	Cell	Filters
20-inch	EMI;1P21	OY4; BG12+GG13; UG2.
26-inch	EMI;1P21	C3384; C5030+GG13; C9863.
50-inch	1P21	C3384; BG12+GG13; UG2.
		C3384; C5030+GG13; C9863.

During the final stages of observation, the 1P21 photomultiplier and Corning filters (C3384, C5030+GG13, C9863) were used.

(1) Johnson, H.L. and Morgan, W.W., Ap.J.,117, 313, 1953.

Observations with the 20-inch were carried out from May 1958 to June 1959, those with the 26-inch during February, April and June 1960, and those with the 50-inch from June 1959 to July 1961. During these periods, the stars discussed in the following chapter also were observed.

As stated, the initial observations were carried out with the 20-inch telescope. However, the nights were rarely of sufficient quality to compare accurately the cluster stars with the equatorial UBV standards of Johnson and Morgan. The mean transformation equations obtained are:

$$V-V_{20} = -0.290(B-V) + A$$
$$B-V = 1.166(B-V)_{20} + B$$
$$U-B = 1.058(U-B)_{20} + C$$

Magnitudes and colours obtained with this telescope were given lower weight than those derived elsewhere.

The 26-inch telescope was used primarily for the transformation of the UBV system from the equatorial standards of Johnson and Morgan to several stars (secondary standards) in the vicinity of the cluster. In this manner, advantage was taken of the greater manoeuvrability of the smaller telescope, and the better quality of the Mount Bingar sky. A total of 23 UBV standards listed by Johnson and Harris[1] was used in the determination of transformation equations; the average number observed on a single night was 12. In general, 16" and 29" focal plane apertures were employed for the observations.

The sensitivity of the photomultiplier was checked frequently with a radium source fitted in the filter wheel.

(1) Johnson, H.L. and Harris, D.L., Ap.J.,120, 196; 1954.

To obtain extinction coefficients for each night, as well as to check on the constancy of transparency throughout it, two stars, one of early, the other of late spectral type, were observed several times. For nights of doubtful quality, the following mean coefficients were used:

$$k_V = 0.18$$
$$k_{B-V} = 0.15 - 0.040\ (B-V)$$
$$k_{U-B} = 0.28$$

The relations between the UBV and the Mount Bingar magnitude systems are shown in figs. 1, 2 and 3, the mean results of observations obtained on five nights of good quality. The least squares solutions are:

$$V-V_{26} = -0.102(B-V) + 0.142$$
$$B-V = 1.156(B-V)_{26} + 1.964$$
$$U-B = 1.051(U-B)_{26} - 1.051$$

with a mean error per single measurement of $0^m.012$ in V

$0^m.015$ in B-V

$0^m.018$ in U-B

The observational procedure with the 50-inch was similar to that with the 26-inch, except that cluster stars were observed with respect to the secondary standards. In general, focal-plane apertures of 14" and 16½" were used.

The reduction of observations was executed in the manner recommended by Johnson and Morgan[1]. After the installation of an IBM 610 computer at Mount Stromlo early in 1960, subsequent reductions were carried out with it. As this computer has a small storage capacity, the reduction program was in two parts. The first consisted of the calculations of the mean value of sec Z per star observation and instrumental magnitudes and colours uncorrected for the

(1) Johnson, H.L. and Morgan, W.W., Ap.J., 117, 313, 1953.

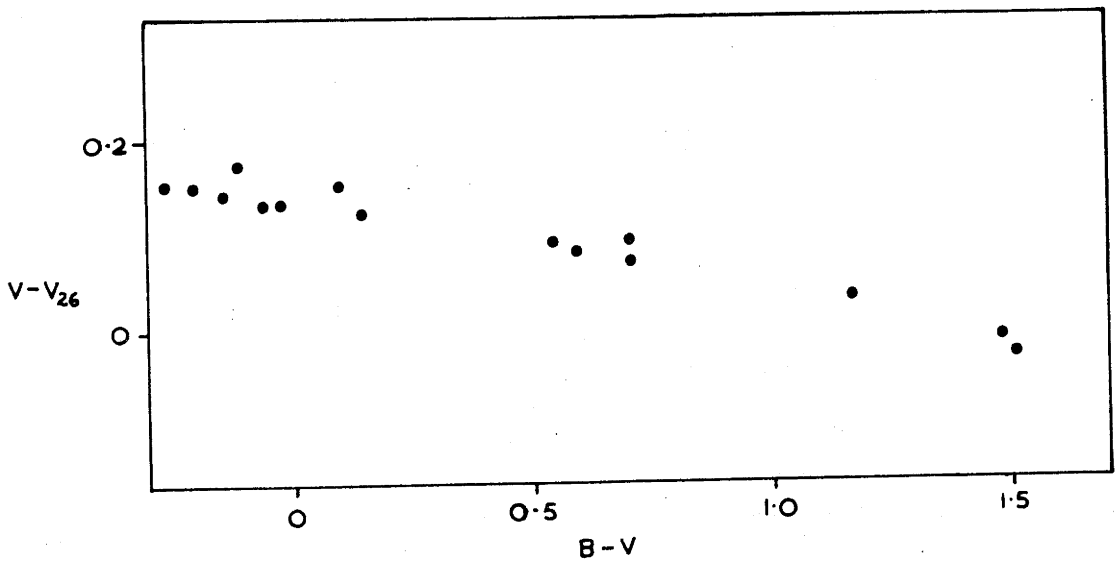

Fig.1. Observed relation between $V-V_{26}$ and B-V.

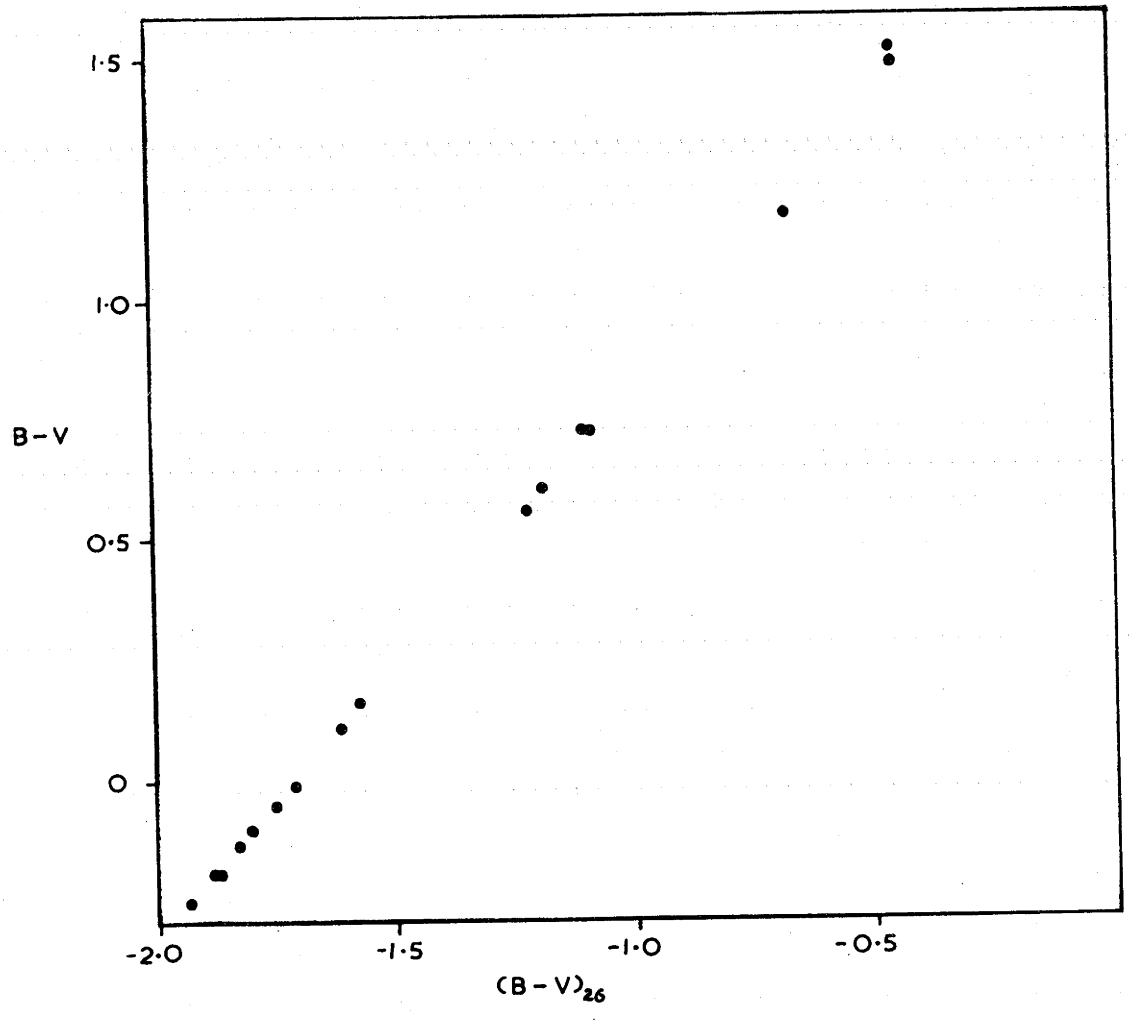

Fig.2. Observed relation between B-V and $(B-V)_{26}$.

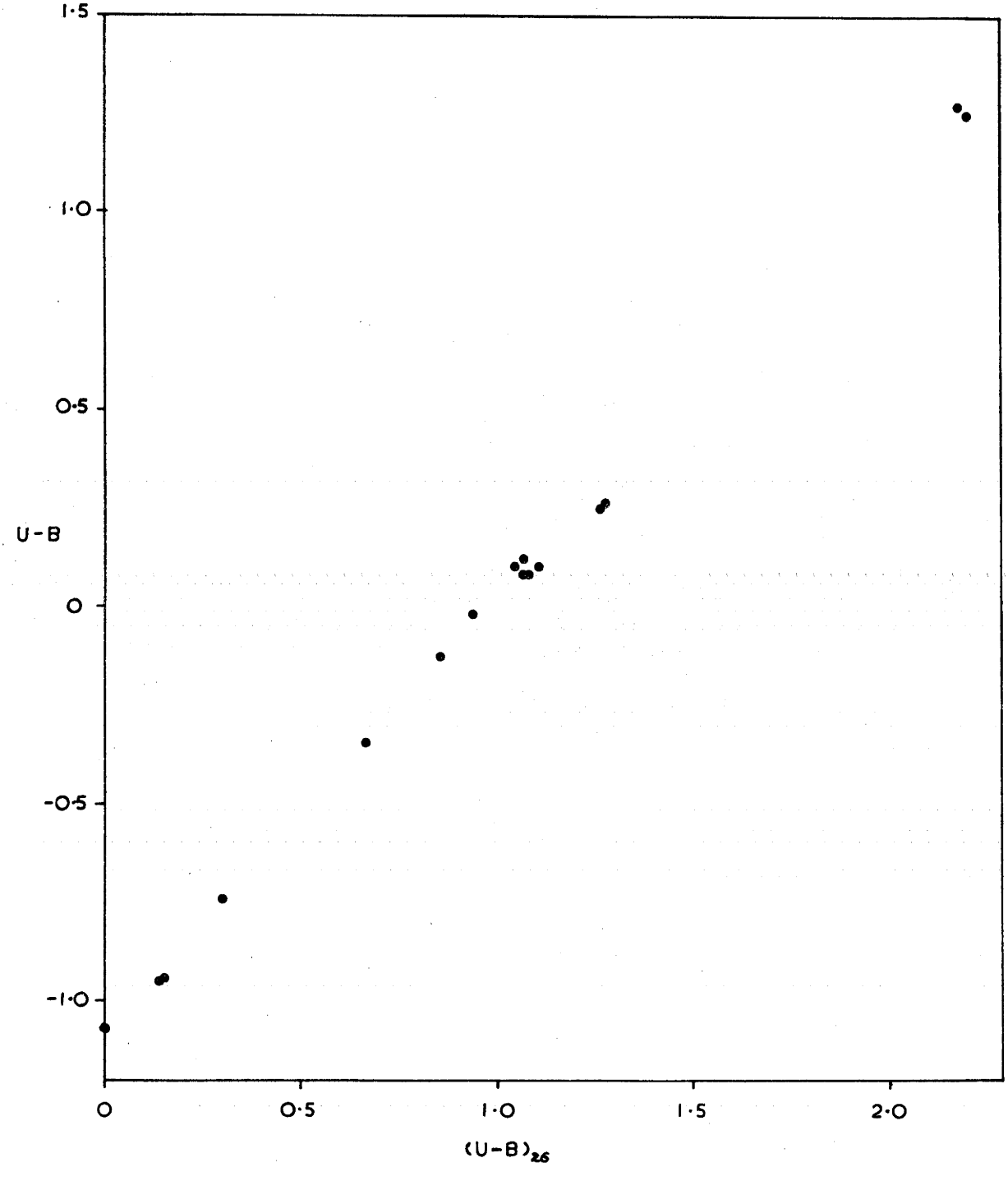

Fig.3. Observed relation between U-B and $(U-B)_{26}$.

effects of extinction. These values were typed, and punched onto output tape. The extinction coefficients were determined graphically in order to correct for the effects of any changes in transparency or any variation of the sensitivity of the photomultiplier. Either these, or mean values, depending on the quality of the night, were entered into the computer, and using the output tape of the first part of the program, the machine calculated instrumental magnitudes and colours, determined the transformation coefficients by the method of least squares, and printed out V, B-V and U-B for all the observed stars.

2. Spectrographic Observations.

To enable the author to effect a luminosity and spectral classification, spectrograms of 35 suspected cluster members, obtained by Drs H. Gollnow and A. Przybylski for the measurement of radial velocities, were kindly made available. The stars were chosen on the basis of their spectral type and apparent magnitude. The spectra were obtained with a Zeiss two-prism spectrograph mounted at the f/5 Newtonian focus of the 74-inch reflector. The dispersion of the spectra is 90A/mm at H-gamma. With Eastman-Kodak IIa-O and 103a-O emulsions and a projected slit-width of 20 microns, the times needed to obtain well-exposed spectra 0.3mm wide varied from a few seconds for Theta Car to 100 minutes for a ninth magnitude F2 star. In the case of the faster 103a-O emulsion, the resolution of the spectra is limited by the grain-size, which is greater than the projected slit-width.

For each star for which spectra were available, an MK spectral type and luminosity class were determined. The classification was effected by visual comparison of the spectra with those of several of the MK standards

listed by Buscombe[1] that have been obtained with the same spectrograph. It was based on the ratios of the spectral-line intensities shown in the MKK Atlas[2] to be sensitive to spectral type and luminosity class. As the dispersion is similar to that of the spectra of the Atlas photographs, a comparison with these provided an initial approximate classification.

3. Photographic Observations.

To carry out a search for fainter cluster members, plates centred at α (1950) = 10^h41, δ (1950) = -64.2°, were taken in blue and visual light with the Schmidt telescope of the Uppsala Southern Station by Dr B. Westerlund and Mr D. Sher, and kindly made available to the author. Exposures were of 20 seconds, 30 seconds and 3 minutes duration; for the last exposure time, the limiting stellar magnitude attained is approximately 17. The emulsion-filter combinations are:

Visual Plates 103a-D + 2mm GG14 filter.
Blue Plates IIa-O + 2mm GG13 filter.

The telescope has a 4° square field; the scale on the plates is 2'/mm.

The images of selected stars were measured with a Haffner Iris Diaphragm Photometer. Only one setting per star per plate was necessary, since the errors in setting are less than those due to variations in the density of the plate emulsion. The photometer readings were converted to V and B magnitudes with stars that had been observed photoelectrically. The derived values needed correcting by amounts depending on the distances of the stars from the centre of the field. Basic calibration curves for B and V magnitudes were constructed

(1) Buscombe,W., Mt. Stromlo Mimeogram, No.3, 1959.
(2) Morgan,W.W., Keenan,P.C. & Kellman,E., 'An Atlas of Stellar Spectra,' Univ.Chicago Press, 1943.

from the results for several members of Mel.101, a group of small angular size; the corrections for stars in other regions of the plates were given by the differences between magnitudes obtained photoelectrically and those deduced from the calibrations on the basis of photometer readings. The mean error of a single reduction, $\pm 0^m.05$, although large, is sufficient to determine whether a star is a possible cluster member.

4. Objective Prism Spectra.

The stars for which photographic magnitudes were obtained, were chosen partly on the basis of their spectral types. In order to classify stars near the cluster, a plate of the field was obtained with the Schmidt telescope equipped with a 4° objective prism. The adopted exposure time of 10 minutes yielded well-exposed spectra, the dispersion of which is 480 A/mm at H-gamma, of stars as faint as magnitude 11.5. Classification was achieved by the comparison of the spectra with those of stars assigned spectral classes in the Henry Draper Extension[1]. Since the choice of fainter possible cluster members depends partly on this objective prism study, the photographic survey was limited to stars brighter than the stated magnitude.

3.4 Results.

1. Cluster Membership.

The stars measured photoelectrically are listed in table 1. The columns are:

1) The star's number in the present study.
2) Its HD or HDE designation.
3) V
4) B-V

(1) Cannon,A.J. and Mayall,M.W., H.A., 112, 1949.

5) U-B

6) The number of times that the star was observed. The stars having a great number of observations were those used as secondary standards.

The stars numbers 1 - 33b were compiled previously, by Dr G. Hagemann at Mt. Stromlo, as a list of possible members (unpublished) for the purpose of a radial velocity study of the cluster; the majority define the visual concentration. During the present study, it was discovered that two of this group, numbers 9 and 33, are visual binaries. With the inclusion of the group numbers 34 - 36, all stars brighter than V = 9.0 in the direction of the cluster have been observed photoelectrically.

B and V measurements of 27 of the listed stars have been made recently by Braes[1]; the mean differences are (Braes - Whiteoak):

in V	-0.017	±0.018 (m.e.)
in B-V	+0.013	±0.014 (m.e.)

In fig.4 is shown the colour-magnitude array of the stars numbers 1 - 33. Although the distribution has not been corrected for the effects of absorption, there is a well-defined main sequence to V = 8.5. Evidence supporting the conclusion that most of the brightest stars are members is provided by radial velocity measurements; of eight stars listed in the catalogue of Wilson[2], and two in the investigation of Braes, all but two, numbers 20 and 31, have similar values.

Fig.5 shows the relation between the colours B-V and U-B of the stars observed photoelectrically. Numbers 1 - 33b

(1) Braes, L.L.E., M.N.A.S.S.A., 20, 7, 1961.
(2) Wilson, R.E., Pub.Carnegie Inst.Washington,No.601,1953.

TABLE 1

Photoelectrically-measured stars.

No.	HD/HDE	V	B-V	U-B	n
1	92385	6.75	-0.08	-0.30	7
2	92467	6.99	0.03	-0.16	8
3	92478	7.56	0.05	0.00	9
4	92492	9.27	0.12	0.04	11
5	92535	8.25	0.21	0.10	9
6	92536	6.34	-0.08	-0.31	8
7	92568	8.58	0.42	0.14	9
8	92569	9.46	0.22	0.15	6
9	92570	8.86	0.47	0.02	1
10	92664	5.52	-0.17	-0.59	7
11	92715	6.82	-0.02	-0.14	9
12	92783	6.74	-0.05	-0.22	13
13	92837	7.18	0.00	-0.08	13
14	92896	7.32	0.22	0.06	7
15	92938	4.81	-0.15	-0.58	20
16	92966	7.28	-0.01	-0.10	14
17	92989	7.58	0.04	-0.01	8
18	93030	2.78	-0.23	-1.03	8
19	93098	7.61	0.04	0.00	9
20	93163	5.79	-0.02	-0.55	11
21	93194	4.84	-0.14	-0.62	9
22	93209	9.41	0.32	0.25	10
23	93405	9.17	0.44	0.01	11
24	93424	8.14	0.15	0.08	14
25	93517	7.86	0.09	0.07	12

No.	HD/HDE	V	B-V	U-B	n
26	93540	5.36	-0.10	-0.48	10
27	93549	5.26	-0.09	-0.48	12
28	93600	8.44	0.50	0.02	15
29	93607	4.87	-0.15	-0.65	9
30	93648	7.85	0.11	0.08	10
31	93714	6.57	0.00	-0.60	7
32	93738	6.48	0.00	-0.16	9
33a	93796	10.28	0.63	0.13	3
33b		9.94	0.58	0.07	3
34	91906	7.46	0.03	0.01	2
35	307860	8.24	0.22	0.03	1
36	307861	10.01	0.50	0.22	2
37	91944	8.68	0.05	-0.38	2
38	91997	8.95	0.04	-0.33	4
39	92066	8.40	0.00	-0.43	4
40	307859	10.35	0.20	0.05	1
41	307842	9.33	0.73	0.33	1
42	307844	9.30	1.41	1.47	1
43	307856	10.58	1.22	1.15	2
44	92663	7.81	1.51	1.68	17
45	307926	9.70	1.34	1.49	6
46	307919	10.06	1.14	0.90	1
47	92821	8.87	1.28	1.31	1
48	307921	9.04	1.58	1.60	2
49	307922	9.99	0.60	0.18	2
50	307924	10.70	0.62	0.02	1
51	307931	10.11	1.21	1.07	14

No.	HD/HDE	V	B-V	U-B	n
52	307937	9.76	0.11	-0.26	4
53	307933	8.90	0.43	0.25	1
54	307934	10.08	1.63	1.90	10
55	93115	7.85	1.52	1.78	6
56	93269	8.15	1.14	1.04	6
57	307963	10.06	1.15	0.89	3
58	308006	9.78	1.53	1.56	5
59	308015	8.95	1.19	0.85	8
60	308012	10.06	0.49	0.03	2
61	93777	8.51	1.16	1.04	3
62	93874	8.20	0.17	0.09	2
63	93892	8.99	0.50	0.06	1
64	94066	7.90	0.08	-0.38	5
65	94174	7.76	0.11	0.06	3
66	94422	8.24	0.10	-0.39	2

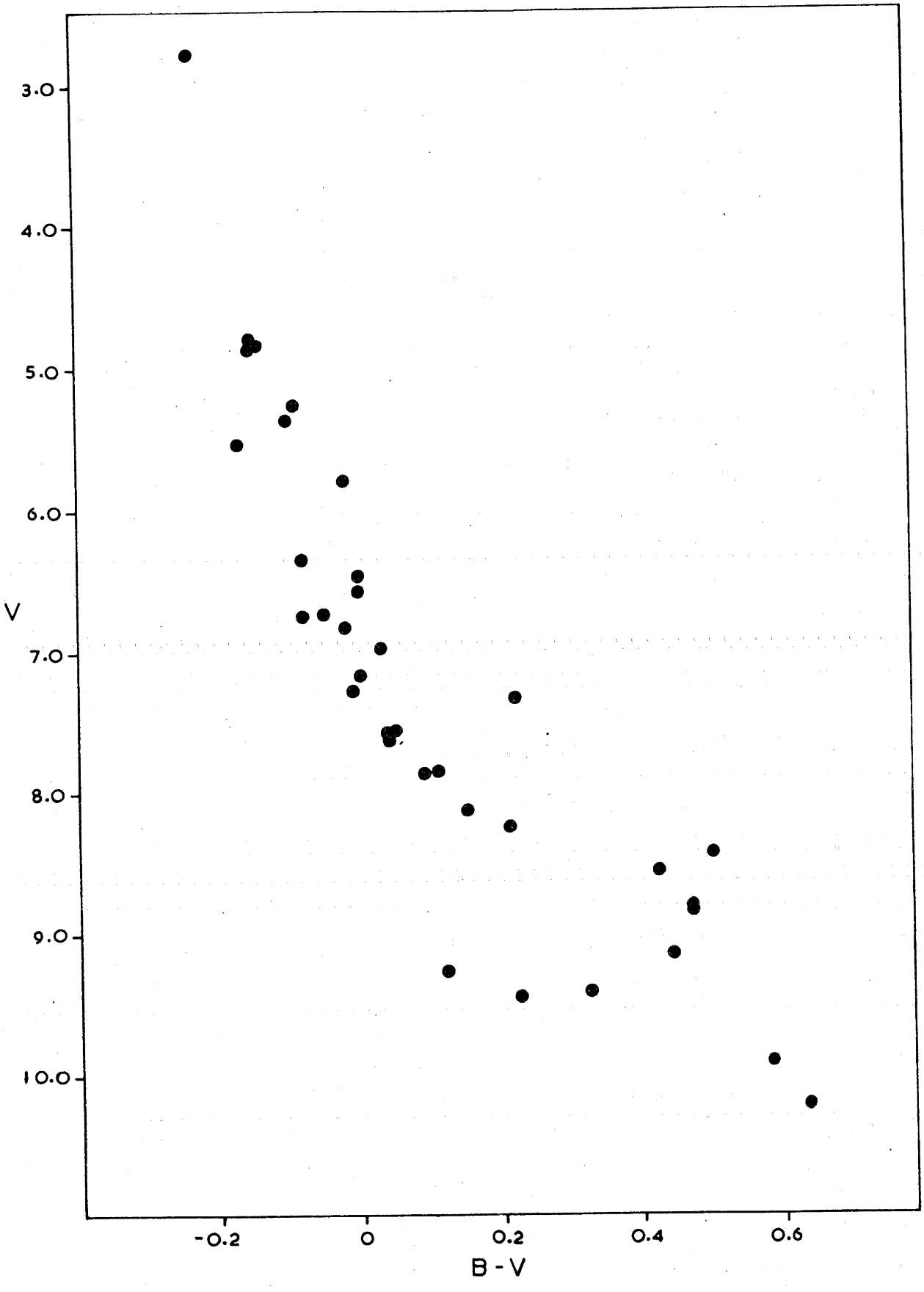

Fig.4. Colour-magnitude array of stars 1-33b.

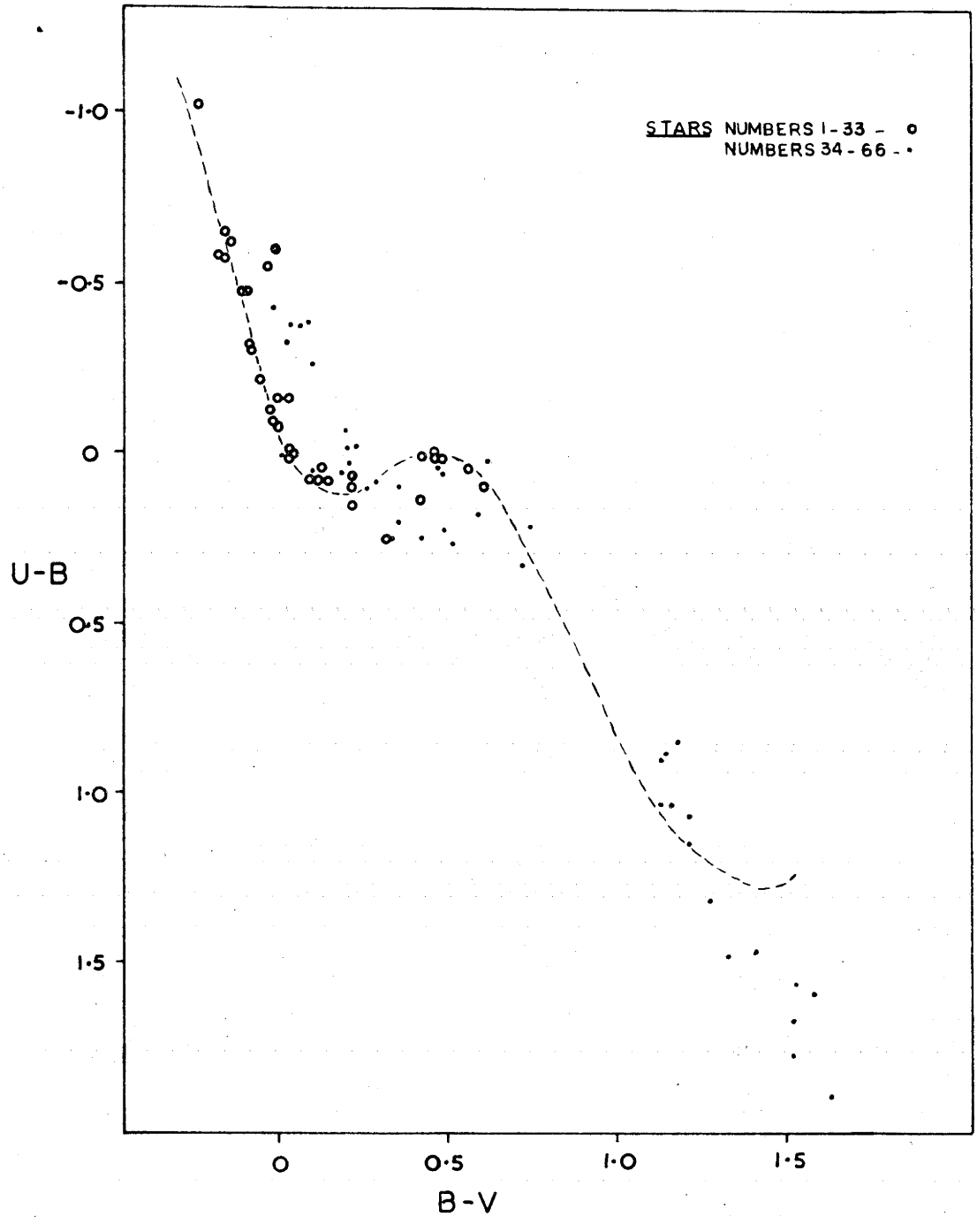

Fig. 5. Two-colour array of stars observed photo-electrically.

are represented by open circles, the remainder by dots. To the former has been fitted the unreddened colour curve given by Arp[1], displaced in B-V by $0^m.04$, the mean colour excess, E_{B-V}, and in U-B by $0^m.03$. From the positions of several of the circles relative to the curve, it appears that numbers 7, 20, 22 and 31 may not be members if it is assumed that they are normal main sequence stars and that the obscuration overlying the cluster is reasonably uniform. Most of the dots appear to represent either more reddened main sequence stars or background giants of late spectral type. Those near the curve are numbers 34, 35, 36, 41, 43, 49, 50, 60, 62, 63 and 65. They may be members of IC 2602; on the other hand, as the cluster reddening is small, they may be foreground or little-reddened background stars. Table 2 contains the results of the spectral and luminosity classification of the numbers 1 - 33b. For the stars of spectral type earlier than A0, the intrinsic values of B-V, (B-V)o, were derived by the "Q" method (Johnson, 1958[2]). This procedure is valid as they are all of luminosity classes IV and V. For those of later spectral types, the values of (b-V)o were derived from the relation given by Arp between the MK classification and UBV photometry. The columns of the table are:

1) Star number.
2) Spectral type and luminosity class.
3) Number of spectra examined.
4) Spectral type from the "Q" method.
5) Colour excess, E_{B-V}.
6) Intrinsic colour, $(B-V)_o$.

(1) Arp,H.C., Handbuch Der Physik, 51, 75, 1958.
(2) Johnson,H.L., Lowell Obs. Bull., No.90, 1958.

7) Visual magnitude corrected for absorption, Vo.

8) Notes on the spectra examined.

The corrected magnitudes and colours listed in columns (6) and (7), of numbers 7 and 10 which have peculiar spectra, were obtained by the reduction of their values of V and B-V by the mean colour excess and visual absorption of cluster members. In column (8), the classifications obtained by other observers are listed. Those followed by (V) were determined by Mme. de Vaucouleurs[1]; that by (M) by Miss Morris[2]. They are in reasonable agreement with those in column (2). Excluding number 10, which has a peculier spectrum, the mean deviation between "Q" spectral types and MK spectral types is half a spectral sub-class.

The distribution in direction of the absorption overlying numbers 1 - 33b is shown in fig.6. To the position of each star is assigned the corresponding colour excess appearing in table 2. The equatorial coordinates included in the diagram are for the epoch 1960. Except possibly for the north-eastern region of the figure, there is little evidence of systematic changes of colour excesses, although there may be small regional variations. Stars numbers 8, 20, 22 and 31 are considerably more reddened than those in similar directions and are presumably background stars. In the case of number 5, the colour excess ($E_{B-V} = 0.12$) is larger than average, but in contrast with the stars mentioned, the corrected magnitude is approximately equal to that of a cluster member of spectral type A3. However, from Johnson's relation,

$$E_{U-B} = 0.71\ E_{B-V}$$

the intrinsic colour $(U-B)_o$ is:

$$(U-B)_o = 0.01$$

(1) de Vaucouleurs,A., M.N., 117, 449, 1957.
(2) Morris,P.M., M.N., 122, 325, 1961.

TABLE 2

Determination of cluster reddening.

No.	Sp.	n	Sp("Q")	E_{B-V}	(B-V)o	Vo	Notes on spectra
1	B9V	4	B8	.00	-0.08	6.75	
2	B9IV	5	B9	.09	-0.06	6.72	
3	AOIV	4	AO	.06	-0.01	7.38	
4	AOIV	4	AO	.12	0.00	8.91	Non-member.
5	A3V	4		.12	0.09	7.89	
6	B8IV	5	B8	.01	-0.09	6.31	
7	A7p	5			0.38	8.46	enhanced lines of Sr and Fe.
8	B9.5IV	7	AO	.23	-0.01	8.77	Non-member.
9	F7V F5IV	4 5			0.43	8.74	Close visual binary.
10	B9p	5	B5		-0.21	5.40	Si star.
11	B9.5V	3	B9.5	.02	-0.04	6.76	
12	B8V	5	B9	.01	-0.06	6.71	
13	B9V	4	B9.5	.03	-0.03	7.09	
14	A5IV	5		.07	0.15	7.11	
15	B3V	5	B5	.01	-0.16	4.78	
16	B9.5V	2	B9.5	.02	-0.03	7.22	
17	A1IV	6	AO	.05	-0.01	7.43	
18	BOV	4	BO	.05	-0.28	2.63	09.5 (V).
19	AOV	5	AO	.05	-0.01	7.46	
20	B3V	4	B4	.15	-0.17	5.34	B3:V (V); non-member.
21	B5V	4	B4	.03	-0.17	4.75	B5 Vn (V).
22	A4IV	5		.20	0.12	8.81	Non-member.
23	F2V	4		.06	0.38	8.99	
24	A4IV	5		.03	0.12	8.05	

No.	Sp.	n	Sp("Q")	E_{B-V}	(B-V)o	Vo	Notes on spectra
25	A2V	4		.03	0.06	7.77	
26	B6V	5	B6	.04	-0.14	5.24	B7:V (V).
27	B7IV	4	B6	.05	-0.14	5.11	
28	F7V	4		.00	0.50	8.44	
29	B4V	6	B4	.03	-0.18	4.78	B4IV(V); B3IV(M).
30	A2V	4		.05	0.06	7.70	
31	B2IV	8	B3	.24	-0.24	5.85	Non-member.
32	AOV	5	B9	.05	-0.05	6.33	
33a	G2IV	2		.00	0.63	10.28	
b	F8V	2		.05	0.53	9.79	

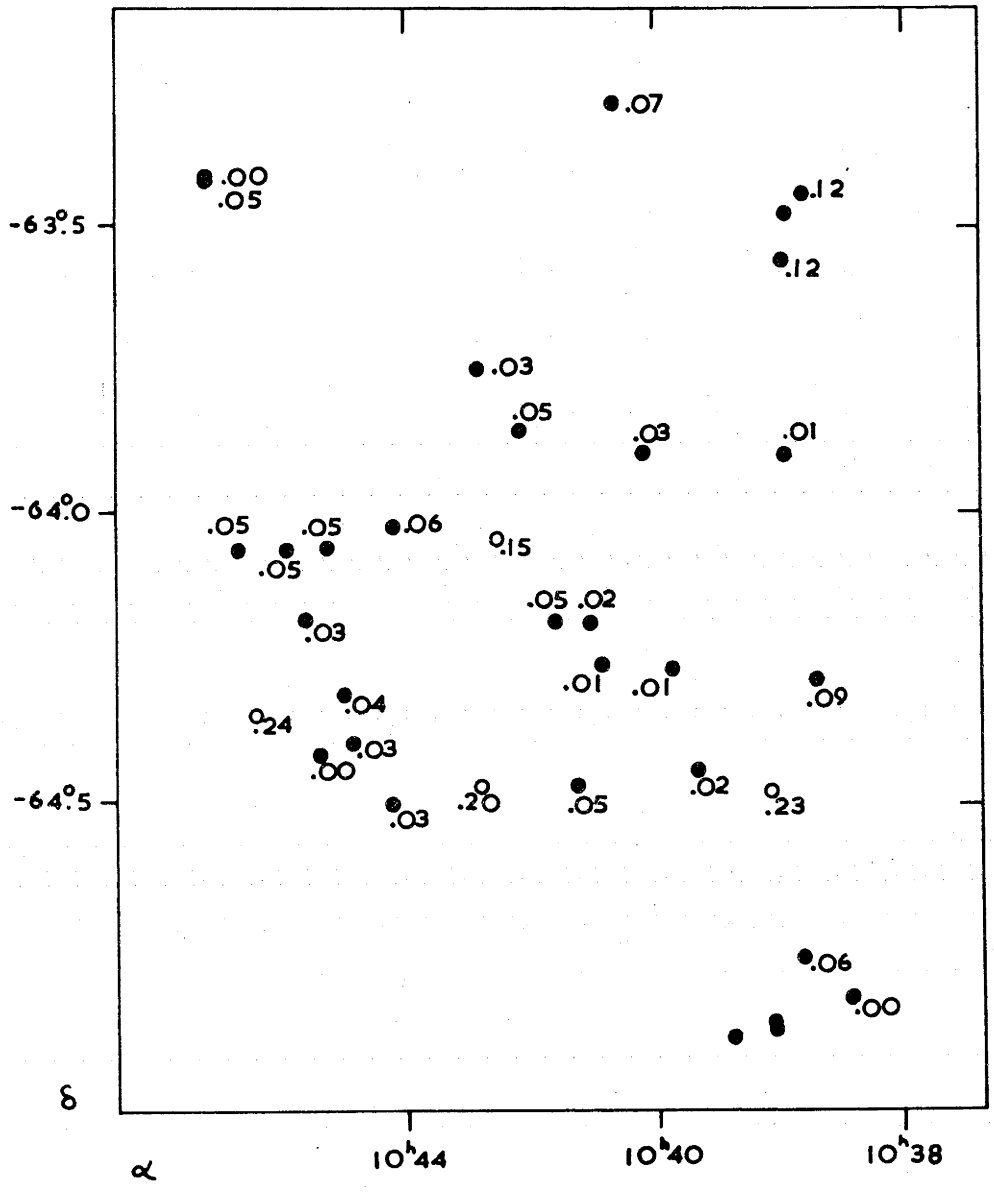

Fig. 6. Colour excesses of stars numbers 1-33b. Doubtful members are shown as open circles.

This is too small for the assigned spectral type; if a later type (A5) is assumed, then not only is the determined colour excess reduced to a value comparable with those of cluster stars, but the modified $(U-B)_o$ corresponds to that of the classification.

For the cluster stars, the mean of the individually-determined colour excesses is:

$$E_{B-V} = 0^m.04$$

From the relation for the visual absorption overlying the cluster (Av):

$$Av = 3.0\ E_{B-V},$$
$$= 0^m.12$$

The stars observed both spectrographically and photo-electrically are represented in a colour-magnitude array corrected for the effects of absorption (fig.7). The doubtful members are shown as open circles; they are numbers 20 and 31 (lower than average radial velocities, large colour excesses), 22 and 8 (large colour excesses). In addition, number 4 is too faint for its spectral type for it to be in the cluster; number 7 is considered doubtful as its Cape proper motion[1] differs considerably from those of members. To the filled circles near $(B-V)_o = 0.0$ has been fitted the zero-age main sequence of Johnson and Iriarte[2], displaced $5^m.94$ vertically, the modulus of the cluster. It is equivalent to a distance of 155 parsecs, in good agreement with the value 150 parsecs determined by Braes. A feature of the main sequence of the cluster is that it does not appear to extend to magnitudes fainter than Vo = 8.7. This could be due to the effects of gravitational contraction for fainter stars, a lack of stars of spectral type F in the cluster, or

(1) Jackson,J. and Stoy,R.H., Ann.Cape Obs., 20, 1958.
(2) Johnson,H.L. and Iriarte,B., Lowell Obs.Bull.,No.91,1958.

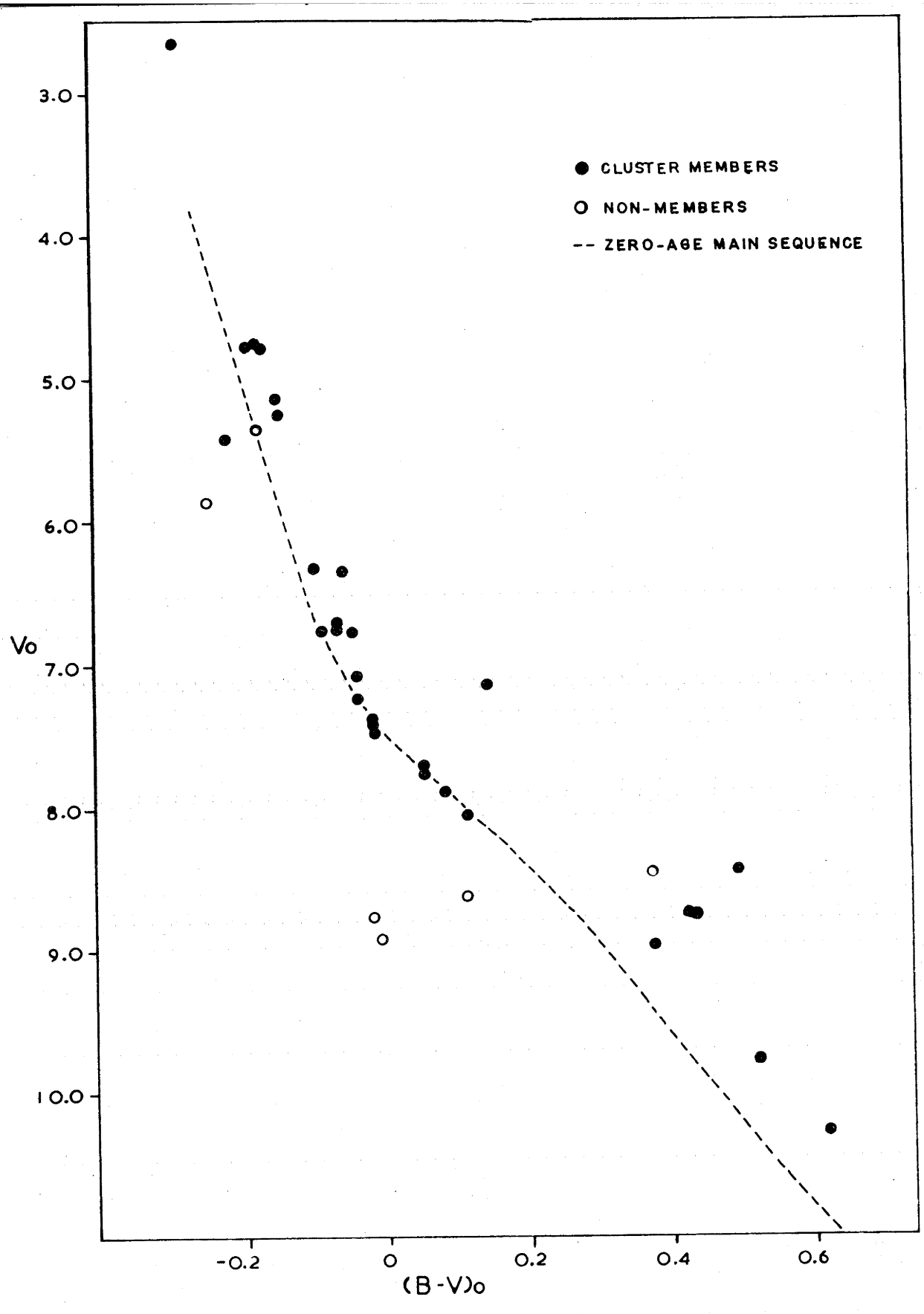

Fig.7. Colour-magnitude array, corrected for the effects of absorption, of stars numbers 1-33b.

incompleteness of the survey for cluster members.

As the brightest members of the cluster are above the main sequence, due to the effects of evolution, their luminosities do not correspond to the absolute magnitudes of the calibration in terms of spectral and luminosity classification (Johnson and Iriarte, 1958). In view of this, a spectroscopic parallax was not obtained. The same effect is encountered for the faint stars that are above the main sequence, although until their radial velocities or proper motions are considered, it cannot be ascertained whether they are cluster members or foreground objects.

On the visual, blue and objective prism Schmidt plates, an area of sky $1\frac{3}{4}^{o}$ in diameter was examined for the presence of fainter members. Stars brighter than V = 11.5 were chosen if the following conditions were satisfied:

(a) their values of (B-V)o derived from spectral types are similar to those of B-V, i.e. little reddening.

(b) their values of V are consistent with those expected for cluster members of similar spectral type. To effect this at faint magnitudes, it was assumed that the gravitational contraction point occurs on the cluster main sequence at V = 8.5 approximately, and that the shape of the colour-magnitude array is similar to that of NGC 2264 (Walker, 1956[1]). In fig.8, the area between the zero-age main sequence and the added curve leaving it at V = 8.5 is that in which the fainter cluster members would be located on these assumptions.

The selected stars and their photographically-determined magnitudes are listed in table 3; the columns are:

(1) Walker,M.F., Ap.J., Supp., 2, 356, 1956.

(1) The number of the star in the survey.
(2) The HD or HDE number of the star.
(3) V.
(4) B-V.
(5) Its spectral type - either that listed in the Henry Draper Extension or that obtained from the objective prism plate.

The method of selection is artificial, in reality, as members were chosen by the adoption of a colour-magnitude array that they should define. Also, the shape of the cluster array that has been suggested by Walker is not well-established.

The total suggested cluster membership is shown in fig.8. Probable members are shown as filled circles, additional photoelectrically-measured stars as open circles, and those measured photographically as dots. To the first grouping has been fitted the Zero-age main sequence. The additional curve leaving the main sequence at V = 8.5 has been mentioned previously. Despite the fact that many of the stars in table 3 may be field stars, there is still the deficiency, mentioned earlier, of F stars. Attempts were made to estimate the number of members brighter than V = 11.5 by a comparison of star counts in the region of the cluster and in a nearby direction, but they were unsuccessful because of the effects of irregular background obscuration.

2. Luminosity Function

The luminosity function of the cluster is shown in fig.9, the distribution of the number of stars per unit magnitude (N[Mv]) with absolute visual magnitude (Mv). The broken line for M_V greater than 3 (V greater than 9) represents the fainter part of the cluster population; as it is based mainly on photographic measurements, it

TABLE 3

Possible members observed photographically.

No.	HD/HDE	V	B-V	SP
67		10.75	1.19	K
68		11.01	1.44	K-M
69	308023	9.80	0.96	KO
70	307885	10.83	1.17	KO
71	308011	9.82	1.16	KO
72		10.42	0.53	GO
73	307942	10.03	0.42	F5
74	307944	9.40	1.07	KO
75		10.93	0.69	GO
76		11.46	0.83	G
77	307918	10.72	0.88	G
78	307938	10.48	0.57	GO
79	307929	10.65	1.03	K2
80		10.96	1.10	G7
81	307960	11.33	0.91	G5
82	307936	10.87	0.70	F7
83	307955	10.84	0.95	KO
84	307969	10.98	1.32	K7
85	307979	10.96	0.68	GO
86	307956	10.96	0.64	G
87	308016	10.59	0.98	K2
88		10.64	0.56	GO
89		10.87	1.55	K5
90		10.12	1.26	K2
91		10.70	1.08	G5-KO

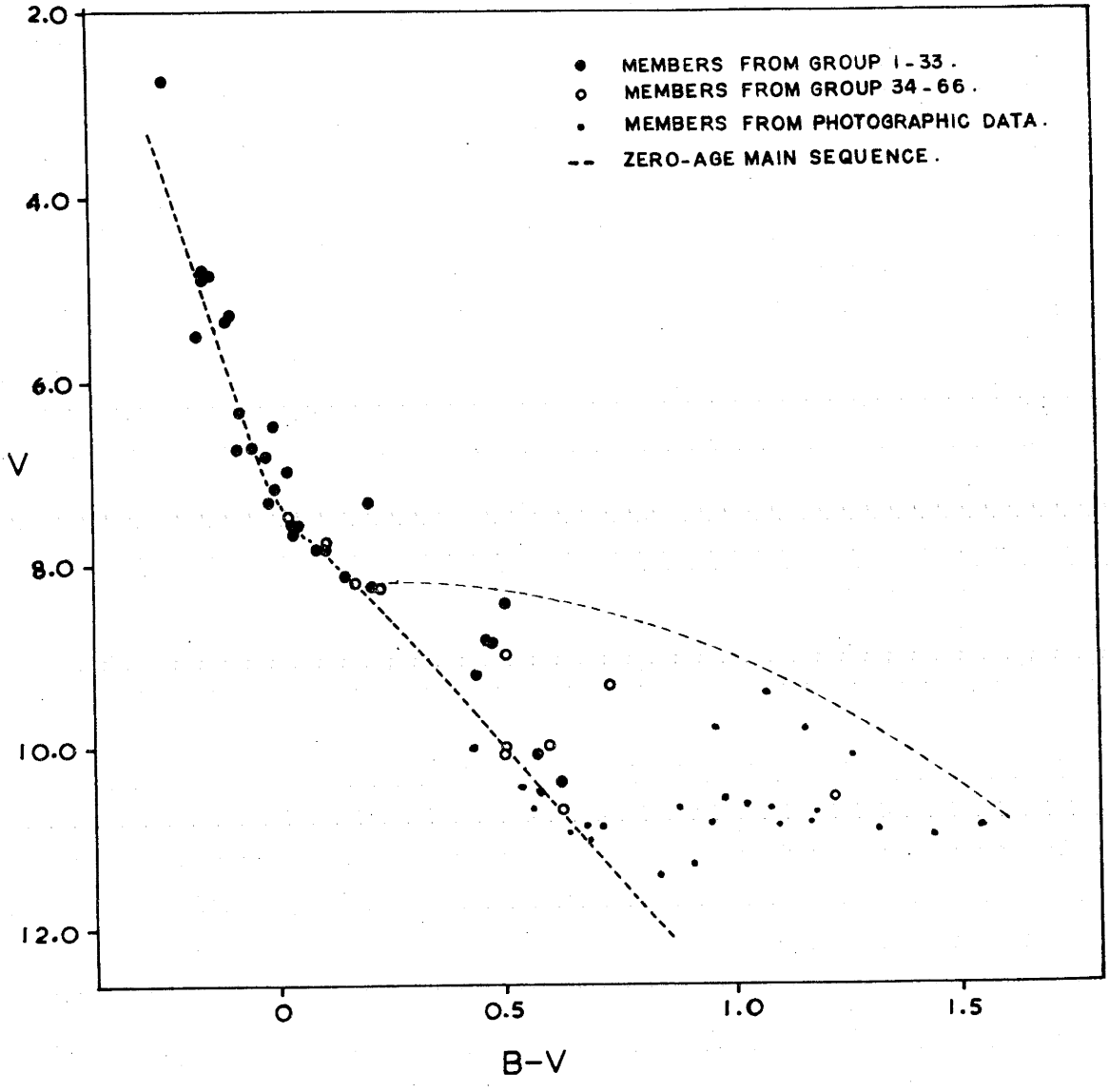

Fig. 8. Colour-magnitude array of IC 2602.

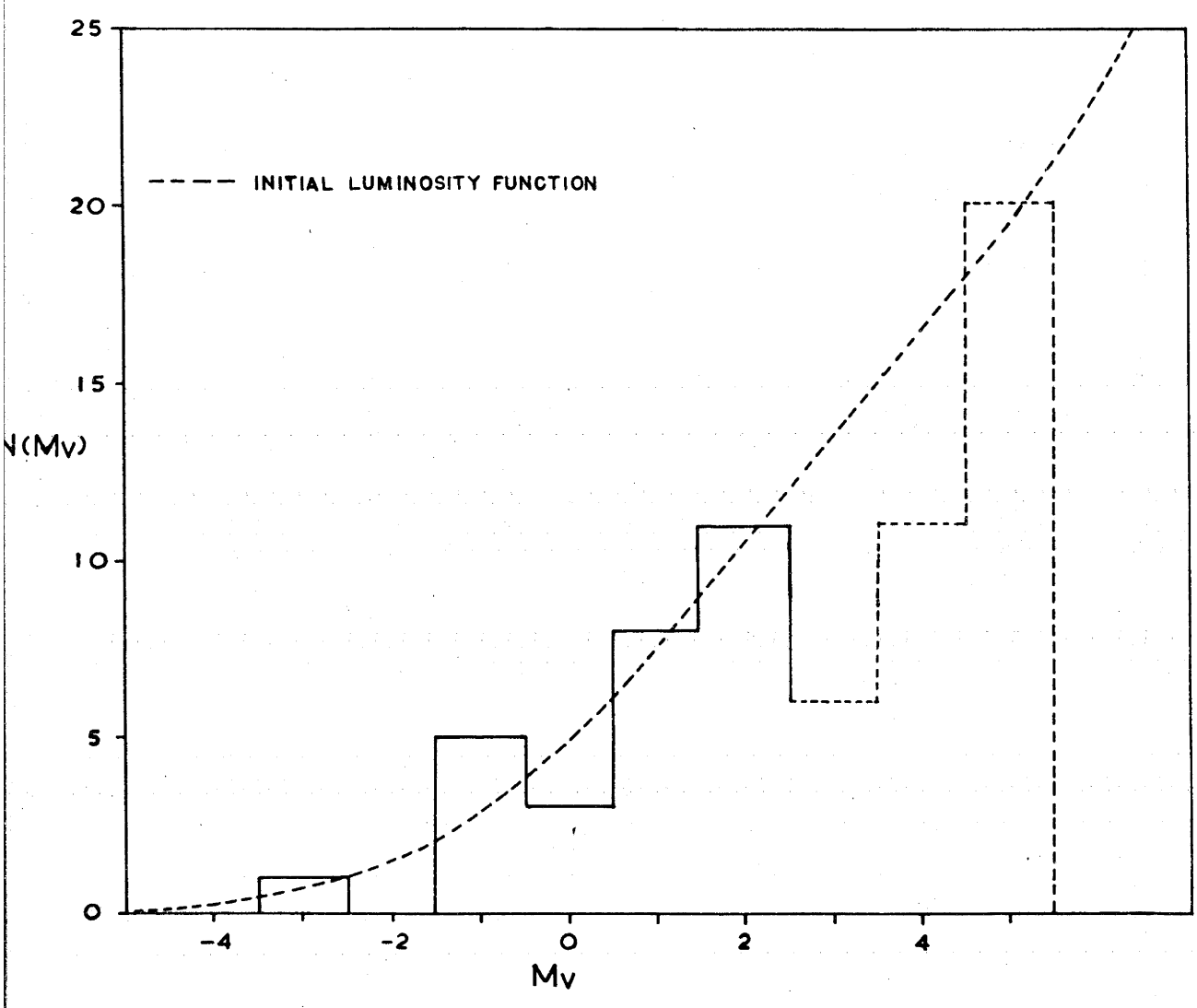

Fig. 9. Luminosity function of IC 2602.

is more uncertain than the brighter region. The curve in the figure represents the Initial Luminosity Function adopted by Limber[1]. It was normalized to the cluster so that the number of members it predicts between the absolute magnitude limits $M_V = -1.5$ and $M_V = 2.5$, a range within which the observed membership is complete but has not been effected by evolution, is equal to the observed number. The adoption of the stated faint magnitude limit was justified by the fact that all stars brighter than V = 9.0 in the general direction of the cluster were observed photoelectrically and investigated for membership. Compared with the population predicted by the Initial Luminosity Function, the cluster appears to be lacking in stars of absolute magnitudes $M_V = +3$ and $M_V = +4$. This disparity is consistent with the conclusion of van den Bergh and Sher[2] that galactic clusters do not have a unique luminosity function.

3. Age of the Cluster.

The cluster's age can be derived from two observable features:

(a) the absolute magnitude of the brightest star near the main sequence.

(b) the position on the main sequence below which stars are still in the process of gravitationally contracting on to it.

The two methods have been discussed in chapter 1.

The brightest star near the main sequence, Theta Car (number 18), has an absolute magnitude $M_V = -3.3$. It is already above the zero-age main sequence due to the effect of evolution; if one assumes that it has moved almost

(1) Limber,D.N., Ap.J., 131, 168, 1960.
(2) van den Bergh and Sher,D., Pub.David Dunlap Obs.,Vol.2, 203, 1960.

vertically from the main sequence, its 'zero-age' absolute magnitude is $(M_v)_o = -2.8$. According to the results of recent calculations of star models (Limber, 1960), such a star would attain an absolute magnitude of $M_v = -3.9$ in a period of 1.2×10^7 years after its formation, before the hydrogen in its core is exhausted and evolution from the neighbourhood of the main sequence begins. Therefore, the age of the cluster is approximately 10^7 years.

The cluster main sequence appears to terminate at $V_0 = 8.7$ i.e. $M_V = 2.8$, equivalent to a star of mass $1\frac{1}{2}$ solar masses. Henyey, Le Levier and Levee[1] have shown that a star of this mass contracts gravitationally on to the main sequence in a time of 8×10^6 years. If it is assumed that the lack of stars on the main sequence at fainter magnitudes is due only to the fact that they are still undergoing this process, the derived age of the cluster would be 8×10^6 years, a value comparable with that previously obtained. However, the termination may be due in part to a deficiency, in the cluster population, of stars with magnitudes between $V_0 = 8.5$ and $V_0 = 10.0$, although it is significant that all members in this range are above the zero-age main sequence. It must be concluded that the 'contraction position' is ill-defined, and that the determined age is possibly an underestimation of the real value.

4. Proper Motions.

Proper motions for eighteen of the cluster stars are listed by Boss[2]. The mean values, corrected to the N30 system with the tables listed by Morgan[3] . are:

$$\bar{\mu}_\alpha = -0^s.0019 \pm .0008/\text{yr}, \quad \bar{\mu}_\delta = +0''.000 \pm .010/\text{yr}.$$

(1) Henyey,L.G.,LeLevier,R. & Levee,R.D.,P.A.S.P.,67,154,1955.
(2) Boss,B., General Catalogue,2-3,1936.
(3) Morgan,H.R., Ast.Pap.Amer.Eph., 13, 109, 1952.

Cape proper motions reduced to the N30 system were employed by Braes[1] to derive means based on a greater number of stars:

$-0^{s}.0011$/yr.; $+0''.008$/yr.

At 150 parsecs in the direction of the cluster, the apparent proper motions due to solar motion are:

$-0^{s}.0015$/yr., + $0''.007$/yr. (for a solar velocity of 19.6 km/sec with apex at A = 271°, D = $+30^{\circ}$).

Therefore, most of the apparent motion of the cluster is due to the effects of solar motion. For this reason, it is difficult to detect members using the criterion of common proper motions - the General Catalogue lists many stars, obviously non-members, but situated in the same direction, that have proper motions comparable with those of cluster stars.

From an analysis using the proper motions of the General Catalogue, Markarian[2] has suggested that the cluster has an age of 3×10^{5} years and is expanding. The results appear doubtful as the expansion age is considerably smaller than the value derived in the present study. A more thorough proper motion analysis is being carried out by Braes (unpublished).

5. The Cluster Mel 101.

The cluster Mel 101 ($\alpha(1950) = 10'41$, $\delta(1950) = -64^{\circ}.9$) is located in the same direction as IC 2602. It is a small compact group of stars approximately 10' in diameter. The cluster is shown in plate (2), an enlargement of plate (1); the 60 stars investigated are those assigned numbers. Of this total, 19 brighter than V = 14.3 were observed photoelectrically with the 50-inch telescope in 1961; values of V and B magnitudes for the remainder were obtained

(1) Braes,L.L.E., Information kindly supplied to the author.
(2) Markarian,B.E., Buir.Soob., 11, 19, 1953.

Plate (2) A 20/26-inch Schmidt photograph in visual light, showing the cluster Melotte 101. North is at the top, East is to the left. The scale of the field is 3'/inch.

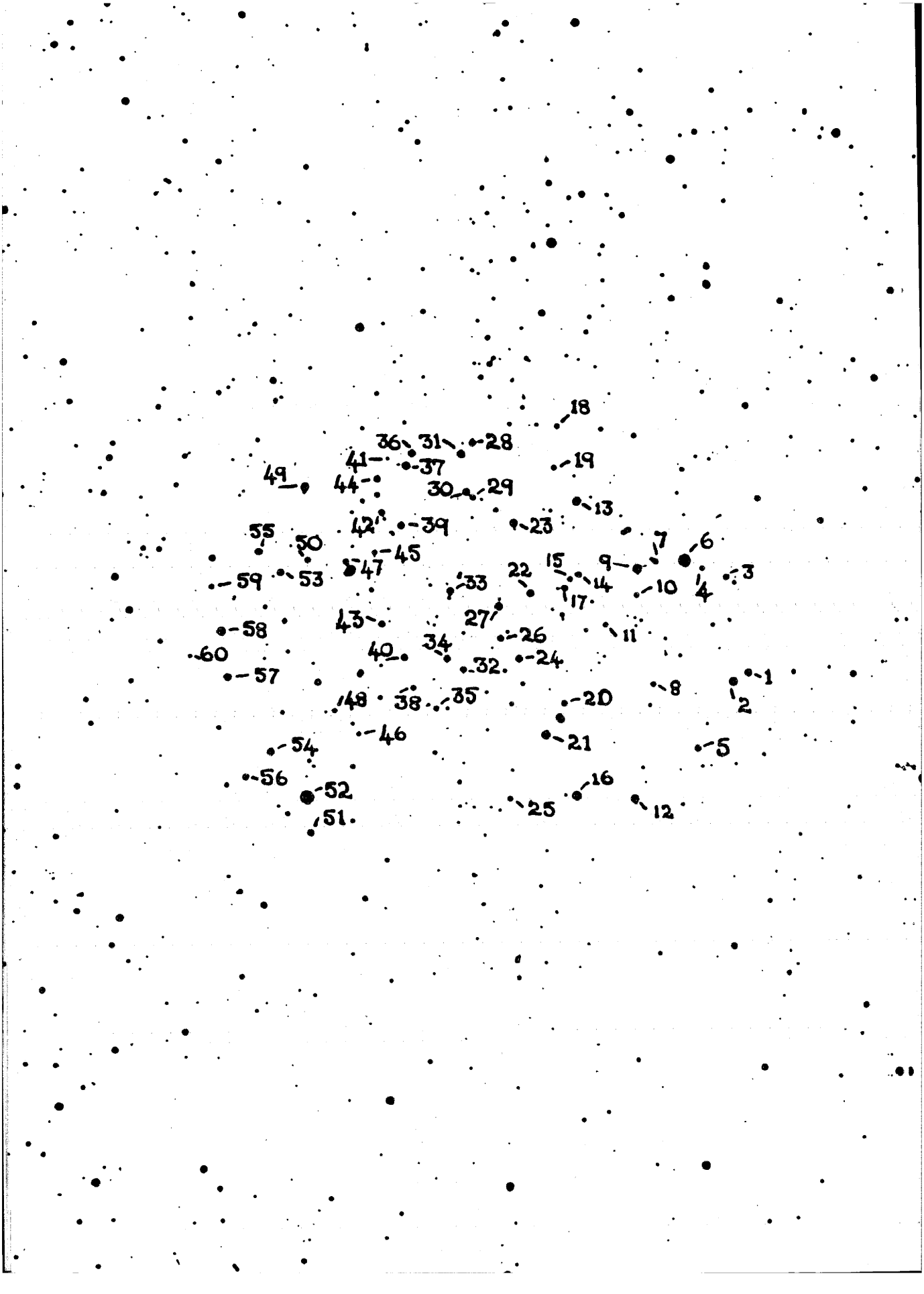
18
36
31
28
41
37
19
49
44
30
29
13
55
42
39
23
7
6
50
45
15
9
47
22
3
59
53
33
14
10
4
17
43
27
58
26
11
34
60
40
24
32
57
1
8
48
38
35
20
2
46
21
54
5
56
16
52
25
12
51

from the Schmidt plates used for the study of IC 2602. The results of the investigation are shown in table 4, the columns of which are:

1) Star number.
2) V.
3) B-V.
4) U-B, if the star was observed photoelectrically.
5) The number of photoelectric observations.
6) Approximate spectral type, derived from the "Q" method where possible, the HDE, or objective prism spectra.

The colour-magnitude diagram of the cluster is shown in fig.10; the stars observed photoelectrically are represented by filled circles, those photographically by open circles. For the stars of spectral type earlier than A0, application of the "Q" method gives a colour excess, $E_{B-V} = 0^m.28$ i.e. a mean visual absorption $A_V = 0^m.84$. A fit of the zero-age main sequence to that of the cluster suggests that the stars are at a distance of 1200 parsecs from the sun. Because of the dispersion of the positions of stars in the colour-magnitude diagram, this value is only approximate. Assuming that the brightest main sequence star, of spectral type B8, is a member, the age of the cluster, derived by the same method as that used for IC 2602, is approximately 10^8 years. The colour-magnitude distribution may include several field stars, but no members of IC 2602, the main sequence of which is considerably higher in the V-(B-V) diagram.

6. The Relation of IC 2602 to the Scorpio-Centaurus Association.

The Scorpio-Centaurus Association (II Sco) is a nearby group of B stars that has been studied extensively during the past few years. Many astronomers believe it to be an

TABLE 4

Stars of the galactic cluster Mel. 101

No.	V	B-V	U-B	n	Sp.
1	12.03	0.21	-0.07	1	B8
2	11.47	0.27	0.10	2	B9.5
3	12.68	0.27			
4	13.31	0.29			
5	12.43	0.43			
6	9.82	1.20	2.02	1	K7
7	13.01	0.37	0.10	1	
8	13.04	0.39			
9	11.21	0.22	-0.01	2	B9
10	13.15	0.26	0.07	1	
11	13.37	0.73	0.26	1	
12	11.59	2.14			
13	11.49	0.23			A2
14	12.75	0.37			
15	13.16	0.39			
16	11.10	0.30	0.08	2	B9.5
17	12.64	0.38			
18	13.22	0.23			
19	13.10	0.40			
20	12.83	0.21			
21	11.32	0.15			A0
22	12.09	0.31			
23	11.82	0.29			
24	11.96	1.42			
25	12.96	0.34			

No.	V	B-V	U-B	n	Sp.
26	12.46	0.30			
27	11.68	0.41			
28	12.26	0.17			A
29	13.01	0.35			
30	12.05	0.33			A
31	11.87	0.23			
32	12,62	0.36			
33	12.09	0.54			
34	12.34	0.38			
35	13.12	0.28			
36	12.18	0.17	-0.06	1	B9
37	11.80	0.15	-0.06	1	B9
38	13.11	0.42			
39	12.14	0.21			
40	12.45	1.48			
41	14.26	0.42	0.27	1	
42	12.54	0.29			
43	12.63	0.38			
44	12.52	0.29			
45	13.22	0.42			
46	13.42	0.64			
47	12.67	0.36			A2
48	13.37	0.42			
49	11.66	0.24	-0.02	2	B8
50	12.75	0.76			
51	12.47	0.35			
52	9.23	0.34	0.26	3	A2
53	12.20	0.30			

No.	V	B-V	U-B	n	Sp.
54	12.01	0.30	-0.03	1	
55	12.43	0.79	0.29	3	
56	12.75	0.34	0.06	1	
57	12.17	1.61			
58	11.43	0.52	0.26	3	A5
59	13.39	0.37	0.20	3	
60	14.05	0.64	0.28	1	

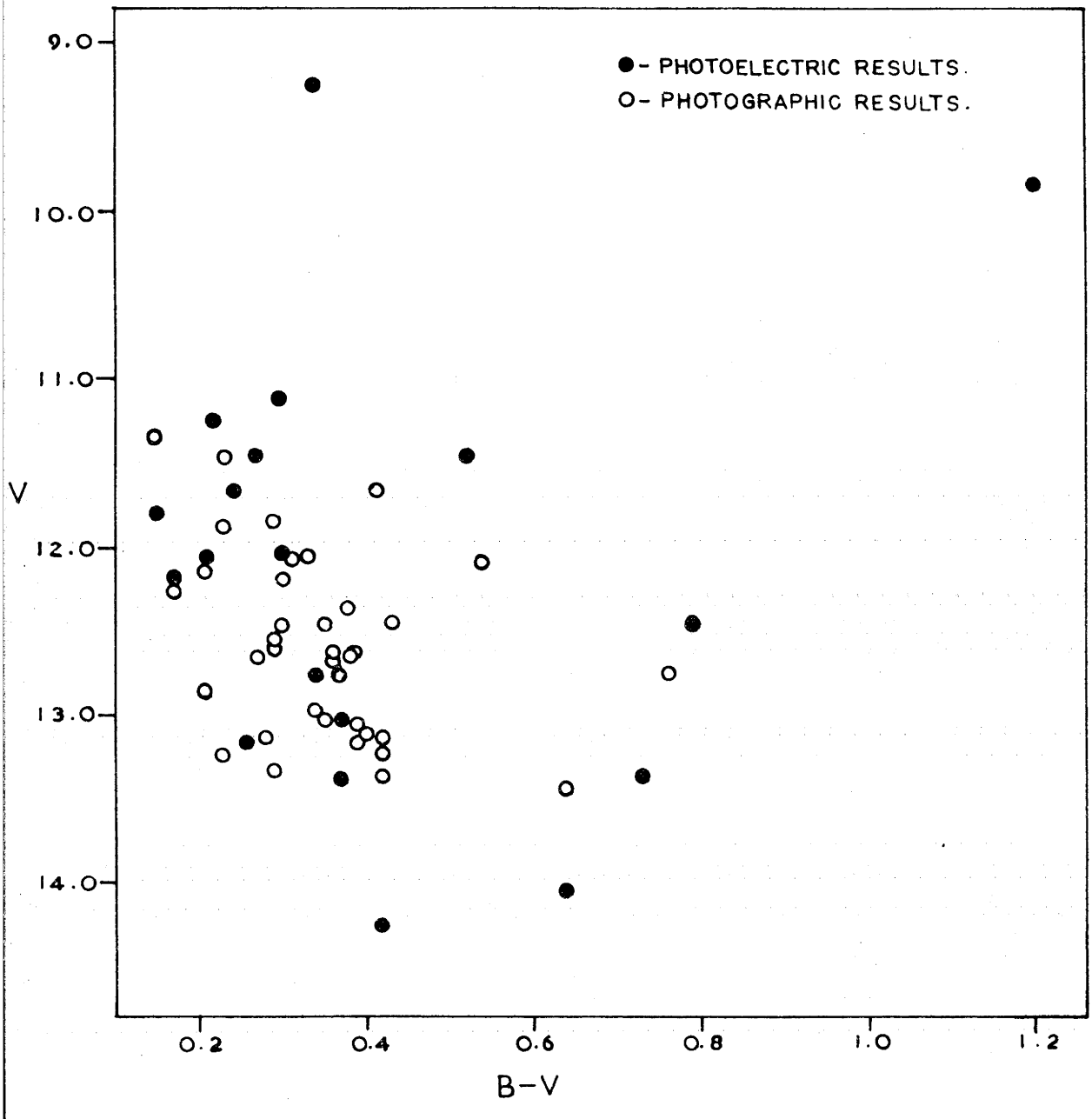

Fig.10. Colour-magnitude array of stars near Melotte 101.

isolated grouping, the members of which can be recognized by their common space motions. However, from an investigation of the distribution and motions of B stars near the sun, Eggen[1] has recently suggested that in reality, the association is not a well-defined grouping, but rather a concentration of stars in a 'local association' that is 1000 parsecs in diameter. In Eggen's opinion this concentration extends from $l^{II} = 280^{o}$, $b^{II} = -10^{o}$, to $l^{II} = 0^{o}$, $b^{II} = +10^{o}$. In the line of sight, distances of the stars range from 50 to 250 parsecs. It appears that IC 2602 is a local condensation in this grouping on the basis of the following membership criteria:

(1) Spatial Position. The cluster is located at a distance of 155 parsecs in the direction $l^{II} = 290^{o}$, $b^{II} = -5^{o}$, well within the spatial boundaries of II Sco.

(2) Space Motions.

(a) Radial velocities of 8 cluster stars have been compiled by Wilson[2]; the mean value is:

$$V_r = +24 \text{ km/sec.}$$

It is similar to the velocities of members of the association that are near the cluster (Buscombe and Morris[3]; Bertiau[4]).

(b) The cluster proper motions derived by Braes have been stated previously. In the galactic coordinate system, they correspond to:

$$\mu_l = -0''.008/\text{yr}$$
$$\mu_b = +0''.004/\text{yr}$$

The proper motions, listed by Bertiau, of the nearest stars of the association are generally more negative e.g.

(1) Eggen,O.J., (in press)
(2) Wilson,R.E., Pub.Carnegie Inst.Washington,No.601,1953.
(3) Buscombe,W. and Morris,P.M., M.N.,121, 263, 1960.
(4) Bertiau,F.C., Ap.J., 128, 533, 1958.

	μ_l	μ_b
HD 103079	-0".035/yr	-0".017/yr
HD 103884	-0".017/yr	-0".012/yr

The agreement is not particularly good, but the accuracy of Braes' values will not be known until the details are published. The mean proper motions obtained from the results listed in the General Catalogue, viz.

$$\bar{\mu}_l = -0".007/yr$$
$$\bar{\mu}_b = -0".004/yr$$

are in better agreement with those of the two stars cited.

(3) Age. The age of IC 2602 was determined on the basis of the brightest main sequence star, of spectral type B0. For II Sco, according to the catalogue of Bertiau, and the list of certain members of Blaauw[1], the brightest stars of luminosity class V are of a similar spectral type. On the assumption that the membership is complete at the high luminosity end of the main sequence, the age of II Sco is similar to that of the cluster.

(1) Blaauw, A., Pub. Kapteyn Ast. Lab. Groningen, No.52, 1946.

CHAPTER 4

A STUDY OF A VISUAL CONCENTRATION OF O AND B STARS IN ARA.

4.1 Summary.

As a result of an objective prism survey of the Southern Milky Way from Crucis to Scorpio ($l^{II} = 298^{o}$ to $l^{II} = 344^{o}$), several visual groupings of stars of early spectral types were detected. Some of these may be caused by the effects, on a reasonably uniform star distribution, of overlying interstellar matter of uneven density, and may not be true associations.

The results are presented of a photoelectric and spectroscopic study of one of the detected visual concentrations located in Ara ($l^{II} = 337^{o}$, $b^{II} = -1.5^{o}$). From an analysis using three-colour photoelectric observations of 127 stars, for 81 of which spectra were obtained, it is found that there is a large grouping of early-type stars at a distance of 1400 parsecs. In addition, there are several stars of high luminosity at distances in excess of 2000 parsecs; there may be a concentration at 3500 parsecs. Photoelectric and photographic studies of two young clusters in the region, NGC 6193 ($l^{II} = 337\overset{o}{.}9$, $b^{II} = -1\overset{o}{.}4$) and NGC 6204 ($l^{II} = 339\overset{o}{.}4$, $b^{II} = -1\overset{o}{.}2$), show that the former is related to the nearest grouping.

4.2 Observations.

1. Photoelectric Observations.

Except for the replacement of the EMI photomultiplier with a refrigerated RCA 1P21 on the 26-inch reflector, the photoelectric equipment and reduction procedure were similar to those described in Chapter 3. A secondary

standard sequence was set up in the region of the visual early-type star grouping by means of 24 UBV standard stars observed at Mt. Bingar. An average of 13 was observed during each night of the 8 used in 1960 to produce the sequence. Extinction coefficients were determined each night. Their mean values are:

$$K_V = 0.165 \pm 0.010 \text{ (m.e.)}$$

$$K_{B-V} = 0.127 \pm 0.006 \text{ (m.e.)} - 0.040 \text{ (B-V)}$$

$$K_{U-B} = 0.329 \pm 0.015 \text{ (m.e.)}$$

These values differ from those of Chapter 3 because they were determined at a different time of the year.
The mean transformation equations are:

$$V-V_{26} = -0.082 \text{ (B-V)} + 0.421$$

$$B-V = 1.242 \text{ } (B-V)_{26} + 1.558$$

$$U-B = 0.996 \text{ } (U-B)_{26} - 1.175$$

with a mean error per measurement of

$0^m.011$ in V

$0^m.013$ in B-V

$0^m.022$ in U-B

As stated previously, the selected field stars were measured with respect to the secondary standards with the 50-inch telescope.

2. Spectrographic Observations.

The spectrographic equipment and method of classification were described in the previous chapter. Spectrograms of several of the MK standard stars listed by Buscombe[1] have been obtained by observers at Mt. Stromlo, and were available for comparison purposes. As mentioned,

(1) Buscombe,W., Mt. Stromlo Mimeogram, No. 3, 1959.

the criteria compiled in the MK Atlas[1] were employed during the process of classification.

3. Photographic Observations.

Plates in blue and visual light of two clusters (NGC 6167 and NGC 6204), that are situated in the direction of the group of stars observed, were obtained at the f/5 Newtonian focus of the 74-inch reflector by Dr S.C.B. Gascoigne. They were of 2 minutes exposure, and centred at α (1950) = 16^h32, δ (1950) = -49^o45, and at α(1950) = 16^h43, δ (1950) = -46^o57 respectively. The following filter-emulsion combinations were used:

Visual Plates	OY4 + 103a-D
Blue Plates	GG13 + 103a-O

The Iris Photometer readings were converted to the UBV system on the basis of stars for which 3-colour photoelectric magnitudes are available. The mean error of a single measurement is $0^m.04$. The limits of the photographic surveys, corresponding to the magnitudes of the faintest stars measured photoelectrically, were approximately V = 13.5 and B = 14.0.

4. Objective Prism Survey.

To investigate the distribution of early-type stars in the Southern Milky Way, objective prism plates were obtained by Dr A. W. Rodgers with the 20/26-inch Uppsala Schmidt telescope; the dispersion of the stellar spectra is 480 A/mm at H-gamma. To avoid overcrowding of spectra on the plates, exposures of 10 minutes duration were used. On the plates, well-exposed spectra of stars as faint as visual magnitude 11.5 were obtained. At the stated dispersion, objective prism spectra of early-type stars have faint absorption lines of the Balmer series or uninterrupted

(1) Morgan,W.W., Keenan,P.C. and Kellman,E., 'An Atlas of Stellar Spectra,' Univ.Chicago Press, 1943.

continua, except in the cases of Of stars, where emission lines of HeII (4686 A) and NIII (4641 A) are present, and Be stars, where Balmer line emission is observed.

The aim of the study was to limit the survey to stars of spectral types equal to or earlier than B3; of the 121 stars in Ara that were selected from objective prism plates, 20 were later discovered to be of later types. An approximate classification was accomplished by a comparison with the spectra of stars that are assigned spectral types in the Henry Draper Extension[1].

4.3 Results.

1. The Early-Type Star Survey.

A spectral survey for the detection of early-type stars was carried out in the Southern Milky Way, extending from $l^{II} = 298^{o}$ to $l^{II} = 344^{o}$ and between $b^{II} = +4^{o}$ and $b^{II} = -4^{o}$. The derived distribution is shown in fig.1 and 2; new galactic coordinates are marked on the diagrams. The continuous lines represent the approximate limits, obtained from the mosaics of 'An Atlas of H-Alpha Emission in the Southern Milky Way,'[2] of areas of heavy obscuration. In the distribution of stars, there are possible visual groupings at:

(1) $l^{II} = 304^{o}$, $b^{II} = 0^{o}$;

(2) $l^{II} = 314^{o}$, $b^{II} = -0.5^{o}$;

(3) $l^{II} = 327^{o}$, $b^{II} = -1.0^{o}$;

(4) $l^{II} = 332^{o}$, $b^{II} = -2.5^{o}$;

(5) $l^{II} = 337^{o}$, $b^{II} = -1.5^{o}$;

(6) $l^{II} = 344^{o}$, $b^{II} = +1.0^{o}$.

(1) Cannon,A.J. and Mayall,M.W., H.A., 112, 1949.
(2) Rodgers,A.W.,Campbell,C.T.,Whiteoak,J.B.,Bailey,H.H. and Hunt,V.O., 'An Atlas of H-Alpha Emission in the Southern Milky Way,' 1960.

Fig.1. Distribution of early type stars between $l^{II}=298°$ and $l^{II}=322°$. The continuous lines represent the limits of heavily-obscured regions.

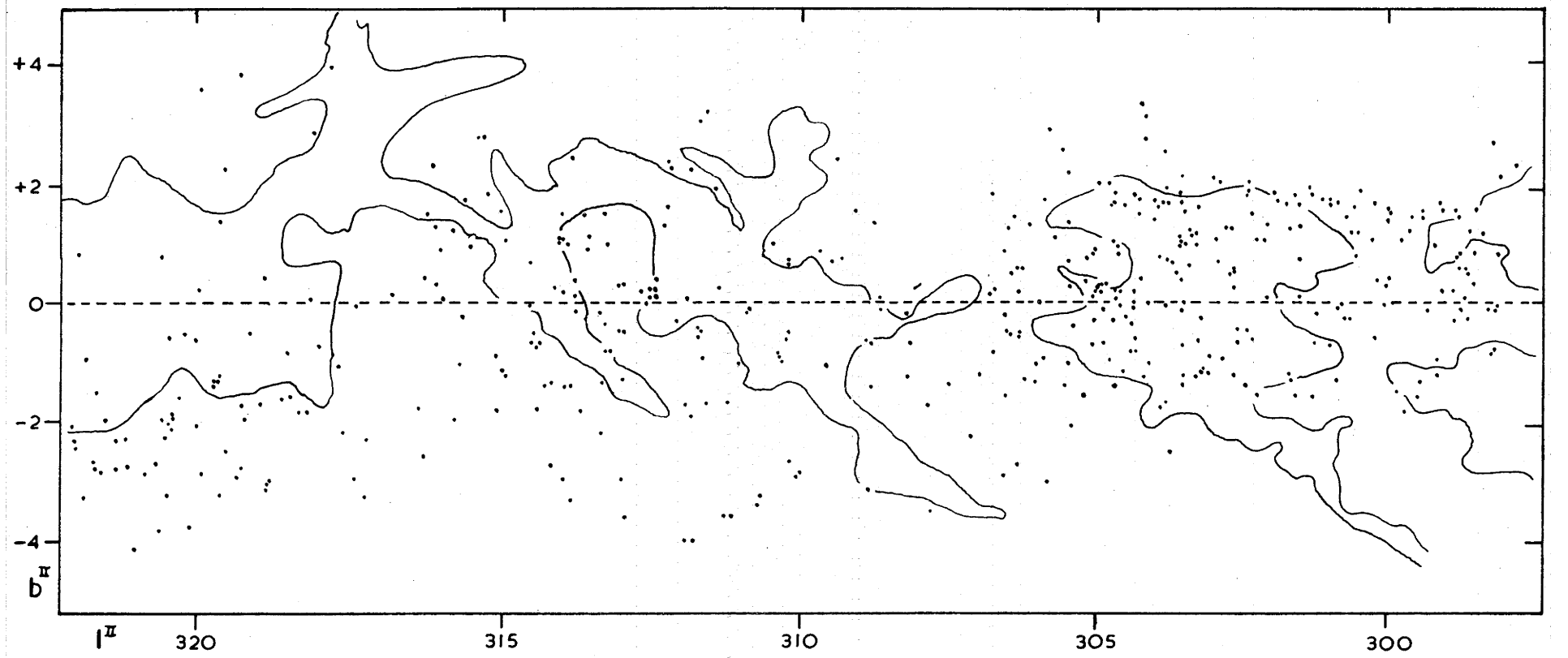

Fig.2. Distribution of early-type stars between $l^{II}=319°$ and $l^{II}=343°$.

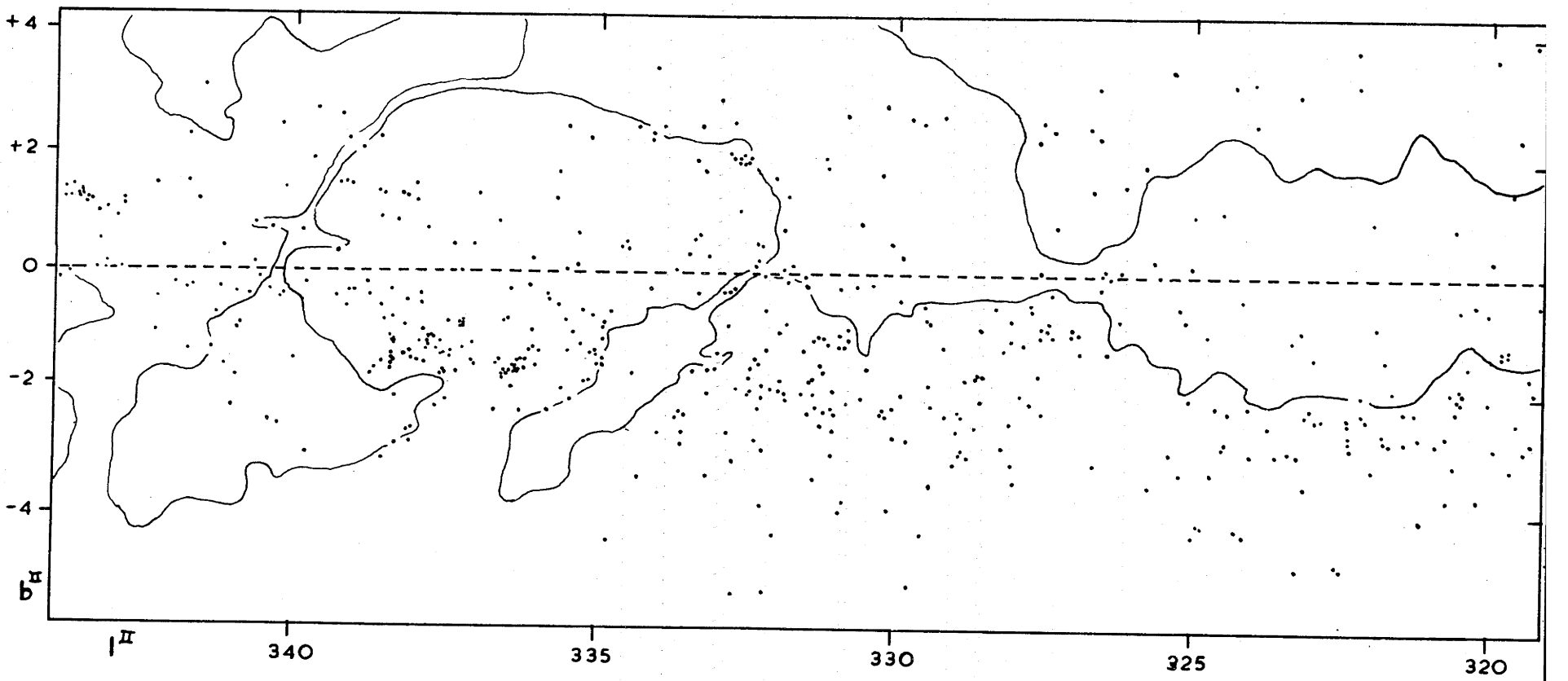

Of these, the first (I Cru association) and the last (I Sco association) have been studied by Houck[1]. From the distribution of the O and B stars listed in the Henry Draper Catalogue, Pannekoek[2], in 1929, detected groupings at $l^{II} = 304^{o}$, 307^{o}, 331^{o}, 338^{o}, 339^{o}, and 351^{o}. Several of the positions agree with those listed above; any noncoincidences are due to the following reasons:

(a) the present study extends to fainter limits.

(b) it includes only stars of spectral types as late as B3. Pannekoek's investigation included stars of later types; these may be older and have a distribution that differs from that of early-type stars.

In the catalogue of associations of Schmidt[3] are listed I Cru, the grouping at $l^{II} = 337^{o}$ (I Ara), and I Sco.

Of the detected groupings, it is difficult without further investigation to decide which are true associations and which are concentrations caused by the irregular distribution of overlying absorption along the Milky Way. It seems significant that, with the exception of the association I Cru which is situated partly behind an area of obscuration (Southern Coalsack) at $l^{II} = 304^{o}$, yet still appears as a grouping in fig.1, the groupings 2 - 6 are confined to parts of the Milky Way that are shown in the two diagrams to be less affected by interstellar absorption.

To study the characteristics of one of the visual groupings, that at $l^{II} = 337^{o}$, $b^{II} = -1^{o}.5$ was chosen. Of those that have not been investigated previously, it appears the most likely to be an association. In addition to the high density of early-type stars, in the direction

(1) Houck,T.E.,Doctoral thesis,Univ.Wisc.,1956, (unpublished).
(2) Pannekoek,A., Pub.Ast.Ins.Univ.Amst.,No.2,1929.
(3) Schmidt,K.H., A.N., 284, 76, 1957.

of the grouping are located two O-clusters, one of which is surrounded by ionized hydrogen; the presence of these infers that parts of the grouping at least are very young. As the Milky Way in this direction appears to be less obscured than at adjacent longitudes, there is a good chance of observing stars at large distances from the sun.

2. Description of the Field in Ara.

The nature of the field in Ara in which is situated the OB grouping is shown in plate (1), a 10-minute exposure in visual light, taken with the 20/26-inch Uppsala Schmidt telescope. The plate includes stars as faint as V = 18.5. As can be seen, parts of the region are heavily obscured by lanes of interstellar matter. According to Dreyer[1], there are four galactic clusters in the field - NGC 6167 (α(1950) = $16^h30.8$, δ(1950) = $-49^\circ40$), NGC 6193 (α(1950) = $16^h37.8$, δ(1950) = $-48^\circ40$), NGC 6200 (α(1950) = $16^h40.5$, δ(1950) = $-47^\circ23$), and NGC 6204 (α(1950) = $16^h42.3$, δ(1950) = $-46^\circ56$). The first is present at the lower right-hand side of the print, the second near the centre, and the last at the top left-hand corner. The third corresponds to the region of higher star density between NGC 6193 and NGC 6204. From its appearance on the plates, it was concluded that it is not a true cluster, but rather a loose visual grouping present as a consequence of lower obscuration in this direction. The selected early-type stars (marked on plate (3)) are situated mostly in the least obscured part of the field.

The distribution of H-alpha emission is shown in plate (2), an exposure in red light (RG1 filter and 103a-G emulsion) taken with the Uppsala Schmidt telescope. NGC 6193 is embedded in the large H II region (no. 107 in

(1) Dreyer,J.L.E., New General Catalogue, 1953.

Plate (1) A photograph, taken in visual light with the 20/26-inch Schmidt, of the field in Ara in which are located the O and B stars studied. North is at the top, East is to the left. (Exposure time 10 minutes). The scale of the photograph is 20'/inch.

Plate (2) Part of the field of plate (1), taken in H-alpha light (exposure time 90 mins.) with the 20/26-inch Schmidt telescope. North is at the top, East to the left. The scale of the photograph is 20'/inch approximately.

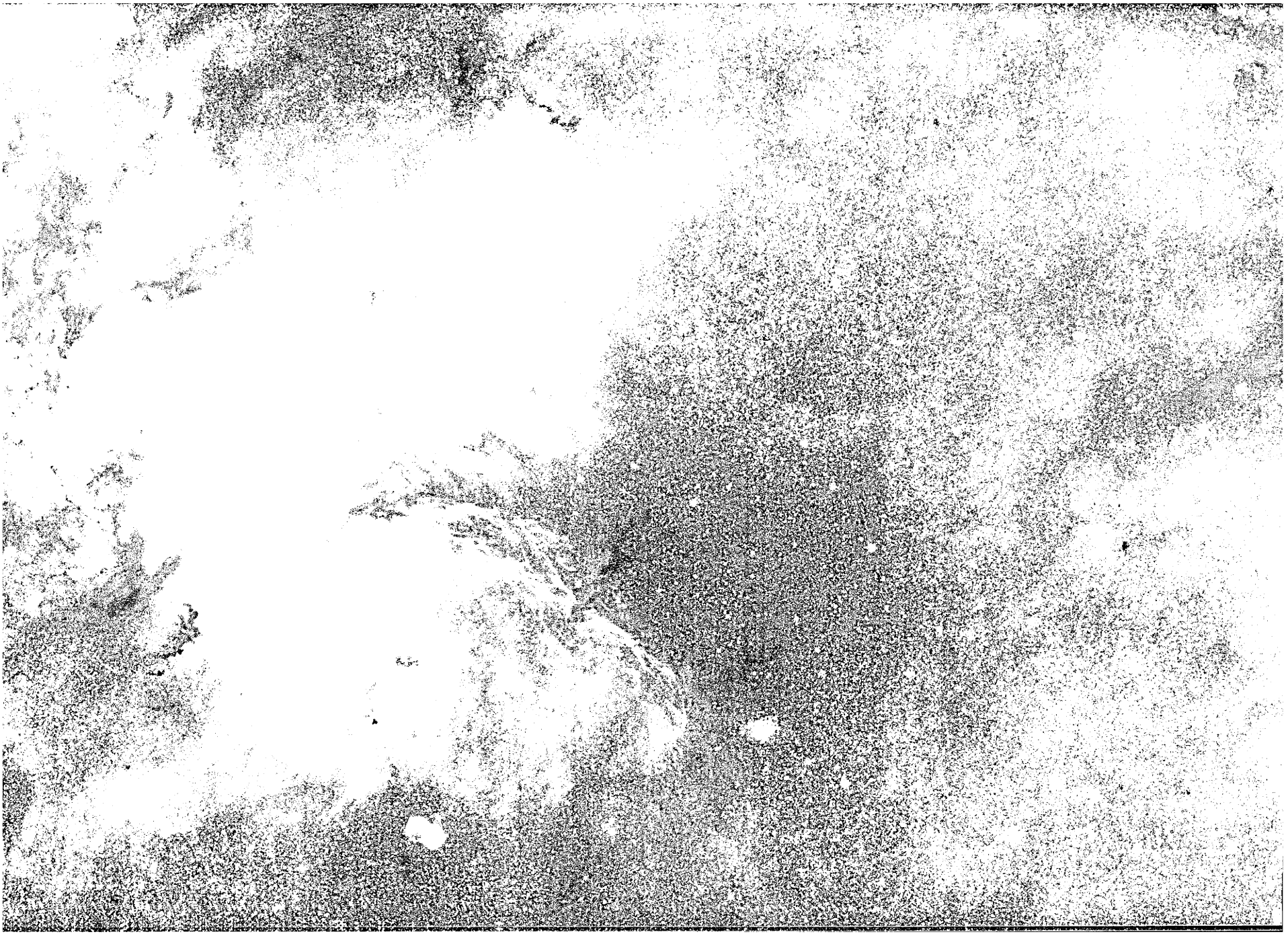

chapter 2); it is probable that most if not all the emission is due to the brightest stars of the cluster. The small but prominent "s"-shaped H II region (no. 108 in chapter 2) has been assigned a tentative distance of 1400 parsecs by Westerlund[1] on the basis of the radial velocities calculated from the interstellar lines in the spectrum of its exciting star (no. 10 of table 1).

3. The OB Grouping.

By means of the objective prism survey, 121 stars of early spectral type in a region of dimensions $4^{\circ}.5 \times 3^{\circ}$, and centred at $l^{II} = 337^{\circ}$ and $b^{II} = -1^{\circ}.5$, were chosen for investigation. In addition, several stars of late spectral type, that are situated in the same direction and have visual magnitudes comparable with those of the brightest O and B stars, were included in the study on the chance that some of them could be supergiants. The selected stars are marked on plate (3), a 10-minute exposure in visual light of the region, taken with the Mt. Stromlo 5-inch f/5.2 Zeiss astrograph. Also shown on the print are the three galactic clusters NGC 6167 ($l^{II} = 336^{\circ}.2$, $b^{II} = -1^{\circ}.4$), NGC 6193 ($l^{II} = 337^{\circ}.9$, $b^{II} = -1^{\circ}.4$), and NGC 6204 ($l^{II} = 339^{\circ}.4$, $b^{II} = -1^{\circ}.2$). In general, the selected stars are grouped near the direction of each cluster; because of this, and the fact that NGC 6193 and NGC 6204 are O-clusters, it was decided that the three clusters could be associated with the OB grouping and that a study of each would be worthwhile.

The positions, photoelectric magnitudes and colours of the selected stars are listed in table 1. The columns are:

(1) The number of the star in the present study.

(2) The HD, HDE or CPD number of the star.

(1) Westerlund,B.E., Upp.Ast.Obs.Medd.,No.133,1960.

Plate (3) The field containing the OB grouping. The photograph was taken in visual light with the 5-inch f/5.2 Zeiss astrograph. North is at the top and East is to the left.

(3) The number assigned in the Tonantzintla objective prism surveys of blue giants[1]. To differentiate between the stars listed in the two catalogues, the numbers of those in the 1954 list are preceded by "1", those of the 1955 compilation by "2".
(4) The right ascension of the star for the epoch 1950.
(5) Its declination for the same epoch.
(6) V.
(7) B-V.
(8) U-B.
(9) The number of times that the star was observed photoelectrically.

The letter "D" following the assigned number indicates that the star is double, or located in a field so crowded that the measures of its brightness may be affected by nearby stars. B and V magnitudes of ten of the stars have been obtained by Feast, Stoy, Thackeray and Wesselink[2]. The mean differences are (South Africa - Whiteoak):

in V	$+0^{m}.014 \pm 0.011$ (m.e.)
in B-V	$+0^{m}.020 \pm 0.016$ (m.e.)

In table 2 are presented the results of the spectrographic study; also listed are the magnitudes and colours corrected for the effects of absorption. The columns are:

(1) The assigned number of the star.
(2) The spectral type and luminosity class.
(3) The number of spectra inspected.
(4) The colour excess, E_{B-V}.
(5) The colour B-V corrected for absorption, $(B-V)_0$.
(6) The colour U-B corrected for absorption, $(U-B)_0$.

(1) Gonzalez,G. and Gonzalez,G., Bol.Ton.Y Tac.,11, 25, 1954; 13, 3, 1955.
(2) Feast,M.W.,Stoy,R.H.,Thackeray,A.D. and Wesselink,A.J., M.N.,122, 239, 1961.

TABLE 1

Photoelectric Measurements.

No.	Cat.No.	Ton	R.A.(1950)	Dec.(1950)	V	B-V	U-B	n
1	330842		$16^h26.7$	-49^o13	10.35	0.14	-0.37	2
2			16 27.1	-49 17	11.37	0.54	0.02	2
3	148610		16 27.9	-49 01	8.22	-0.02	-0.59	3
4			16 28.0	-49 19	11.38	0.59	0.42	2
5	330938	2-47	16 28.1	-48 53	10.43	0.52	-0.32	2
6		2-48	16 28.5	-49 21	10.90	0.50	-0.38	3
7			16 29.4	-49 27	9.85	0.84	-0.03	3
8	148851		16 29.6	-48 20	8.72	-0.03	-0.58	4
9	330928		16 29.8	-48 34	10.82	0.59	0.13	2
10	148937	1-34	16 30.2	-48 01	6.71	0.34	-0.66	6
11	330947		16 30.4	-49 20	10.52	0.90	-0.10	2
12	148989	1-35	16 30.5	-48 47	8.81	0.63	-0.40	2
13			16 30.5	-49 30	10.47	0.76	-0.29	2
14			16 30.7	-49 02	11.32	0.60	-0.28	2
15			16 30.7	-49 32	10.84	0.70	-0.37	3
16	149019	2-50	16 30.7	-49 40	7.45	0.88	0.17	5
17	149076		16 31.0	-46 54	7.48	0.47	-0.05	1
18	330950	2-51	16 31.0	-49 25	9.49	0.51	-0.51	2
19	330946	2-52	16 31.1	-49 13	8.94	0.45	-0.53	3
20	149065		16 31.1	-49 45	8.41	-0.02	-0.68	5
21			16 31.5	-49 40	10.99	0.63	-0.12	2
22			16 31.8	-47 51	11.06	0.95	-0.16	2
23	149277		16 32.2	-45.34	8.38	0.02	-0.63	1
24	149298	1-36	16 32.5	-49 09	9.90	0.45	-0.46	3
25	330044		16 33.0	-49 45	10.13	0.79	-0.08	2

No.	Cat.No.	Ton	R.A.(1950)	Dec.(1950)	V	B-V	U-B	n
26	149426	2-56	$16^h33.4$	$-48^\circ33$	9.51	0.62	-0.38	2
27			16 33.4	-49 41	11.02	0.79	-0.11	2
28	149452	1-38	16 33.5	-47 01	9.05	0.59	-0.43	3
29	330003	2-58	16 34.4	-48 06	10.00	0.53	-0.37	2
30	149589		16 34.4	-48 53	9.39	0.26	-0.55	2
31	149610		16 34.5	-48 06	9.05	0.04	-0.59	3
32	331019		16 34.6	-48 45	10.73	0.43	-0.41	3
33	149658		16 34.8	-48 42	9.63	0.39	-0.50	2
34	328530	2-60	16 35.2	-45 30	10.64	0.54	-0.61	1
35			16 35.5	-49 31	11.76	0.74	-0.21	1
36	331051		16 35.7	-49 45	9.82	0.36	-0.28	3
37	149834		16 35.9	-48 45	9.13	0.21	-0.56	4
38	331023	2-61	16 36.0	-48 58	9.67	0.54	-0.36	4
39	149855	2-62	16 36.0	-49 15	8.98	0.33	-0.47	3
40			16 36.3	-48 40	10.91	0.40	-0.33	2
41	331053		16 36.5	-49 58	10.24	0.44	-0.27	2
42			16 36.7	-48 49	10.87	0.38	-0.41	2
43			16 36.9	-48 47	10.35	0.33	-0.55	2
44			16 37.0	-48 43	10.69	0.18	-0.50	3
45	150041	1-39	16 37.1	-48 39	7.06	0.08	-0.83	13
46	$-47^\circ10939$	2-63	16 37.2	-47 39	11.13	0.70	-0.41	2
47			16 37.2	-48 39	11.21	0.22	-0.42	3
48	$-47^\circ10941$	2-64	16 37.3	-47 39	9.98	0.58	-0.46	2
49			16 37.3	-47 41	10.09	0.50	-0.42	2
50			16 37.3	-48 48	11.37	0.29	-0.31	2
51	150083		16 37.4	-47 40	7.26	0.01	-0.33	2
52			16 37.4	-48 47	11.03	0.25	-0.41	2
53			16 37.6	-48 39	9.51	0.15	-0.56	1
54			16 37.7	-48 39	8.45	0.16	-0.70	2
55	150135	1-40	16 37.7	-48 40	6.89	0.17	-0.80	2

No.	Cat.No.	Ton	R.A.(1950)	Dec.(1950)	V	B-V	U-B	n
56	150136		$16^h37.7$	$-48^\circ40$	5.62	0.16	-0.79	2
57			16 37.8	-48 27	10.10	0.39	-0.50	2
58	$-48^\circ11078$	2-65	16 37.9	-48 39	10.02	0.26	-0.57	2
59			16 37.9	-48 41	10.28	0.29	-0.50	1
60	150168	1-41	16 37.9	-49 33	5.63	-0.02	-0.87	11
61	150197	1-42	16 38.0	-47 28	9.51	0.40	-0.57	2
62	$-47^\circ10950$		16 38.0	-47 58	8.92	0.06	-0.31	2
63	$-48^\circ11082$	2-67	16 38.0	-48 42	10.35	0.24	-0.56	2
64	328686	2-68	16 38.1	-46 48	10.44	0.45	-0.34	3
65			16 38.1	-48 39	10.36	0.38	-0.36	2
66			16 38.2	-48 36	9.99	0.35	-0.40	1
67			16 38.3	-48 37	10.55	0.39	-0.37	2
68	150288	2-70	16 38.6	-46 55	8.67	0.15	-0.61	4
69(D)	150312	2-71	16 38.9	-48 56	8.92	0.42	-0.42	2
70	328678		16 39.2	-46 45	10.37	0.35	-0.35	3
71	150373	2-72	16 39.2	-47 27	9.92	0.32	-0.54	2
72	150421		16 39.5	-45 59	6.23	0.85	0.59	3
73	150422	1-43	16 39.5	-46 25	8.90	0.28	-0.60	3
74	150401	2-73	16 39.5	-48 05	9.23	0.53	-0.32	2
75	150423		16 39.6	-48 11	9.25	0.20	-0.58	2
76			16 39.6	-49 15	10.00	0.58	0.08	3
77	150500		16 40.0	-47 01	7.04	-0.03	-0.51	5
78	150533	1-45	16 40.2	-45 22	9.47	0.64	-0.46	1
79(D)	328867	2-74	16 40.2	-47 25	9.29	0.35	-0.54	2
80	328693		16 40.2	-47 34	10.25	0.37	-0.52	2
81			16 40.2	-47 46	10.53	0.67	0.36	2
82	328864	2-75	16 40.4	-47 19	9.19	0.30	-0.52	3
83	150574	1-47	16 40.5	-46 03	8.47	0.24	-0.72	4
84			16 40.6	-47 49	11.29	0.41	0.20	2
85(D)	150627	1-46	16 40.8	-47 23	9.17	0.36	-0.58	3

No.	Cat.No.	Ton	R.A.(1950)	Dec.(1950)	V	B-V	U-B	n
86			$16^h40.8$	$-47^\circ36$	10.94	0.49	-0.54	2
87	328862	2-76	16 40.9	-47 07	10.12	0.30	-0.53	3
88	328869		16 40.9	-47 24	10.04	0.22	-0.53	3
89			16 40.9	-47 43	11.28	0.30	-0.45	3
90	150658		16 41.0	-46 57	8.87	0.13	-0.40	10
91	328811		16 41.1	-46 12	10.89	0.28	-0.47	3
92	150675		16 41.1	-47 34	7.07	1.20	1.08	9
93			16 41.1	-48 02	11.14	0.36	-0.53	2
94(D)			16 41.2	-46 29	11.32	0.35	-0.18	3
95	328870	2-69	16 41.2	-47 26	10.63	0.34	-0.55	2
96			16 41.5	-48 57	10.68	0.88	-0.09	3
97			16 41.6	-47 28	11.30	0.38	-0.47	2
98	328806		16 41.7	-45 58	11.16	0.34	-0.42	3
99	328865	2-77	16 41.9	-47 17	10.80	0.38	-0.48	3
100	328833		16 42.0	-46 41	10.68	0.29	-0.35	3
101			16 42.1	-47 49	9.79	0.62	-0.34	3
102	150884		16 42.4	-46 24	7.01	0.87	0.49	3
103	150897		16 42.5	-46 27	6.47	0.10	0.04	3
104			16 42.7	-46 55	10.91	0.36	-0.52	3
105			16 42.8	-47 00	10.49	0.59	0.10	1
106	328856	1-49	16 42.8	-47 01	8.50	0.44	-0.55	17
107	328872	2-79	16 42.8	-47 36	10.05	0.37	-0.44	4
108			16 42.9	-47 01	10.27	0.31	-0.59	3
109	$-46^\circ11017$	1-50	16 42.9	-47 01	9.18	0.40	-0.57	3
110	150958	1-51	16 42.9	-47 01	7.31	0.35	-0,63	14
111			16 43.0	-47 23	10.63	0.53	-0.39	2
112	328871	2-80	16 43.0	-47 26	10.38	0.44	-0.40	2
113	151018	2-81	16 43.2	-45 48	8.67	0.63	-0.42	4
114	151040		16 43.4	-46 05	9.98	0.23	-0.29	3
115	328857	2-82	16 43.7	-47 16	9.95	0.52	-0.43	3

No.	Cat.No.	Ton	R.A.(1950)	Dec.(1950)	V	B-V	U-B	n
116(D)	329034		$16^h43.9$	-47^o04	10.31	0.43	-0.36	2
117	151115		16 44.0	-48 16	8.13	0.41	0.00	1
118	329033	2-83	16 44.3	-47 09	9.96	0.50	-0.40	4
119	151196		16 44.5	-45 52	6.67	0.37	0.04	5
120	329032	2-84	16 44.5	-47 10	10.79	0.60	-0.30	3
121	151213	1-53	16 44.6	-47 12	7.64	0.29	-0.64	18
122	151300	1-54	16 45.1	-47 06	9.29	0.47	-0.53	8
123			16 45.3	-47 17	11.01	0.38	-0.26	3
124	151318		16 45.3	-48 13	8.29	0.03	-0.52	6
125	151475		16 46.1	-47 03	8.01	0.17	-0.53	18
126	329027	2-85	16 46.7	-47 07	9.85	0.82	-0.22	5
127	329038	2-86	16 46.9	-47 35	10.01	0.55	-0.33	2

(7) The visual magnitude corrected for absorption, V_0.

(8) The spectral type inferred from the intrinsic colours in (5) and (6), assuming that the star is of luminosity class V.

(9) The distance modulus of the star, Vo-Mv.

Following the table are notes concerning the appearance of the star spectra, together with a list of types and luminosity classes determined by other observers.

The values of E_{B-V}, $(B-V)_0$ and $(U-B)_0$ were derived by three methods:

(a) for stars of luminosity classes IV and V, and for those for which spectra are not available, by the "Q" method (Johnson[1]).

(b) for stars with higher luminosity classes, from Johnson's calibration of intrinsic colours in terms of spectral types and luminosity classes.

(c) for stars with spectral types later than A0, from the tables of intrinsic colours, compiled by Arp[2].

In column (7), $V_0 = V-A_V$, where A_V, the visual absorption, is given by the relation $A_V = 3.0\ E_{B-V}$. For the determination of the distance moduli that are listed in column (9), absolute magnitudes were obtained from:

(a) the zero-age main sequence of Johnson and Iriarte[3] (stars of luminosity class V and spectral types B0 and later).

(b) the absolute magnitudes of Johnson and Iriarte (early-type stars with high luminosity classes).

(c) the tables of Arp (stars with spectral types later than B).

(1) Johnson, H.L., Lowell Obs. Bull.,No.90, 1958.
(2) Arp, H.C., Handbuch der Physik, 51, 75, 1958.
(3) Johnson,H.L. and Iriarte,B., Lowell Obs.Bull.,No.91,1958.

TABLE 2

Spectroscopic Results.

No.	Sp.	n	E_{B-V}	$(B-V)_o$	$(U-B)_o$	Vo.	Sp"Q"	Vo-Mv
1			0.29	-0.15	-0.56	9.48	B5	
2			0.66	-0.12	-0.42	9.39	B7	
3	B3V	2	0.17	-0.19	-0.70	7.71	B3	8.8
4			0.66	-0.07	-0.22	9.40	B9	
5	B3V	1	0.76	-0.24	-0.86	8.15	B2	10.0
6			0.75	-0.25	-0.91	8.65	B1.5	
7	B3IV	1	1.06	-0.22	-0.78	6.67	B2.5	9.4
8	B5IV	4	0.15	-0.18	-0.68	8.27	B4	10.1
9			0.69	-0.10	-0.32	8.75	B8	
10	O6	5	0.65	-0.31	-1.13	4.76	O8	10.3
11			1.16	-0.26	-0.93	7.04	B1	
12	BOII	2	0.92	-0.29	-1.10	6.05	B0	11.8
13			1.05	-0.29	-1.08	7.32	B0	
14			0.84	-0.24	-0.88	8.80	B2	
15			1.00	-0.30	-1.12	7.84	O9	
16	A1Ia	3	0.84	+0.04		4.93		11.9
17	B6Ia	4	0.67	-0.08	-0.73	5.30	B4	12.2
18	B1Ve	1	0.81	-0.30	-1.11	7.06	O9.5	10.7
19	B5IV	1	0.74	-0.29	-1.08	6.72	B0	8.9
20	B2IV	3	0.20	-0.22	-0.82	7.81	B2	11.1
21			0.83	-0.20	-0.70	8.50	B3	
22			1.24	-0.29	-1.10	7.34	O9.5	
23	B2IV	1	0.23	-0.21	-0.78	7.69	B3	10.9
24	B2Vne	1	0.71	-0.26	-0.98	7.77	B1	10.3
25	B2IV	1	1.01	-0.22	-0.80	7.10	B2.5	10.3

No.	Sp.	n	E_{B-V}	$(B-V)_o$	$(U-B)_o$	Vo.	Sp"Q"	Vo-Mv
26	B0.5Ib	1	0.82	-0.20	-1.01	7.05	B0.5	13.2
27			1.02	-0.23	-0.86	7.96	B2	
28	09V	1	0.88	-0.29	-1.08	6.40	B0	11.1
29	B3IV	1	0.79	-0.26	-0.95	7.63	B1	10.3
30	B2IV	1	0.51	-0.25	-0.91	7.86	B1	11.0
31	B5V	1	0.24	-0.20	-0.75	8.33	B3	8.8
32			0.67	-0.24	-0.88	8.72	B2	
33	B2IV	1	0.65	-0.26	-0.97	7.68	B1	11.0
34			0.87	-0.33	-1.24	8.03	05	13.6
35			0.99	-0.25	-0.93	8.79	B1	
36	B3V	2	0.54	-0.18	-0.64	8.20	B4	9.2
37	B3IV	1	0.45	-0.24	-0.87	7.78	B2	10.4
38	B2V	1	0.79	-0.25	-0.93	7.30	B1	9.2
39	B1.5IV	1	0.57	-0.24	-0.87	7.27	B2	10.9
40			0.61	-0.21	-0.74	9.08	B3	
41	B2IV	1	0.63	-0.19	-0.70	8.35	B3	11.5
42			0.61	-0.23	-0.83	9.04	B2	
43			0.59	-0.26	-0.97	8.58	B1	
44			0.39	-0.21	-0.76	9.52	B3	
45	B01b	3	0.30	-0.22	-1.05	6.16	09.5	12.4
46			1.03	-0.31	-1.18	8.04	08	13.5
47			0.41	-0.19	-0.69	9.98	B3	
48	B0IV	1	0.88	-0.30	-1.11	7.34	09.5	12.3
49	B1II	1	0.74	-0.24	-1.00	7.87	B1	14.2
50			0.46	-0.17	-0.59	9.99	B5	
51	B6III	1	0.15	-0.14	-0.51	6.81	B7	8.7
52			0.45	-0.20	-0.71	9.68	B3	
53	B2IV	1	0.37	-0.22	-0.82	8.40	B2	11.6
54	B0V	2	0.43	-0.27	-1.01	7.16	B0.5	11.1
55	07	4	0.48	-0.31	-1.15	5.45	06	10.9

No.	Sp.	n	E_{B-V}	$(B-V)_o$	$(U-B)_o$	Vo.	Sp"Q"	Vo-Mv
56	O7	3	0.46	-0.30	-1.12	4.24	O9	9.7
57	B1IV	2	0.65	-0.26	-0.97	8.15	B1	12.3
58	B2V	2	0.51	-0.25	-0.93	8.49	B1	10.4
59			0.53	-0.24	-0.87	8.69	B2	
60	BOII	4	0.27	-0.29	-1.10	4.82	BO.5	10.5
61	O9.5II	1	0.70	-0.30	-1.12	7.41	BO	13.3
62	B8III	1	0.15	-0.09	-0.32	8.47	B7	9.5
63	B2IV	1	0.48	-0.24	-0.89	8.91	B2	12.2
64	B3Vnn	2	0.66	-0.22	-0.80	8.46	B2.5	10.2
65			0.59	-0.21	-0.77	8.59	B3	
66			0.57	-0.22	-0.79	8.28	B2.5	
67			0.61	-0.22	-0.79	8.72	B2.5	
68	B3V	2	0.39	-0.24	-0.88	7.50	B2	8.7
69	B1V	1	0.67	-0.25	-0.90	6.91	B1.5	9.2
70	B3IV	1	0.55	-0.20	-0.72	8.72	B3	11.2
71	B1III	1	0.58	-0.26	-0.96	8.18	B1	12.6
72	F2Ib	2	0.51	+0.34	+0.32	4.70		9.2
73	B2Vnne	1	0.55	-0.27	-1.00	7.25	BO.5	8.8
74	B3V	1	0.77	-0.24	-0.86	6.92	B2	8.1
75	B2IV	1	0.44	-0.24	-0.88	7.93	B2	11.2
76	B5III	1	0.74	-0.16	-0.59	7.78	B7.5	10.0
77	B9 pec	1	0.13	-0.16	-0.63	6.61	B4	6.3
78	BOIV	1	0.96	-0.32	-1.18	6.59	O5-O8	11.7
79	BO.5 pec	2	0.61	-0.26	-0.98	7.46	B1	11.4
80	BO.5III	1	0.65	-0.28	-1.03	8.30	B1	13.2
81			0.71	-0.04	-0.12	8.40	B9.5	
82	B1IV	1	0.55	-0.25	-0.91	7.54	B1	11.6
83	O9III	2	0.55	-0.31	-1.12	6.82	O9.5	12.9
84			0.44	-0.04	-0.10	9.97	B9.5	
85	BOIV	2	0.64	-0.28	-1.04	7.25	BO.5	12.3

No.	Sp.	n	E_{B-V}	$(B-V)_o$	$(U-B)_o$	Vo	Sp"Q"	Vo-Mv
86			0.79	-0.30	-1.12	8.57	09	
87	B0.5III	1	0.58	-0.28	-1.03	8.38	B1	13.3
88	B2V	2	0.45	-0.23	-0.84	8.69	B2	10.6
89			0.52	-0.22	-0.81	9.72	B2.5	
90	B5IV	3	0.29	-0.16	-0.58	8.00	B5	9.8
91			0.50	-0.22	-0.82	9.39	B2.5	
92	KIIb	2	0.19	+1.01		6.50		11.0
93			0.63	-0.27	-0.98	9.25	B0.5	
94			0.49	-0.14	-0.50	9.85	B6	
95			0.61	-0.27	-0.99	8.80	B0.5	
96			1.13	-0.25	-0.92	7.29	B1	
97			0.63	-0.25	-0.92	9.41	B1	
98			0.56	-0.22	-0.81	9.48	B2.5	
99	B0.5II	1	0.64	-0.26	-1.05	8.88	B1	14.4
100			0.50	-0.19	-0.69	9.18	B3	
101	B0II	1	0.91	-0.29	-1.10	7.06	B0.5	12.8
102	F8Ia	1	0.19	+0.68	+0.50	6.44		11.4
103	A1V	1	0.11	-0.01	-0.03	6.14	A0	4.8
104			0.62	-0.26	-0.97	9.05	B1	
105			0.70	-0.11	-0.38	8.39	B7.5	
106	09.5III	4	0.74	-0.30	-1.10	6.28	09.5	12.1
107	B2V	1	0.61	-0.24	-0.87	8.22	B2	10.1
108	B0.5III	3	0.60	-0.29	-1.03	8.47	B0.5	13.3
109	B0III	4	0.70	-0.30	-1.09	7.08	B0	12.6
110	06	5	0.65	-0.30	-1.10	5.36	09.5	10.8
111			0.79	-0.26	-0.97	8.26	B1	
112			0.68	-0.24	-0.88	8.34	B2	
113	09.5Iab	2	0.88	-0.25	-1.10	6.03	09	12.2
114	B3V	1	0.38	-0.15	-0.53	8.84	B5	9.8
115	B1	1	0.79	-0.27	-1.01	7.58	B0.5	

No.	Sp.	n	E_{B-V}	$(B-V)_o$	$(U-B)_o$	Vo.	Sp"Q"	Vo-Mv
116			0.65	-0.22	-0.81	8.36	B2.5	
117			0.50	-0.09	-0.33	6.63	B8	
118	B1III	2	0.76	-0.26	-0.96	7.68	B1	12.1
119	A7IV	1	0.17	+0.20	+0.08	6.16		3.7
120	B2V	1	0.85	-0.25	-0.90	8.24	B1.5	10.2
121	BOIV	4	0.57	-0.28	-1.06	5.96	BO	10.9
122	O6	1	0.77	-0.30	-1.10	6.98	O9.5	12.4
123			0.53	-0.17	-0.60	9.42	B5	
124	B3IV	4	0.21	-0.18	-0.65	7.66	B4	10.1
125	B2V	4	0.39	-0.22	-0.80	6.84	B2.5	8.7
126	BO	1	1.10	-0.28	-1.06	6.55	BO.5	
127	B2IV	1	0.80	-0.25	-0.91	7.61	B1.5	9.5

Notes on the stars in tables 1 and 2

5 Feast et al.[1] give V=10.44, B-V=0.52, B2Vn.

10 Westerlund[2] gives V=6.81, B-V=0.42, U-B=-0.65; O6 or Of, and a tentative value Vo-Mv=10.7.

18 Spectra show H , , emission. Feast et al. give V=9.68, B-V=0.46; B1Vne.

24 Spectra show H , emission. Feast et al. give V=9.94, B-V=0.45; B1:Ve.

29 Feast et al. give V=10.01, B-V=0.53; B2.5V.

45 Classified as BOII by Feast, Thackeray and Wesselink.[3]

55 Classified as O6 by Hoffleit[4], and F, T and W.

56 Classified as O7: by Hoffleit.

60 Classified as BO.5I by F, T and W.

61 Classified by Hoffleit as BOI.

64 Feast et al. give V=10.44, B-V=0.47; B2Vn.

71 Feast et al. give V=9.92, B-V=0.33; B3V.

73 Broad absorption lines; H emission.

77 Si.star.

79 Spectra show broad absorption lines with square profiles.

101 Feast et al. give V=9.79, B-V=0.67; BO.5Ia.

110 Classified as O6 by Hoffleit and F, T and W.

115 Feast et al. give V=9.96, B-V=0.57; BO.5Ia.

116 Feast et al. give V=10.33, B-V=0.46; B3V.

118 Feast et al. give V=10.01, 0.52; BO.5III.

122 Classified as O6 by Hoffleit.

125 Variable magnitude and colours.

126 Feast et al. give V=9.85, B-V=0.83; O9.5I.

Refs. 1. Feast,M.W.,Stoy,R.H.,Thackeray,A.D. and Wesselink,A.J., M.N. (in press) 1961.

2. Westerlund,B., Upp.Ast.Obs.Medd.No.133,467,1960.

3. Feast,M.W., Thackeray,A.D. and Wesselink,A.J., Mem.R.A.S., 67,51,1955; 68,1,1957.

4. Hoffleit,D., Ap.J., 124,61,1956.

The use of (a) is valid if the stars are members of associations, since they would be too young for their absolute magnitude to have changed appreciably from their 'zero-age' values as a result of evolution.

For the main sequence stars that were observed spectroscopically, the main deviation between the MK classifications and the "Q" classifications is half a spectral sub-class. The spectral types and luminosity classes assigned by Feast, Stoy, Thackeray and Wesselink to 11 of the stars are in reasonable agreement with those of the present investigation.

The colour-magnitude array of the observed stars is shown in fig.3. The distribution of the early-type stars effectively demonstrates the presence of irregular absorption in the field. The values of the corrected visual magnitude, V_0, and intrinsic colour, $(B-V)_0$, of table 2 were used to construct a colour-magnitude diagram in which the effects of absorption have been eliminated (fig.4). All stars of spectral types later than B3, and low luminosity classes, have been omitted. The stars for which no spectra were obtained, and which are assumed to be of luminosity class V, are represented by open circles, the remainder by filled circles. The figure shows a well-defined main sequence which is almost vertical for a range of six magnitudes. The distance modulus, obtained by a fitting of the zero-age main sequence of Johnson and Iriarte to the fainter stars in the diagram, is $10^m.7$. The accuracy of the fit is no better than $\pm 0^m.3$, irrespective of the uncertainties of the absolute magnitudes of the zero-age main sequence ($\pm 0^m.2$). Therefore, the derived mean distance, at least for the fainter stars of the main sequence, is 1400 $\pm$ 200 parsecs. Including the possible mean error of zero-age absolute magnitudes,

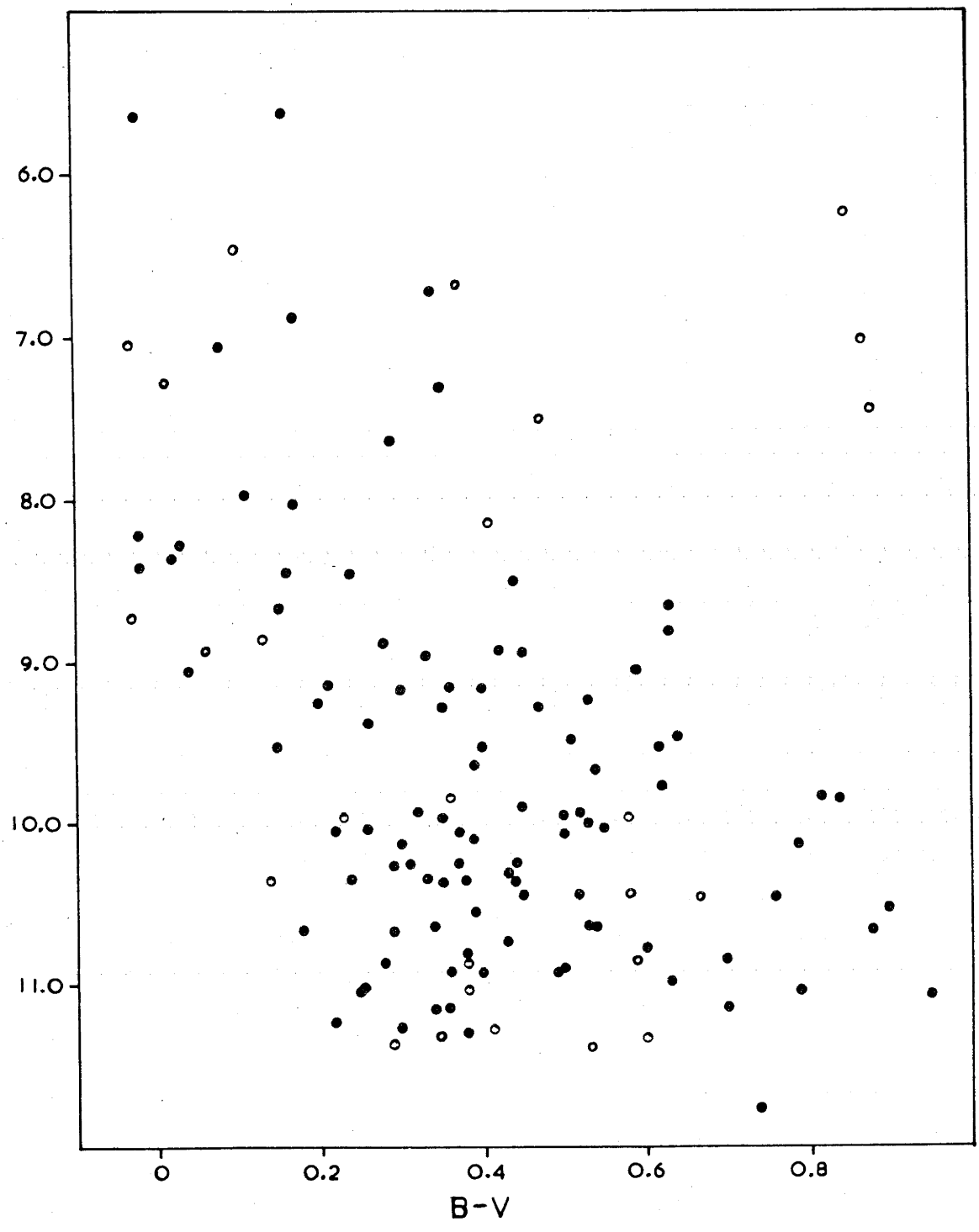

Fig.3. Colour-magnitude array of early-type stars (filled circles) and later-type stars (open circles) of table I.

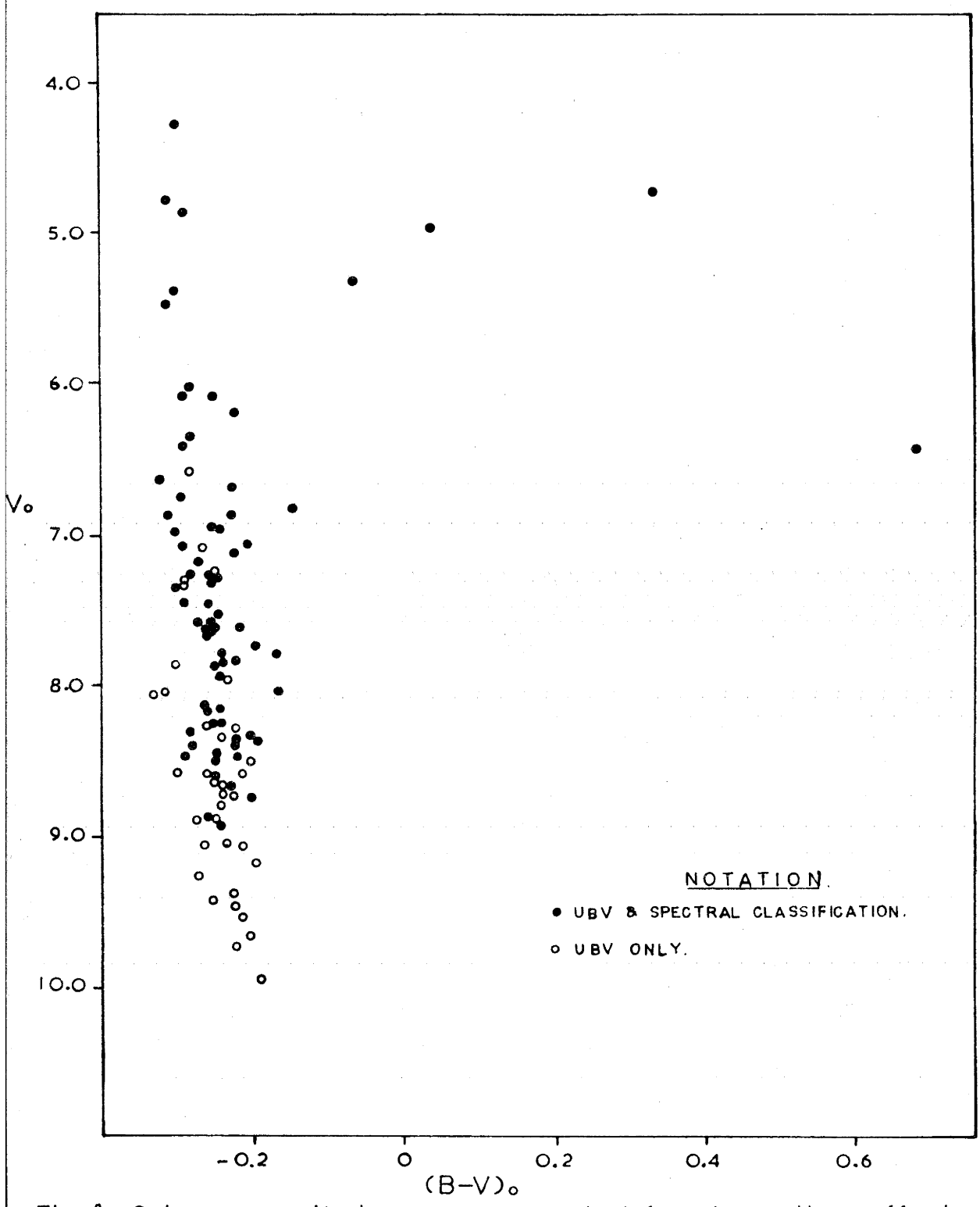

Fig.4. Colour-magnitude array, corrected for absorption effects.

the distance is accurate only to $\pm$350 parsecs.

4. More Distant Stars.

An inspection of table 2 reveals that there are several high luminosity stars that have distance moduli well in excess of $10^{m}.7$. To investigate their distribution with distance, they have been represented in a diagram showing the relationship between the distance modulus of each star ($V_o - M_v$) and the overlying absorption, A_v (fig.5). In addition, the assigned spectral type and luminosity class of each are marked on the figure. Most of the moduli are in excess of that of the OB grouping discussed previously. As might be expected, there is a general increase in absorption with increasing distance, but the great variations that occur for the nearest stars render impossible any chance of isolating groupings by the selection of stars with similar colour excesses. Before the distribution in fig.5 can be interpreted, the uncertainties in the estimated moduli should be assessed. The classification carried out by the author and that of Feast, Stoy, Thackeray and Wesselink are in agreement to within an average of half a spectral type and half a luminosity class. Excluding star no.71, which Feast et al. appear to have misclassified (both the "Q" and MK spectral types listed in table 2 disagree with that of the South African observers, and the difference between spectra of stars of types B1III and B3V is too great not to be recognized during classification of well-exposed spectrograms), the average difference in assigned distance moduli is (South Africa - Whiteoak) $+0^{m}.6$. This value is greater than that implied by the disparity in the classifications, since for main sequence stars, the author used 'zero-age' absolute magnitudes, whilst the other observers used the calibration derived from stars near the

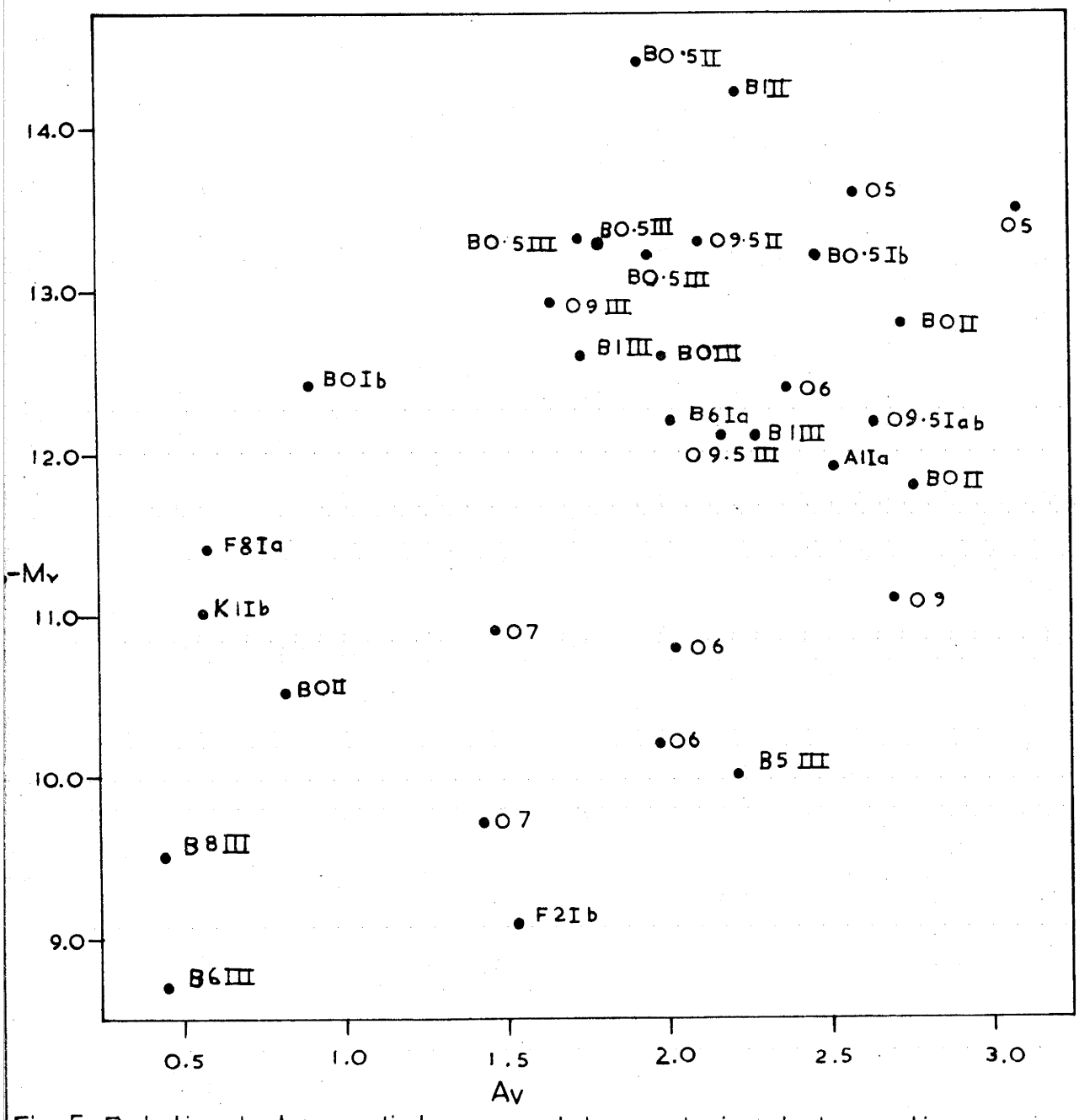

Fig.5. Relation between distance modulus and visual absorption.

sun. However, it is an indication of the limits of the accuracy with which absolute magnitudes can be derived.

In the figure, there is a broad grouping at Vo-Mv=10.5, with a mean error of $\pm 0^m.6$. This corresponds to the distance of the OB grouping discussed previously, and as the mean error is equal to the mean difference between the present classification and that of Feast et al., the stars may be more spatially concentrated than suggested by the distribution in the diagram. There is a second grouping at Vo-Mv= $12^m.7 \pm 0.5$ (3500 $\pm$ 900 parsecs). Amongst the grouping is one star classified as 09III (Mv=-6.1), three between 09.5III - 09.5Iab (Mv=-5.8 to Mv=-6.2), four between BOIII - BOIb (Mv=-5.4 to Mv=-6.2) and four between BO.5III - BO.5Ib (Mv=-4.9 to Mv=-6.2). Hence, the values of absolute magnitude vary slowly within the stated range of spectral types and luminosity classes. As a result, it is possible that the average uncertainty of the absolute magnitudes of the stars is less than ± 0.6, and that the stars are, in actual fact, spread over several hundred parsecs in the line of sight. Naturally, the whole argument relies on the accuracy of the calibration of absolute magnitudes in terms of MK spectral types and luminosity classes. The discussion shows that, in the direction of the OB grouping, there are several stars more distant than Vo-Mv=12 (2500 parsecs). The two stars, with Vo-Mv= 14.2 (7000 parsecs) approximately, must be more distant than the others if the MK classes and luminosity types are accurate within the stated uncertainties, though they may be as close as 5500 parsecs.

5. The Star Grouping, NGC 6167.

The cluster NGC 6167 (α (1950) = $16^h 30.8$, δ (1950) = $-49^\circ 40$) is located near the boundary of the selected OB grouping. It is shown as a small concentration

of stars in the lower regions of plates (1) and (3). Plate (4) is a 2-minute exposure in visual light of the cluster, taken by Dr S.C.B. Gascoigne with the 74-inch reflector. Three of the brightest stars in the field are listed in tables 1 and 2 (numbers 16, 20 and 21). With the 50-inch reflector, three colour photoelectric observations to a limiting magnitude V = 12.6 were obtained for 7 stars near the cluster. Photographic B and V magnitudes for an additional 32 stars were measured using two 74-inch plates in each colour. The colour-magnitude array is shown in fig.6. To the limits of the investigation there is little evidence of a main sequence, and it was concluded that if any cluster exists in this direction, it is considerably more distant than the early type stars which are present in the same direction, and which have magnitudes between V = 7.5 and V = 11.0. The apparent visual grouping in plates (1) and (3) may be due to the effect of interstellar matter of irregular distribution.

6. The Galactic Cluster NGC 6193.

The galactic cluster NGC 6193 (α (1950) = $16^h37.8$, δ (1950) = $-48^\circ40$) is an open grouping of stars, approximately 15' in diameter, that is present also in the direction of the OB concentration. The surrounding region of intense H-alpha emission (plate (2)) suggests that the cluster is very young. Several of the stars are listed in tables 1 and 2 (numbers 40,42,43,44,45,47, 50,52,53,54,55,56,58,59,63,65,66, and 67). Included amongst these are two O stars and a BO supergiant.

The cluster is being studied by Westerlund who, in advance of publication, has kindly made available his photoelectric magnitudes, extending to V = 12.5, and

Plate (4) A photograph, taken in visual light with the 74-inch f/5 reflector, of the field in which is situated the star-grouping NGC 6167. North is at the top, East is to the left. The scale of the photograph is 2'/inch.

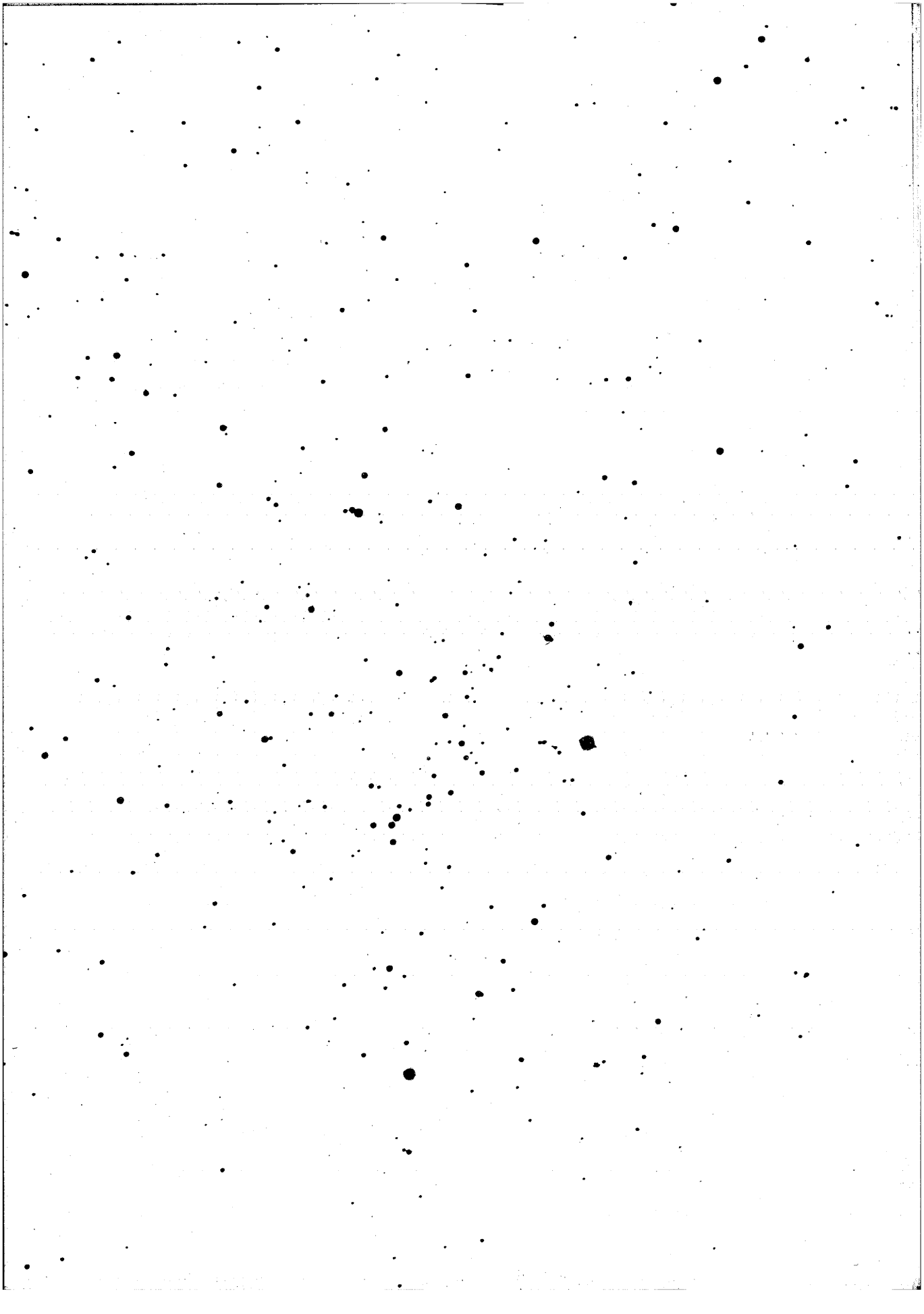

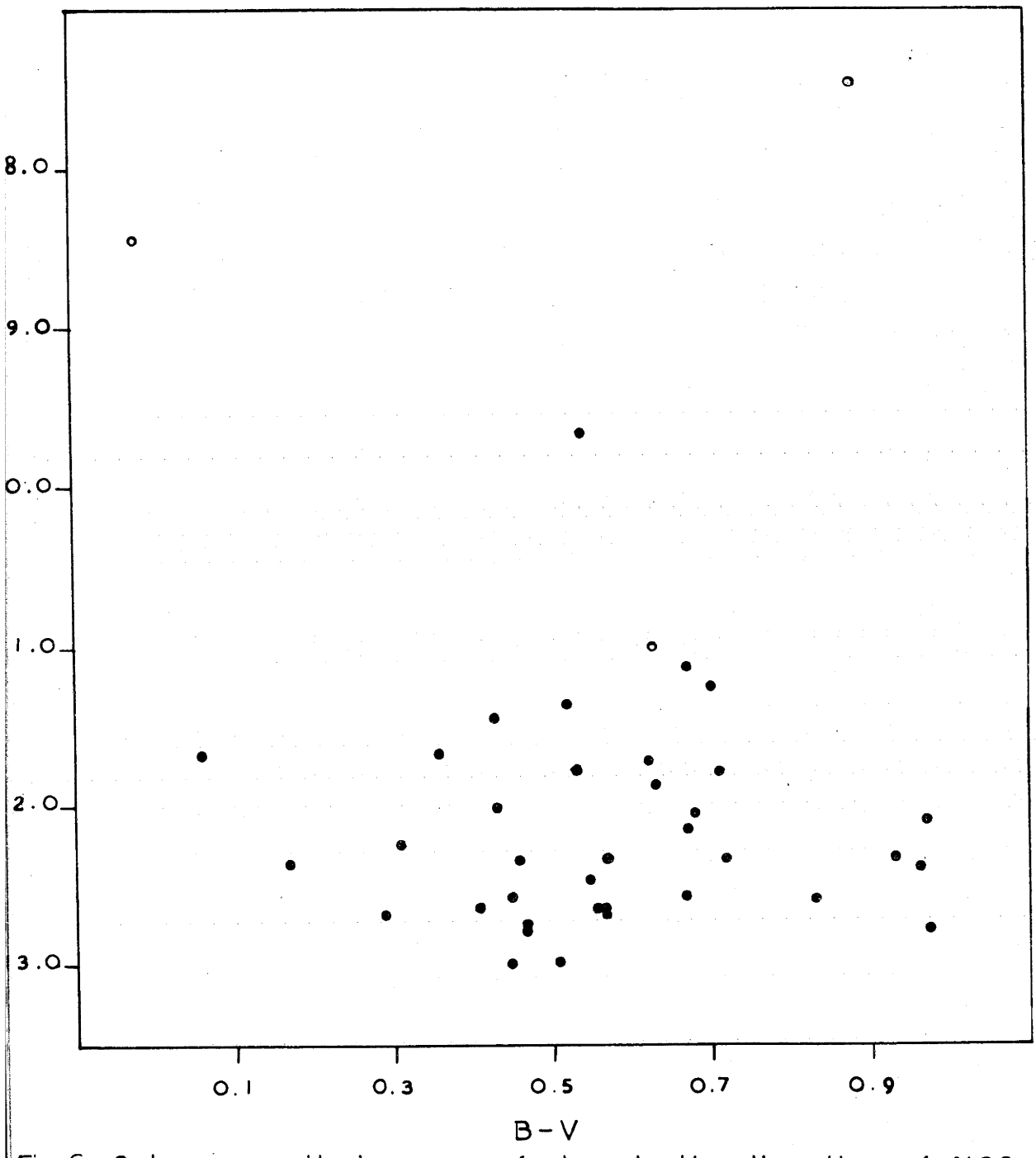

Fig. 6. Colour-magnitude array of stars in the direction of NGC 6167. Filled circles represent stars not listed in table I.

colours. From the application of the "Q" method to his colours of the early-type members, a mean cluster reddening of $0^m.49 \pm 0.07$ was obtained. A fit of the zero-age main sequence to the colour-magnitude array yields a mean modulus of $10^m.6 \pm 0.4$, equivalent to a distance of 1300 ± 300 parsecs. The brightest star near the main sequence (number 56) has an absolute magnitude of -6.4; if it is assumed that it is about to evolve, then from the calculations of the times that stars of certain masses remain near the main sequence (Limber[1]), its age, and therefore that of the cluster, is 5×10^6 years. The absolute magnitude that is assigned to this star in table 2 is fainter than that derived above; the disparity is due to the fact that the former represents the value for a main sequence O star, whilst number 56 is above the zero-age main sequence in the colour-magnitude array.

The surrounding H II region is not centred on the cluster, and although the most intense part of it surrounds, and presumably is caused by, the brightest members, it is possible that other stars of the OB grouping contribute to the ionization.

7. The Galactic Cluster NGC 6204.

A third cluster in the vicinity of the stars studied is the galactic cluster NGC 6204 (α (1950) = $16^h42.3$, δ (1950) = $-46^\circ56$). It is present on plates (1), (2) and (3) as a small group of stars on the outskirts of which is a compact set of five bright stars of early spectral type (numbers 105,106,108,109 and 110 in tables 1 and 2), possibly associated with the cluster. Plate (5) is a 2-minute exposure, in visual light, of the field containing the cluster, taken with the 74-inch reflector. Photo-

(1) Limber, D.N., Ap.J., 131, 168, 1960.

Plate (5) A photograph, taken in visual light with the 74-inch f/5 reflector, showing the galactic cluster NGC 6204. North is at the top, West is to the left. The scale of the photograph is 2'/inch.

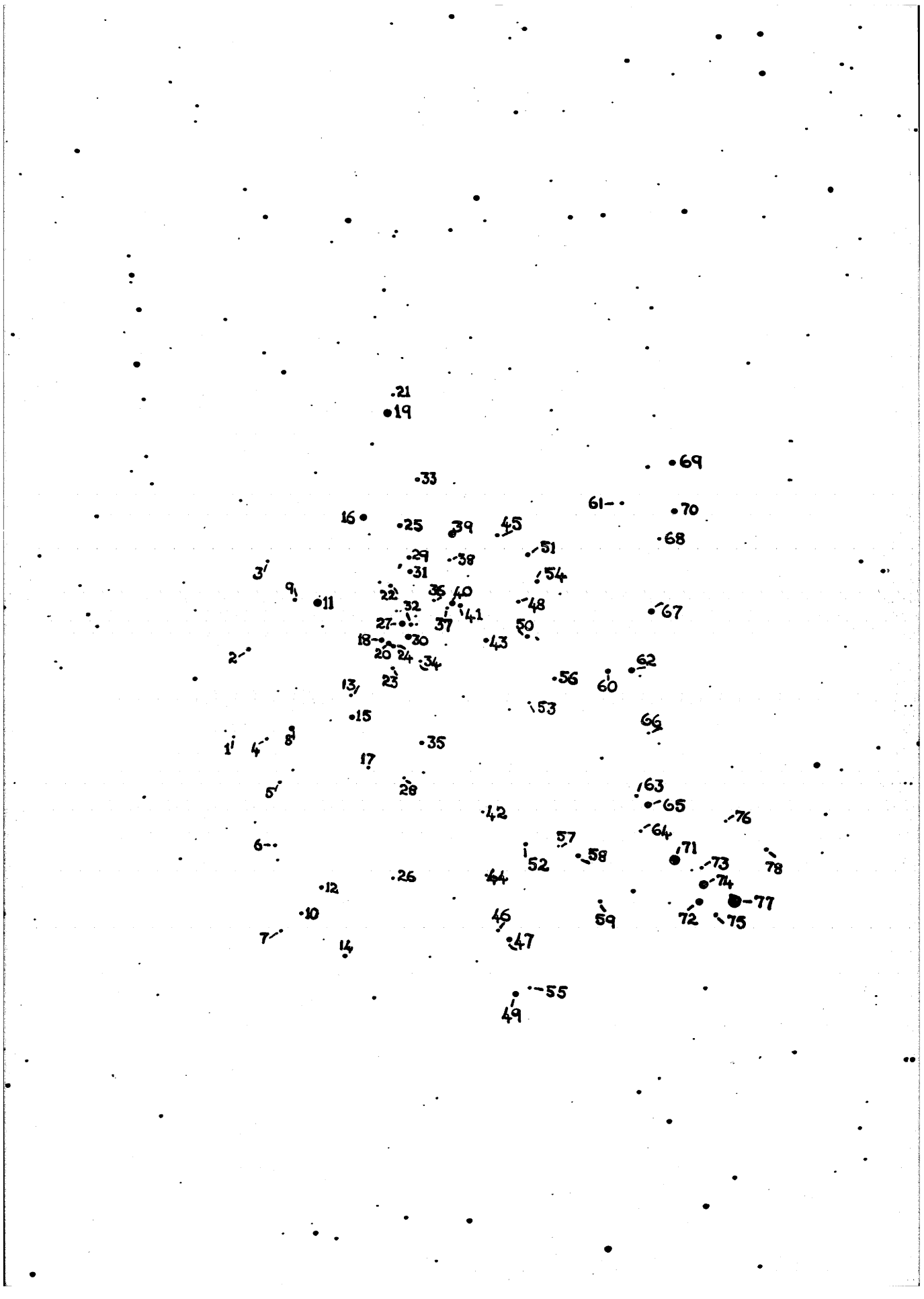
21
19
69
33
61
70
16
25
39
45
68
51
29
38
3
31
54
9
22
35
40
11
32
48
67
41
27
37
50
18
30
43
2
20
24
34
62
23
56
60
13
53
15
66
1
4
8
35
17
5
28
63
65
42
76
64
6
57
71
58
52
73
78
26
44
74
12
77
10
46
59
72
75
7
14
47
55
49

graphic B and V magnitudes for 68 stars in the field were determined; the conversion from iris photometer measurements of images on 74-inch plates to the UBV system was effected with 11 stars which also were observed photoelectrically. The brightest stars selected define the visual grouping, and consequently, most should be members of the cluster. The results are presented in table 3, the columns of which are:

(1) The number of the star marked on the plate. If the star is in table 1, the number assigned in that list is in parenthesis.
(2) V.
(3) B-V.
(4) U-B, if the star was observed photoelectrically.
(5) The colour excess, E_{B-V}, determined by the "Q" method, for main sequence stars with spectral types earlier than A0, or from the MK classification for stars of high luminosity classes.

The colour-magnitude array of the cluster, not corrected for the effects of interstellar absorption, is shown in fig.7. Photoelectric and photographic observations are represented by open circles and filled circles respectively. Although several of the stars may be non-members, there is a reasonably well-defined main sequence to V = 12.3. The stars near the most concentrated part of the clustering mostly comprise the almost vertical grouping on the blue side of the distribution in the figure. The individually-determined values of colour excess, E_{B-V}, range from $E_{B-V} = 0^m.40$ near the main grouping of faint stars to $E_{B-V} = 0^m.70$ in the direction of the brightest stars. This variation in the obscuration is visible in plates (1) and (2). The average value in the former region would be

TABLE 3

Stars of the Cluster NGC 6204.

No.	V	B-V	U-B	E_{B-V}
1	13.49	0.56		
2	12.19	0.35		
3	13.09	0.35		
4	13.05	0.65		
5	13.01	0.46		
6	12.90	0.55		
7	13.00	0.45		
8	11.28	1.43		
9	12.65	0.60		
10	12.64	0.54		
11	9.69	0.31		
12	12.32	0.73		
13	13.19	0.44		
14	12.27	0.50		
15	11.46	0.45		
16	10.46	0.28		
17	13.07	0.46		
18	11.63	0.35		
19	9.73	1.11		
20	11.73	0.30		
21	13.19	0.23		
22	12.61	0.32		
23	12.97	0.47		
24	12.20	0.34		
25	11.89	0.44		

No.	V	B-V	U-B	E_{B-V}
26	13.26	0.56		
27	10.86	0.26		
28	13.46	0.45		
29	12.34	0.75		
30	10.92	0.30		
31	11.94	0.30		
32	12.58	0.37		
33	12.26	0.42		
34	13.45	0.35		
35	12.53	0.51		
36	13.38	0.72		
37	13.20	0.48		
38	13.08	0.47		
39	9.89	0.30		
40	11.21	0.28		
41	12.14	0.35		
42	13.49	0.43		
43	11.85	0.30	-0.08	0.40
44	13.42	0.56	0.37	
45	12.58	0.46	0.12	0.53
46	12.96	0.52		
47	11.47	0.57		
48	12.91	0.38		
49	11.01	0.67		
50	12.22	0.36		
51	12.02	0.69		
52	12.54	0.35	-0.13	0.48
53	13.50	0.39		
54	12.15	0.32		
55	13.00	0.54		

No.	V	B-V	U-B	E_{B-V}
56	12.60	0.49		
57	13.12	1.08		
58	11.92	0.49	0.26	0.53
59	12.66	0.47		
60	11.63	0.42		
61	12.76	0.67		
62	10.92	0.33		
63	12.82	0.39		
64	13.09	1.11		
65 (105)	10.49	0.59	0.10	0.70
66	13.55	0.32		
67	10.91	0.60		
68	13.06	0.37		
69 (104)	10.91	0.36	-0.52	0.62
70	11.19	0.25		
71 (106)	8.50	0.44	-0.55	0.74
72 (108)	10.27	0.31	-0.59	0.60
73	13.11	0.41		
74 (109)	9.18	0.40	-0.57	0.70
75	12.28	0.61		
76	13.39	0.39		
77 (110)	7.31	0.35	-0.63	0.65
78	12.51	0.43		

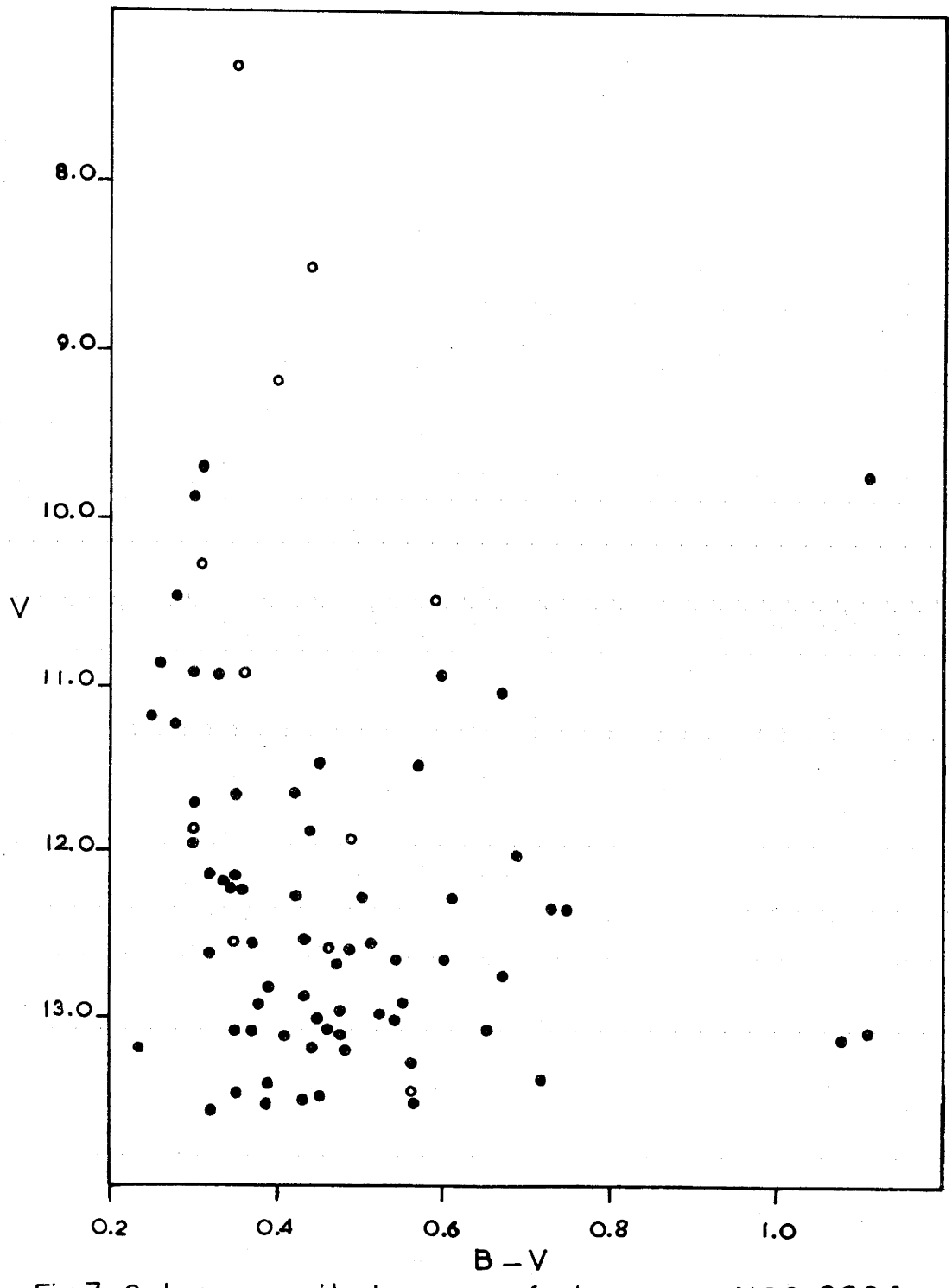

Fig.7. Colour-magnitude array of stars near NGC 6204. Photoelectric observations are shown as open circles.

$\overline{E_{B-V}}$ = 0.^m50 approximately; if this is used to correct the magnitudes and colours of the fainter members of the cluster, a fit of the zero-age main sequence to the blue side of the corrected distribution yields a distance modulus of Vo-Mv= 11.5 ±0.4 (2000 ± 400 parsecs).

With reference to table 2, the spectroscopic moduli of the brightest stars near the cluster (the small grouping at the lower edge of the cluster, present in plates (1), (2) and (3)) are:

No.	Sp.	Vo-Mv
71 (106)	09.5 III	12.1
72 (108)	B0.5 III	13.3
74 (109)	B0 III	12.6
77 (110)	06	10.8

All except number 77 have moduli in excess of that determined for the cluster. To explain the disparity, it is necessary to review the procedures carried out previously. One must assume that the grouping is associated with the cluster since it is located within the boundaries, and less than 6 minutes of arc from the centre, of the visual concentration. In the analysis of the photoelectric results, the value of the mean reddening used was $\overline{E_{B-V}}$ = 0.^m50. It is not well-defined, since the variations in the amount of obscuration overlying the cluster are greater than originally suspected. If a larger value, E_{B-V} = 0.^m60, representing the average of all determined colour excesses, was adopted, the derived modulus would be increased to Vo-Mv = 12.2 ± 0.4, in better agreement with the values for the four listed stars. From the results, it appears that star number 72 has been classified too luminous, compared with the others. Number 77 has a spectrum that shows Of characteristics (emission lines of He II (4686A) and C III (4651A)), and its absolute

magnitude for a modulus Vo-Mv = 12.2 would be Mv = -6.9, a more likely value than Mv = -5.5, which was used to derive the modulus assigned in table 2 (10.8).

On the basis of the photoelectric and spectroscopic results, a tentative distance of 2500 ± 500 parsecs is adopted. To obtain a more accurate distance of the cluster, a more thorough determination of individual colour excesses is needed, as they appear to vary considerably in the region. The fact that there is no H-alpha emission near the early-type stars suggests that the cluster may not be associated with the OB grouping around NGC 6193, where there is prolific ionization. In addition, although its distance is uncertain, the available evidence indicates that it is greater than that of NGC 6193.

4.4 Conclusion.

1. Distances.

Approximately centred on the coordinates $l^{II} = 337^{\circ}$, $b^{II} = -1^{\circ}.5$, in a region $4^{\circ}.5 \times 3^{\circ}$, is a visual grouping of 101 stars of early type, and 6 of late type and high luminosity class. The concentration has the following features:-

(1). The majority of stars are concentrated at a distance of 1400 parsecs - an approximate analysis of the data in table 2 reveals that about 75% of the stars have estimated moduli near Vo-Mv = 10.7, if it is assumed that the stars lacking spectroscopic observations are of luminosity class V. Very few have moduli less than 9.0 (equivalent to a distance of 700 parsecs).

(2). The galactic cluster NGC 6193, at a determined distance of 1300 parsecs from the sun, may represent the nucleus of the grouping.

(3). There are approximately 26 stars with determined distance moduli between Vo-Mv = 12.0 and Vo-Mv = 14.2.

It has been shown that they form a broad grouping at the distance 3500 parsecs, and that two may be as distant as 7000 parsecs.

(4). The young galactic cluster NGC 6204 is at an estimated distance of 2500 parsecs and may be associated with the more distant stars.

2. The OB Grouping.

At a distance of 1400 parsecs, the dimensions of the OB grouping (designated as the association I Ara, after the name of the grouping, listed by Schmidt, that is in the same direction) are 110 x 75 parsecs. Since for early-type stars, the absolute magnitude scale in terms of spectral types and luminosity classes is coarse, early-type stars with estimated distances between 1000 and 2000 parsecs (using the same assumption as in 1 (1)) were included as possible members. The number of such stars of spectral type B3 or earlier is 75. In addition, there are 3 of later spectral types and luminosity classes I - II (numbers 72, 92 and 102 of table 2); they were selected on the basis of the groupings of fig.5. The colour magnitude array of the grouping is essentially the same as in fig.4.

In visual appearance, I Ara has the typical characteristics of associations i.e a grouping of O and B stars surrounding a young galactic cluster (NGC 6193). The ionized hydrogen near the cluster may indicate the presence of remnants of the parent gas from which the stars were formed. According to the Oort-Spitzer 'rocket' mechanism[1] (discussed in chapter 1), one would expect the gas to be expanding; to date, unfortunately, no study of motions of the gas has been attempted. That

(1) Oort,J.H., B.A.N., 312, 177, 1954.

some parts of the gas have expansion velocities is suggested by the filaments visible on the H-alpha plate of the region (plate (2)). Westerlund[1] has postulated that they are caused by the deceleration, by interstellar material, of a shell of gas expanding away from the region near the central star of the "S" nebula (number 10 in tables 1 and 2). The colour-magnitude array of the grouping is quite narrow, since it is almost vertical, and any spread in the individual distances of the stars will not be reflected greatly in the width of the main sequence.

It is of interest to examine the luminosity function of the 78 stars of the association; this is shown in fig.8. The broken line represents the Initial Luminosity Function of Limber[2], normalized to the population so that the predicted number of stars with absolute magnitudes between Mv = -6.5 and Mv = -2.5, a range in which the membership should be virtually complete (for an absorption Av = $2^{m}.0$, an absolute magnitude Mv = -2.5 corresponds to V = 10.2 at the distance of the association), is equal to the observed number. The agreement between the curve and the histogram is quite reasonable. The greater number of observed stars with Mv = -6 is due probably to the addition of the late-type supergiants (F2 Ib, F8 Ib, and K1 Ib). However, until the radial velocities of these stars have been obtained, it is not possible to ascertain that they are members. Associations containing late-type stars of high luminosity are not common; the best known case is that in which is located the double cluster h and χ Per (I Per), and in which are several M-type supergiants.

(1) Westerlund,B.E., Upp.Ast.Obs.Medd.,No.133,1960.
(2) Limber,D.N., Ap.J., 131, 168, 1960.

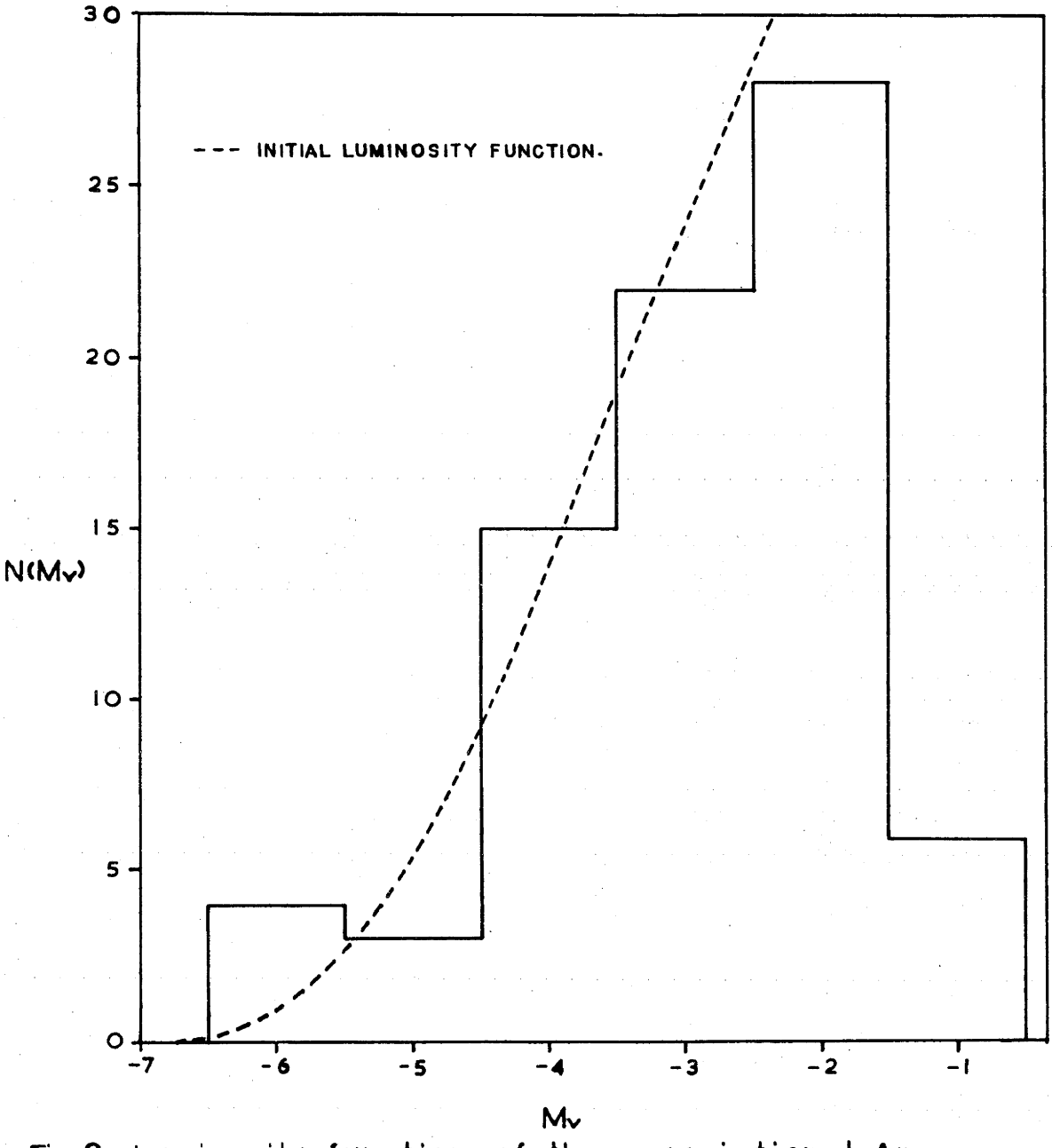

Fig. 8. Luminosity function of the association I Ara.

As the brightest star near the main sequence of the association is the most luminous member of the related cluster, NGC 6193, the age of I Ara is presumably close to 5×10^6 years. It is unlikely that the ages of association members not in the cluster differ appreciably from this value, for amongst these are stars comparable in brightness with the earliest of NGC 6193.

CHAPTER 5

SUMMARY

5.1 Spiral Structure.

In the preceding chapters, the distributions of H II regions and early-type stars in the Southern Milky Way have been discussed. The distances of several of the former are known from studies of their exciting stars (chapter 2). Groupings of young stars have been studied photoelectrically and spectroscopically (chapters 3 and 4). In the present chapter, these results will be used to define more accurately the spiral structure of the inner part of the galaxy.

1. The Distribution of Population I Objects.

(a). H II regions.

Fig.1 represents the distribution, in the galactic plane, of the H II regions listed in table 3 of chapter 2 (H II regions for which distances have been estimated). The continuous lines represent the approximate limits, suggested by the grouping in the diagram, of almost circular spiral arms.

(b). Southern O and B stars.

In chapter 4, a study of a group of high-luminosity stars at $l^{II} = 337^{o}$ with distances greater than 2000 parsecs was described. These are represented as dots in fig.2, the distribution, in the galactic plane, of early-type stars, OB associations and neutral atomic hydrogen. Also shown as dots are the early-type stars observed between longitudes $l^{II} = 265^{o}$ and $l^{II} = 50^{o}$ by Hiltner (1954)[1], Hiltner and Iriarte[2], Hiltner (1956)[3], and Feast, Stoy, Thackeray and

(1) Hiltner,W.A., Ap.J., 120, 41, 1954.
(2) Hiltner,W.A. and Iriarte,B., Ap.J., 122, 185, 1955.
(3) Hiltner,W.A., Ap.J.Supp., 2, 389, 1956.

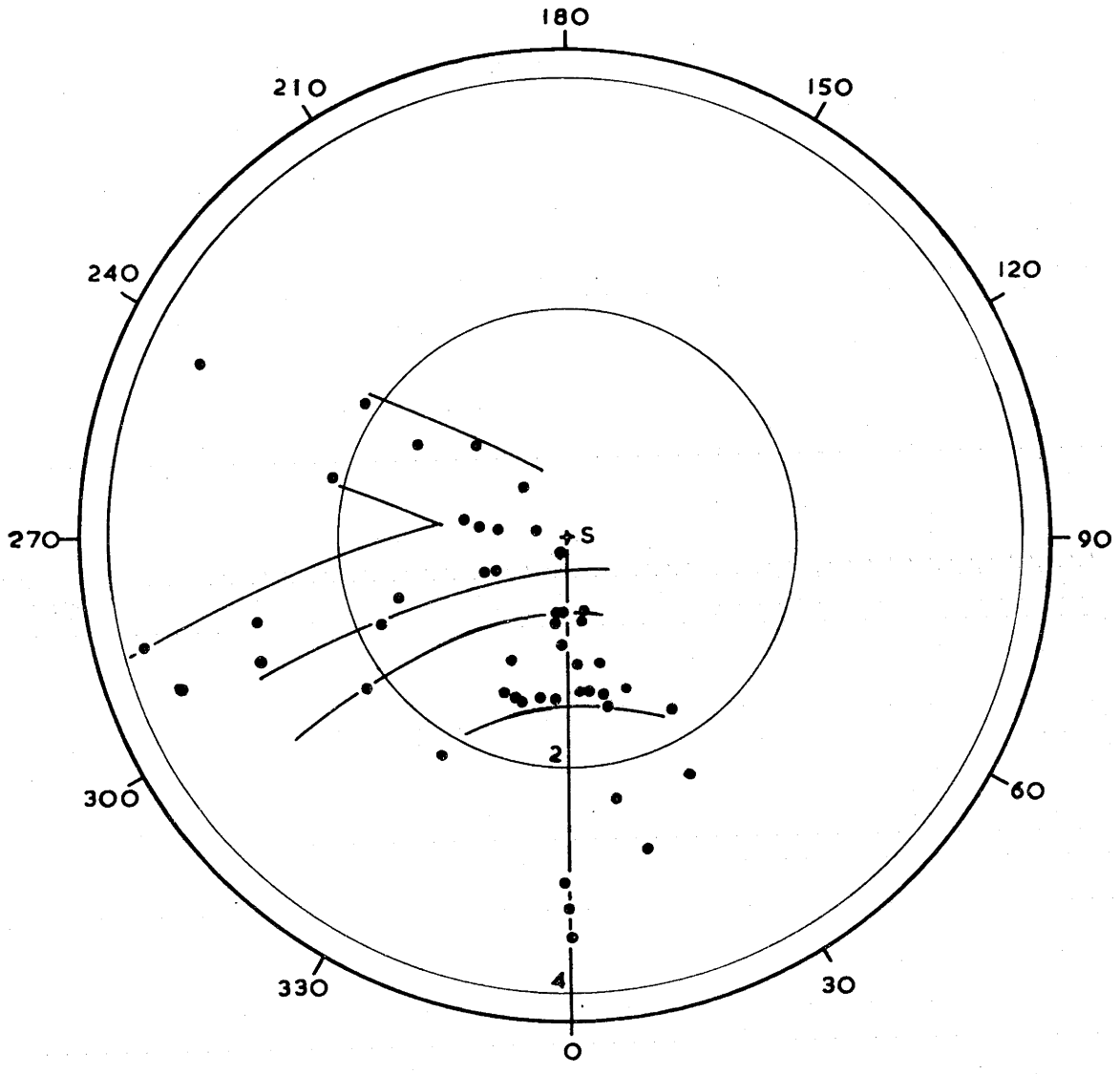

Fig.1. Distribution of HII regions in the galactic plane.

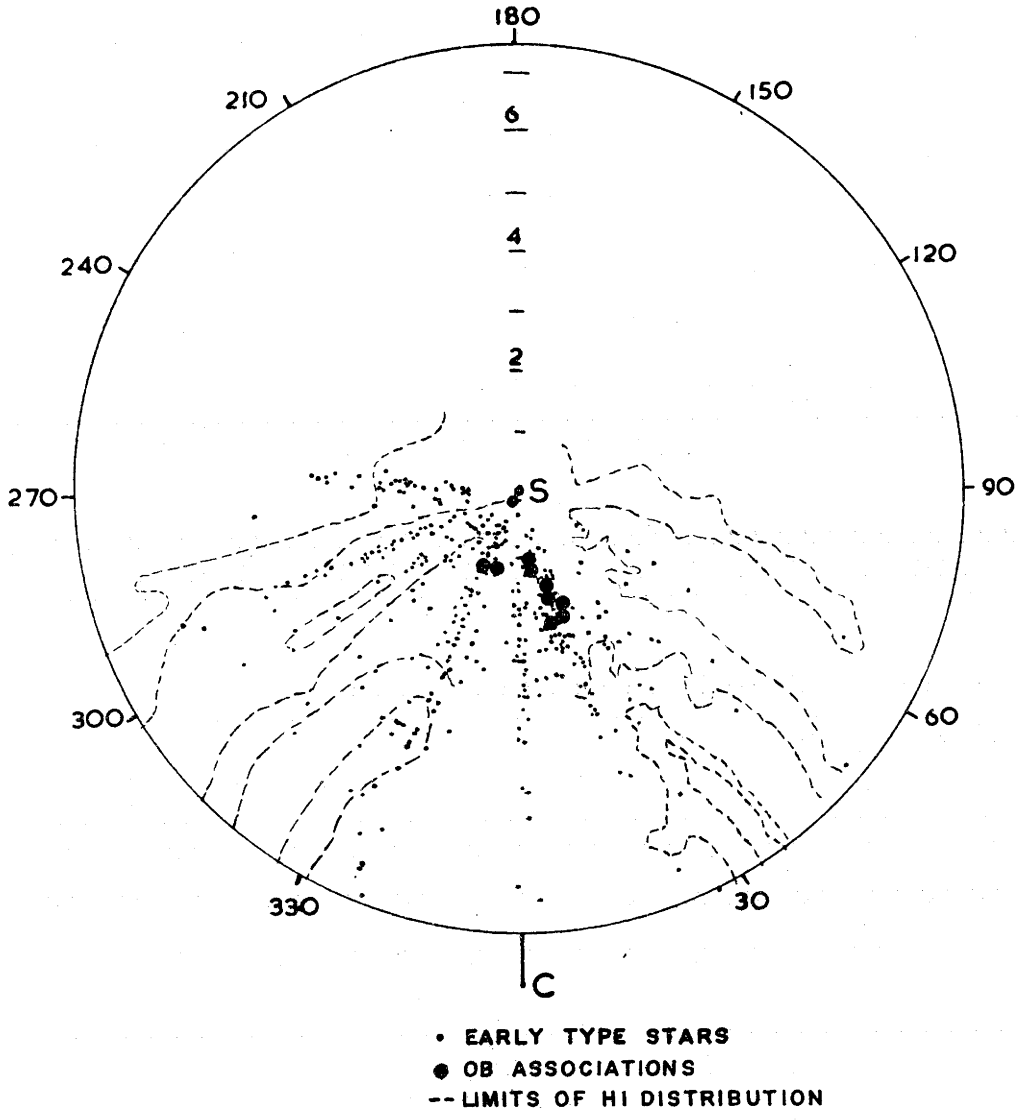

Fig.2. Distribution of southern early-type stars, OB associations and neutral atomic hydrogen.

Wesselink[1]. The distance moduli of stars in the lists of Hiltner and Hiltner and Iriarte have been redetermined using the latest tables of absolute magnitudes as functions of spectral type and luminosity class (Johnson and Iriarte[2]); these tabulations were employed by the other observers. The filled circles represent the positions of the associations of Morgan, Whitford and Code[3], and those discussed in the previous chapters (II Sco, I Ara). The broken lines represent the limits of the distribution of neutral atomic hydrogen with a density equal to, or greater than 0.6 atoms/cm^3 (Kerr, unpublished). The figure is complete only between longitudes $l^{II} = 265^o$ and $l^{II} = 40^o$.

(c). Clusters and associations.

In fig.3 is reproduced Becker's[4] diagram showing the distribution, in the galactic plane, of clusters, associations (filled circles) and H II regions (open circles). Added to the figure are the star groups discussed in chapters 3 and 4 (IC 2602, Mel. 101, NGC 6193, NGC 6204); their positions are represented by crosses. As in the previous figure, the broken lines represent the distribution of neutral atomic hydrogen.

2. Southern Spiral Structure.

(a). Previous evidence.

It was indicated in chapter 1 that there are at present two accepted patterns:-

(1) spiral structure similar to that inferred from the diagram of Morgan, Whitford and Code, i.e. highly-inclined spiral arms;

(2) spiral structure as suggested by the distribution

(1) Feast,M.W., Stoy,R.H., Thackeray,A.D. and Wesselink,A.J., M.N., 122, 239, 1961.
(2) Johnson,H.L. and Iriarte,B.,Lowell Obs.Bull.,No.91,1958.
(3) Morgan,W.W.,Whitford,A.E. and Code,A.D.,Ap.J.,118,318,1953.
(4) Becker,W., Z.f.Ap., 51, 151, 1961.

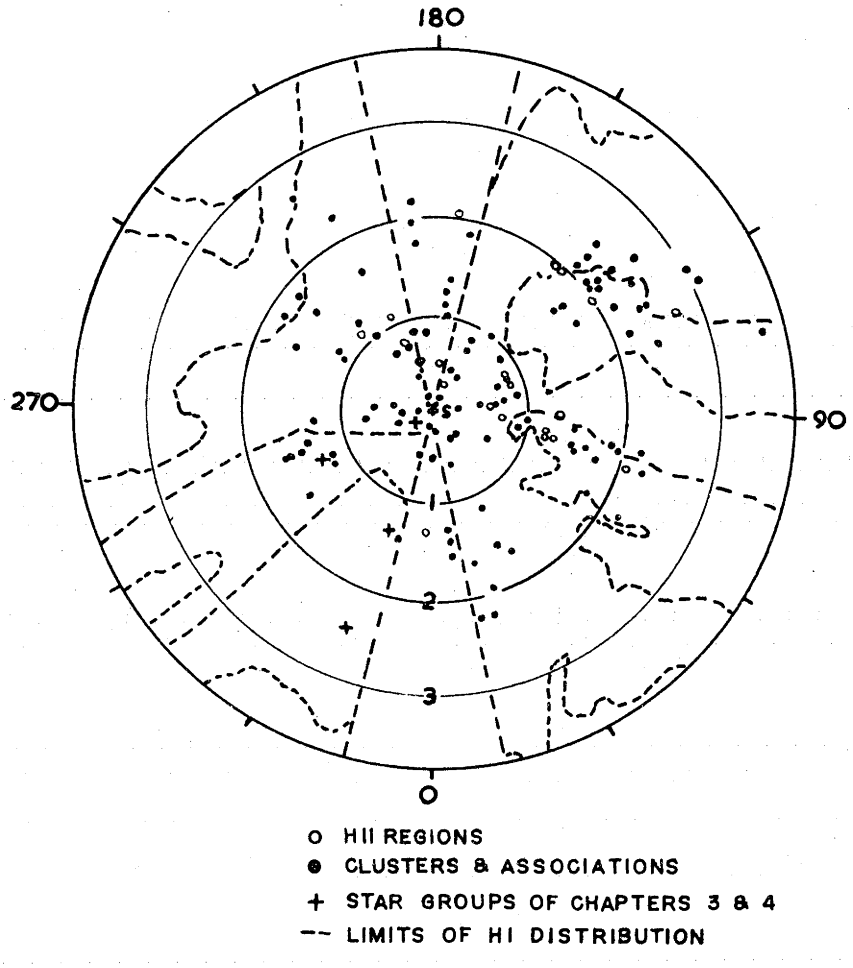

Fig. 3. The distribution in the galactic plane, according to Becker, of HII regions, OB associations & clusters

of neutral atomic hydrogen, i.e. nearly circular arms.

If (2) is the correct interpretation, the spiral-tracing features in Carina should be rather uniformly distributed along the line of sight in the tangential direction, as believed by Bok[1]. The results of the study of early-type stars in the region by Hoffleit[2] were not sufficiently conclusive to be able to choose between (1) and (2). Furthermore, confirmation of (2) depends on the detection of an interarm region between $l^{II} = 300^{o}$ and $l^{II} = 0^{o}$.

With these points in mind, let us examine the various distributions of Population I objects, described in chapter 1. Those not covering the Southern Milky Way, e.g. the diagram of associations of Morgan, Whitford and Code, will be excluded because of insufficient data. The highly inclined arms of Gum[3] and Kopylov[4] can be criticized; in both, the gap in the distributions between $l^{II} = 310^{o}$ and $l^{II} = 330^{o}$ has been ignored, and it could represent an interarm region. On the basis of the diagram of Kopylov, one would be quite justified in concluding that the continuation of the Orion Arm extended along the line of sight $l^{II} = 290^{o}$. Bearing in mind the inaccuracies of distances of early-type stars, the inclusion of a double Sagittarius Arm may be the result of over-interpretation. With the model of Elsasser and Haug[5], it has been shown that a representation in the form of (1) or (2) can be constructed, depending on which pairs of tangential points are joined. It is significant that all radioastronomical models would be included in category (2).

(1) Bok,B.J., Obs., 79, 58, 1959.
(2) Hoffleit,D., Ap.J., 124, 51, 1956.
(3) Gum,C.S., Mem.R.A.S., 67, 155, 1955.
(4) Kopylov,I.M., A.J.U.S.S.R., 35, 359, 1958.
(5) Elsasser,H. and Haug,U., Z.f.Ap., 50, 121, 1960.

According to Bok, the optical evidence in favor of circular arms is:

(1) Between $l^{II} = 300^{o}$ and $l^{II} = 330^{o}$, the H II regions are considerably smaller in size than those at adjacent longitudes.

(2) Between $l^{II} = 285^{o}$ and $l^{II} = 300^{o}$, there is a high concentration of early-type stars; it has a physically significant edge at the lower longitude. He reported recently[1] that at $l^{II} = 294^{o}$, there is a rather uniform distribution of B stars along the line of sight, and suggested that in this direction, the inner edge of the Carina-Cygnus Arm is present.

(3) In the direction of Carina, the polarization measurements of van P. Smith[2] show the disorderly arrangement expected along the line of sight of a spiral arm.

(4) The distribution of cepheids in the galactic plane shows a concentration between $l^{II} = 285^{o}$ and $l^{II} = 300^{o}$, a fact adding strength to the points (2) and (3), although several of such stars are associated with galactic clusters which are not sufficiently young to be extreme Population I.

(b). Evidence of structure in figs. 1, 2 and 3.

In each of the figures, there is a group of H II regions, clusters, associations and stars that extends almost continuously along the line of sight at longitude $l^{II} = 290^{o}$, suggesting the continuation of the Orion Arm (i.e. Bok's Carina-Cygnus Arm). In support of this conclusion, there is a common lack of Population I objects at $l^{II} = 275^{o}$, which, judging from an inspection of the mosaics described in chapter 2, is not due to the presence

(1) Bok,B.J., Obs., 81, 118, 1961.
(2) van P.Smith,E., Ap.J., 124, 43, 1956.

of heavier obscuration in this direction. The tangential longitude is in agreement with one of those of Elsasser and Haug. Only in fig. 3 is there a small discontinuity, in the line of stars, that might be called an inter-arm region by those astronomers supporting (1), although it is not a particularly prominent feature.

In figs. 1 and 3, there is a gap in the distributions between $l^{II} = 300^{o}$ and $l^{II} = 320^{o}$; it is not prominent in fig.2, the outstanding features of which are the lines of stars in directions which are either not affected greatly by obscuration, or which have been studied more extensively. The distribution of H II regions in chapter 2 also shows that most of the regions within these longitudes are small, which suggests that they are distant. The fact that they are present within these longitudes has led some astronomers to believe that the direction does not correspond to an inter-arm region. In fig.1 of chapter 4, the distribution of early-type stars on the celestial sphere, it is seen that at longitude $l^{II} = 303^{o}$, there is a large grouping (I Cru); Houck[1] has estimated that it is at a distance of 2200 parsecs, which places it near the edge of the Sagittarius Arm. In support of the association of I Cru with this arm, Rodgers[2], from a study of interstellar absorption in the direction, $l^{II} = 303^{o}$, has suggested that behind the Coalsack (i.e. at distances greater than 170 parsecs from the sun), there is an inter-arm region for at least 800 parsecs.

In all figures, a group of Population I objects define well the Sagittarius Arm from $l^{II} = 330^{o}$ to $l^{II} = 30^{o}$. The presence of an isolated arm is not shown clearly by the star distribution of fig.2; this is probably due to

(1) Houck,T.E., Doctoral Thesis,Univ.Wisc.,1956 (unpublished).
(2) Rodgers,A.W., M.N., 120, 163, 1960.

the small scale of the diagram, the preferential treatment given to some directions, and the masking of the true distribution by the errors in the determination of individual stars, for on the average, an error of one spectral sub-division, or one luminosity class in the classification of early-type stars, will change the distance modulus by $0^m.5$. From the positions of H II regions, clusters and associations, the arm is about 800 parsecs wide, extending from 800 to 1600 parsecs approximately, in the direction of the galactic centre.

Other features suggesting the presence of the Sagittarius Arm can be found in the results of the investigation reported in chapter 2. In the figure showing the distribution of H II regions on the celestial sphere, at longitudes greater than $l^{II} = 320^o$, the sizes of the regions are greater, suggesting that they are closer than those between $l^{II} = 300^o$ and $l^{II} = 320^o$. In the 19.7 Mc/s survey, it has been noted that the longitude $l^{II} = 318^o$ marks the direction in which the characteristics of the distribution of brightness temperature change; from this longitude to $l^{II} = 40^o$ there is an absorption 'trough' present along the galactic equator, suggesting the existence of an almost continuous band of H-alpha emission that is presumably in the Sagittarius Arm. According to the models of Elsasser and Haug, and of Mills[1], there are tangential directions at $l^{II} = 307^o$, $l^{II} = 49^o$, and $l^{II} = 310^o$, $l^{II} = 41^o$, respectively, that could correspond to this arm.

Between $l^{II} = 330^o$ and $l^{II} = 30^o$, the presence of another arm, the Scutum-Norma Arm, was originally noted by Thackeray[2]. In fig.1, the distant H II regions near

(1) Mills,B.Y., P.A.S.P., 71, 267, 1959.
(2) Thackeray,A.D., Nature, 178, 1458, 1956.

$l^{II} = 0$ could belong to it. In chapter 4, it was suggested that at longitude $l^{II} = 337^{o}$, there is a group of high luminosity stars at a distance of 3500 parsecs. Added to the results of other observers in fig.2, it appears to be part of a loose concentration, which could be associated with the Scutum-Norma Arm, at a distance of 4000 parsecs in that direction. There appears to be little other evidence in the diagram of the position of the arm; if it is assumed that it is nearly circular (and possibly contains the galactic cluster NGC 6204, discussed in chapter 4), it would extend from 2500 to 3500 parsecs in the direction of the galactic centre. Its existence between longitudes $l^{II} = 0$ and $l^{II} = 20^{o}$ is shown in Kopylov's results by the presence of several OB groupings with distances between 3000 and 4000 parsecs, although it should be realized that a grouping may consist of as little as two stars, and the distribution may suffer the same uncertainties as when dealing with the distances of single stars. Tangential directions of the arm are $l^{II} = 331^{o}$, $l^{II} = 27^{o}$ according to Elsasser and Haug, and $l^{II} = 325^{o}$, $l^{II} = 24^{o}$ according to the model of Mills. These results are in reasonable agreement, considering the difficulty in the former survey of eliminating the effects of large regions of heavy obscuration, although, as will be discussed later, there is some doubt as to whether the optical and the hydrogen arms are coincident. In addition, recent unpublished work by D.S. Mathewson and associates shows that the brightness of the radio continuum at a frequency 1440 Mc/s changes suddenly at $l^{II} = 327^{o}$ approximately, indicating the existence of the tangential direction discussed above.

To summarize, the optical evidence favours the existence of nearly circular spiral arms, in agreement with 21 cm results.

3. Comparison of Optical and Radio Distributions.

Becker[1] concluded from his diagram showing the distribution in the galactic plane of clusters, associations, H II regions and neutral hydrogen according to Westerhout[2] (similar to fig.3) that there is little coincidence in positions of the optical spiral tracers and the gas. The same applies to figs. 1, 2 and 3; many of the optical objects are concentrated at the inner edges of the H I arms. The existence of such a feature in the Perseus Arm has been known for some time, and it has been suggested that the presence of heavy obscuration in the arm prevented the detection of all but the innermost stars. However, this explanation could not apply for the Carina-Cygnus Arm, since the interstellar absorption at $l^{II} = 275^{o}$, the direction in which the H I arm extends along a line of sight, does not appear to be sufficiently high to cause the gap in the distribution of Population I objects. In the case of the Sagittarius Arm, Kerr has offered an explanation dependent on the stars being on the outer edges of the arms, an arrangement that does not apply, for in the figures, the objects defining the optical arm are within the limits of the broad hydrogen distribution. However, this is not a true test of coincidence, for many of the optical spiral tracers are located between longitudes $l^{II} = 345^{o}$ and $l^{II} = 15^{o}$, where the hydrogen model is uncertain because the random velocity fluctuations of the gas are of the same order of magnitude as the velocities due to galactic rotation. The represented parts of the

(1) Becker,W., Z.f.Ap., 51, 151, 1961.
(2) Westerhout,G., Sky and Telescope, 18, 367, 1959.

innermost H I arm appears to be located near the Optical Scutum-Norma Arm, but with the available data it is difficult to ascertain whether their positions coincide.

At this stage, it is appropriate to examine the limitations of the arguments for and against coincidence. For the optical distributions, the shape of the Carina-Cygnus Arm is real so long as the effects of interstellar matter are similar in the directions where the arm is tangential to the line of sight, and at adjacent longitudes. For example, the presence of heavier interstellar obscuration at $l^{II} = 280^{o}$, than at $l^{II} = 290^{o}$, could cause an apparent deficiency in the number of stars at the lower longitude, in which case the spiral arm could be thicker than shown in the diagrams, and its position may be in better agreement with the hydrogen distribution. However, it is significant that the distribution of H II regions is similar to those of stars and clusters, for this suggests that hydrogen must be present in detectable amounts outside the limits assigned by Kerr. The disparity in position cannot be due wholly to inaccuracies in the distances assigned to the H II regions, since it occurs in regions where the hydrogen arms and optical arms have different tangential directions. With the hydrogen model, it must be realized that near the sun, the derived results depend greatly on small irregularities in the motions, and the applied corrections, for the smoothing of the observed scans, caused by random velocities, are least effective. In support of Kerr's version of the Carina-Cygnus Arm, an important feature is that its tangential directions agree well with those of the model of Mills, derived independently from radio continuum radiation. We also may ask ourselves, how correct is the adopted velocity-distance model? Kerr's model was derived on the basis of an ex-

pansion hypothesis and inverse square relationship fitted to two points, viz. the 'expanding arm' near the galactic centre, and a postulated expansion velocity of 7km/sec at the distance of the sun. The existence of the latter has yet to be confirmed. The relationship was based on a distance of 8.2 kpc from the galactic centre to the sun; if as some astronomers believe, this value is too low, then the distance of the hydrogen Perseus Arm would be greater and the non-coincidence of position with the optical arm more pronounced. To be able to assess the accuracy of the adopted velocity-distance model, radial velocities of optical spiral tracers are needed - if the non-coincidence is real, one will not expect to have clusters, associations and H II regions with velocities similar to those of concentrations of hydrogen in slightly different positions of the sky. One might expect a tendency for stars and clusters with ages of the order of 100 million years to be inside the H I arms, for, once formed from the gas, they would take no further part in expansion, but would move in an orbit about the galactic centre and therefore would be eventually left behind by the gas. However, as most of the early-type stars considered are much younger, it is difficult to understand how they could be so far behind the gas, as suggested in the figures.

5.2 Future Work.

The results presented in this thesis suggest several problems for future investigation. Similar studies as reported in chapters 3 and 4 should be carried out using the remainder of the OB groupings detected. Previous arguments showed that, as derived distances of star concentrations are more accurate than those of individual stars, more meaning can be given to their distribution in

the galactic plane. Studies should be carried out particularly in the regions between $l^{II} = 265^{o}$ and $l^{II} = 285^{o}$ (to confirm the lack of spiral features) and between $l^{II} = 300^{o}$ and $l^{II} = 330^{o}$. If studies concerning the distances of individual stars are attempted, unless all directions are investigated to great distances, it is too easy to mistake a more thoroughly-studied direction for a line of sight along a spiral arm, and a more heavily obscured longitude for an inter-arm region.

As mentioned, there is an urgent need for radial velocities of optical spiral tracers. Such would act as a check on the velocity-distance relationship adopted in the reduction of H I observations. As mentioned in chapter 1, Pismis[1] detected a mean outward expansion of 4km/sec in a study of the motions of several associations. However, little confidence should be placed in the result for very few southern associations were included, although the velocity compares favourably with the 7km/sec expansion that Kerr has suggested for the hydrogen at the same distance as the sun from the galactic centre.

Another necessary study is that of the intensities and radial velocities of interstellar material, shown by interstellar lines in stellar spectra. One should extend the type of study carried out by Munch and Thackeray (chapter 1) to obtain more knowledge of southern spiral arms. If a sufficient number of distant stars were studied, it would not be difficult to obtain the directions in which the arms are tangential to the line of sight. As mentioned before, this type of study suffers from the same defects as radio investigations, viz. the determined

(1) Pismis,P., Ton.Bol., 19, 3, 1960.

distances depend on the rotation law. However, the velocities of the interstellar lines can be used for comparison with those of H I concentrations in an investigation of the coincidence in positions of optical and radio spiral features.

It is probable that polarization studies could assist in the determination of spiral structure. It has been shown that stars in a spiral arm viewed tangentially show polarized light with randomly distributed directions of preference. On the other hand, stars in spiral arms viewed normal to the line of sight show polarized light with directions aligned along the arms. There are of course difficulties in the cases of distant stars that are located behind several spiral arms. To date, little work of this nature has been carried out in the Southern Milky Way.